Phenomenological aspects of E_6 superstring-inspired models

Fabio Zwirner
International School for Advanced Studies
Trieste - Italy

April 1987

Contents

E.P. [illegible] PHD.
(5.5.87) [illegible] 86/87

Relatore: Prof John ELLIS

Acknowledgements

I would like to thank the Theoretical Physics Divisions of CERN and of the Lawrence Berkeley Laboratory for their warm hospitality during the preparation of this work, and Fondazione A. Della Riccia, Fondazione Ing. A. Gini and Istituto Nazionale di Fisica Nucleare for their financial support.

Many thanks go to my collaborators B. Adeva, F. del Aguila, V. D. Angelopoulos, K. Enqvist, S. Ferrara, F. Feruglio, G. L. Fogli, F. Gabbiani, C. Kounnas, H. Kowalski, A. B. Lahanas, D. V. Nanopoulos, K. Olive, S. Petcov, M. Quirós and N. Tracas for several useful discussions and for making my job more pleasant.

I am deeply indebted to my supervisor, Prof. John Ellis, for his precious scientific and human advice.

Last, but not the least, I would like to express my gratitude to Prof. Giovanni Costa for his constant help and encouragement during the last six years.

Chapter 1

Introduction

1.1 The way up

The standard model of strong and electroweak interactions, based on the gauge group $H_0 \equiv SU(3)_C \times SU(2)_L \times U(1)_Y$, successfully describes, or is at least consistent with, all confirmed experimental data in particle physics [1]. Despite this remarkable achievement, few physicists believe that it is really the ultimate theory of elementary particles, since, among the other things, it has a large number of arbitrary parameters and it leaves several unanswered questions. Outstanding theoretical problems that can find a solution only beyond the framework of the standard model are those of *unification*, of *flavour*, and of the *hierarchy* of different mass scales in physics.

The *unification* problem is related to the gauge interactions, whose pattern of groups and representations is complicated and arbitrary. Why should there be three different factors in the gauge group, with the associated coupling constants taking the values they do? Why should the fermions transform according to chiral representations of $SU(2)_L \times U(1)_Y$, so that parity is violated in weak interactions? Why should the electromagnetic charges of quarks and leptons be related by simple rational factors? Moreover, gravitational interactions are not included in the standard model: how could one give a consistent description of all elementary particle interactions, including gravity, compatible with the principles of quantum

mechanics?

The *flavour* problem has to do with the Yukawa interactions of the standard model, which introduce several arbitrary parameters into the game. There is no explanation for the existence of (at least) three fermion generations with the same gauge quantum numbers nor for the complicated pattern of masses, mixing angles and phases.

The *hierarchy* problem is connected with the scalar sector, which is used to describe spontaneous symmetry breaking of $SU(2)_L \times U(1)_Y$ down to $U(1)_Q$ via the Higgs mechanism, and which has not been checked experimentally at all. If one takes seriously the possibility of fundamental scalar fields, then one has to face the problem of quadratic divergences in perturbation theory. If one regards the standard model as a low-energy approximation of a more fundamental theory which explains the origin of the different mass scales in physics, in particular the smallness of the electroweak scale ($m_W \simeq 82\,GeV$) with respect to the Planck scale ($M_P \simeq 2.4 \times 10^{18}\,GeV$), such a hierarchy can be stable against radiative corrections only if quadratic divergences are cut-off at a certain mass scale, which must roughly correspond to the mass of the scalar(s) involved in the electroweak breaking. This mass, if we want the couplings in the Higgs sector to stay in the perturbative regime, cannot be much larger than 1 TeV.

Many attempts to go beyond the standard model, solving at least some of the problems outlined above, have been made over the last years: in particular, grand unified theories (GUTs) [2] with simple groups like $SU(5)$, $SO(10)$ or E_6 are able to give some partial answers to the unification problem (though there is still some arbitrariness left in the choice of the gauge group and of its representations, and gravity is not included), but they do not improve significantly our understanding of the flavour problem and they make the hierarchy problem even more acute. In addition to that, the scale of grand unification ($M_X \geq 10^{15}\,GeV$) is many orders of magnitude above the electroweak scale m_W, so that it is very difficult to

extract phenomenological consequences from GUTs. Indeed, the most dramatic suggestion, that of nucleon decay, has not yet been verified experimentally, and the present limits already rule out the 'minimal' $SU(5)$ model.

Among the problems listed above, the hierarchy problem is the only one whose formulation implies that some new physics *must* appear within the TeV region. Two main lines of attack on it have been pursued. One is the attempt to formulate models which do not contain fundamental scalar particles: the so-called technicolor or composite models, where the Higgs sector of the standard model is replaced by a strongly interacting gauge system, and fermion condensates are supposed to realize gauge symmetry breaking and the associated mass generation. No completely satisfactory model of this kind has been formulated until now. Another approach, which will be followed in the present work, is $N = 1$ supersymmetry (SUSY), which produces automatic cancellation of the dangerous quadratic divergences between boson and fermion loops. Of course, supersymmetry cannot be an exact symmetry of Nature but, as long as it is broken 'softly' and the mass splittings inside the supermultiplets containing the ordinary particles are not much larger than 1 TeV, it still provides a solution, in the technical sense, to the hierarchy problem.

Models with low-energy supersymmetry have been extensively investigated in the last few years [3], with particular regard to the problem of having a phenomenologically acceptable scenario for the spontaneous breaking of supersymmetry. Explicit 'soft' SUSY-breaking would solve technically the hierarchy problem, but it is theoretically unsatisfactory, since it introduces by hand several new dimensional parameters and it is incompatible with further unification with gravity. Earlier attempts focused on models with spontaneously broken global supersymmetry, with or without the inclusion of grand unification. It is not impossible to formulate realistic models of this kind, but in general one needs rather ugly constructions to avoid problems with the mass spectrum, chiral anomalies, etc..

The most natural framework for low-energy supersymmetry turns out to be

$N = 1$ supergravity in four dimensions, which automatically includes gravitational interactions. In these models spontaneous breaking of local supersymmetry takes place in a 'hidden' sector of the theory, constituted by fields which are singlets under the standard model gauge group and therefore communicating with the 'observable' sector only through gravitational interactions. This allows the generation of a mass $m_{3/2}$ for the gravitino and is compatible with a vanishing cosmological constant. Moreover, soft supersymmetry breaking scalar masses, trilinear scalar couplings and gaugino masses can be generated in the observable sector, with a common mass scale m related (in a model-dependent way) to the gravitino mass $m_{3/2}$. If m is of order m_W this scenario allows one to describe electroweak symmetry breaking as an effect of radiative corrections, which generate a negative mass-squared in the effective potential.

While supersymmetry and supergravity are able to solve the technical aspect of the hierarchy problem, they do not explain, in general, the origin of the observed hierarchy of mass scales, $(m_W/M_P) < 10^{-16}$, nor the observed smallness of the cosmological constant. An ambitious attempt in this direction is represented by the so-called 'no-scale' supergravity models, in which the small scales of physics are undetermined at the tree level and could be fixed by radiative corrections, and the tree level cosmological constant automatically vanishes.

Even four-dimensional $N = 1$ supergravity models cannot be the final word, however, since although they improve the ultraviolet behaviour of conventional quantum gravity, they are still affected by incurable divergences. One could imagine going beyond them to extended $N > 1$ supergravities or to more dimensions $d > 4$. The requirement of chirality strongly argues against extended $N > 1$ supergravities, which have left-right symmetric fermion spectra, with no way of pushing the unwanted 'mirror' fermions beyond the 1 TeV region. One is therefore left with higher dimensional theories: most of them also conserve parity, but one can incorporate chirality by introducing elementary gauge fields and going to an even

number of dimensions. The largest even number of dimensions in which $N = 1$ supersymmetry can be incorporated is $d = 10$, so interest naturally focuses on $N = 1$, $d = 10$ Yang-Mills supergravity. Anomalies are a danger for chiral theories, but they can be compensated by a Wess-Zumino term if the Yang-Mills group is $O(32)$ or $E_8 \times E_8'$. Of these possible choices, only $E_8 \times E_8'$ gives an acceptable chiral fermion spectrum. These last two results were derived from work on the superstrings.

1.2 The way down

We have seen in the previous section how, when trying to go beyond the standard model, one can make contact with the less empirical, more cartesian approach to physics represented by string theories [4].

In contrast with conventional point-particle theories, string theories describe extended one-dimensional objects, strings, each of which has an infinite number of states with masses and spins increasing without limit. The scale for the mass splitting between these states is set by the string tension, T, with dimension of $(mass)^2$. The first string theories, like the bosonic string or the spinning string, were developed originally in the early 1970's as models for strong interaction physics. These theories, however, had severe theoretical inconsistencies, because the string ground state always turned out to be a tachyon. Superstring theories, which evolved from the spinning string theory, incorporate supersymmetry and do not suffer from tachyonic ground states. In fact, the ground states have zero mass and are simply the fundamental states of interesting supergravity point field theories. Superstring theories are therefore re-interpreted as theories that include gravity and the natural mass scale set by T is the Planck scale M_P.

Some other remarkable properties of string theories show up only at the quantum level: for example, the consistency of the quantum theory selects a special dimension for space-time, the 'critical dimension'. For the original (bosonic) string

theory this was $d = 26$, whereas superstring theories (in their usual formulation) require 10-dimensional space-time. Another important fact is that superstrings can be formulated in d=10 with chiral fermions and Yang-Mills gauge symmetry, but in this case the theory is free of Yang-Mills and gravitational anomalies only if the gauge group is $SO(32)$ or $E_8 \times E_8'$. If so, the theory is also finite to one loop and possibly to all orders. Therefore superstring are candidates for a mathematically consistent theory unifying gravity with all the other interactions.

The main phenomenological problem with superstrings is to relate these theories of extended objects, formulated in ten dimensions and supposed to describe physics at the Planck scale, with a low-energy four-dimensional effective field theory of point-like particles, with chiral fermions and a realistic gauge group [5]. The most promising theory in this respect is the 'heterotic' string, in the version with gauge group $E_8 \times E_8'$.

One step in trying to descend from $SO(32)$ or $E_8 \times E_8'$ superstrings to the standard model is to consider, as a low-energy approximation, the corresponding field theory in the zero-slope limit, i.e. the field theory of the (massless) ground states of the string, disregarding the excited states. As a result, one obtains $N = 1$, $d = 10$ supergravity coupled with Yang-Mills theory: the physical fields in the supergravity multiplet are the graviton g_{MN}, the gravitino ψ_M, an antisymmetric tensor B_{MN}, a spinor λ and a real scalar ϕ, the dilaton; the super-Yang-Mills multiplet contains the gauge vectors A_M^α and the associated gauginos χ^α. All the fermion fields are Majorana-Weyl spinors, α are group indices and $M, N = 0, 1, \ldots, 9$. In addition to the terms already present in the conventional formulation, the resulting lagrangian contains some higher-derivative bosonic interaction terms which are essential for the mechanism of anomaly cancellation discovered by Green and Schwarz, and terms which supersymmetrize them.

Another step in the approach to the standard model is the compactification from $d = 10$ to $d = 4$. If one considers the standard formulation of $N = 1$, $d = 10$

supergravity, without higher-derivative terms, there are powerful no-go theorems which forbid compactifications to $d = 4$ with chiral fermion representations. This obstacle can be circumvented if one allows for the higher-derivative terms which are induced by the massive modes of string theories. Some of the possible vacuum states are of the form $\mathcal{M}_4 \times K$, where $\mathcal{M}_4$ is four-dimensional Minkowski space-time and K is a compact six-dimensional *Kähler* manifold of $SU(3)$ holonomy, a so-called 'Calabi-Yau' manifold. In this case it is possible to have in $d = 4$ unbroken $N = 1$ supersymmetry, a realistic gauge group and fermions in chiral representations. A series of results on Calabi-Yau compactification will be presented in section 2.1, as the starting point for the following phenomenological discussion.

With the present knowledge, nothing prevents the optimist from regarding the heterotic superstring as a candidate 'Theory of Everything', answering all the questions that are not answered by the standard model. It fixes almost uniquely its gauge group (at the moment $E_8 \times E_8'$ is preferred over $SO(32)$ for phenomenological reasons, without a deeper theoretical explanation) and the number of space-time dimensions, $d = 10$. It includes automatically gravitational and Yang-Mills interactions with chiral fermions, is anomaly-free and possibly finite. Compactification from $d = 10$ to $d = 4$, for example on a Calabi-Yau manifold, can determine dynamically the number of generations and the Yukawa couplings in the four-dimensional theory, solving therefore the flavour problem. Unbroken $N = 1$ supersymmetry can allow for a solution of the hierarchy problem, and the second E_8 is a natural candidate for the hidden sector of supergravity models. Moreover, the no-scale structure that seems to emerge could permit a dynamical determination of the scales of SUSY and electroweak breaking, reproducing some mechanisms previously suggested on phenomenological grounds. Up to now, there could be an answer for any of the questions raised in the previous section.

However, many problems have to be solved before a rigorous connection (or absence of connection) between string theories and low-energy phenomenology can

be established. First of all, a covariant second-quantized description of interacting strings is not available, so that non-perturbative questions like the determination of the correct vacuum of the theory cannot be addressed. First-quantized string perturbation theory, the only viable calculational scheme at present, can be used to impose consistency conditions that restrict the class of possible vacua. However, even in this approach there are several unsolved technical problems in the computation of multiloop amplitudes, and a rigorous proof of perturbative finiteness is still lacking. Finally, there are several gaps to be filled in our understanding of the low-energy limit of string theories, especially when $N = 1$ supersymmetric compactifications are considered and one wants to determine the structure of the effective four-dimensional pointlike theory in order to discuss problems like supersymmetry breaking and the low-energy spectrum.

In view of the above considerations, trying to do superstring phenomenology in the absence of a better understanding of the theory might seem premature or even foolhardy. However, as physicists we should not be only interested in the mathematical beauty and the internal consistency of the theories, but also in their chances to describe the real world. Indeed, phenomenological constraints are already playing an important role in guiding the theoretical investigations about string theories, helping to bypass some dynamical aspects which are very poorly understood. The fact that at low energy space-time is four-dimensional and there are at least three generations of chiral fermions, with a gauge group containing $SU(3)_C \times SU(2)_L \times U(1)_Y$ and, possibly, $N = 1$ supersymmetry broken in the TeV region, is already focusing the theoretical efforts on a restricted class of possible compactifications of the $E_8 \times E_8'$ heterotic string theory, leaving aside many other possibilities (e.g., type-II superstrings formulated in flat ten-dimensional space) that seem equally good from the point of view of the mathematical consistency alone. Of course, we are still very far from the stage of giving unequivocal and detailed predictions from string first principles. What we can do, however, is to

explore in detail different plausible scenarios, trying to understand their problems in reproducing the known experimental facts and the possible new phenomena they suggest: this is the spirit of the present work.

1.3 Outline

The present work is organized as follows.

Chapter 2 is meant to be a more extended introduction to the original part of this work. There general issues, associated with compactification of the heterotic string with gauge group $E_8 \times E_8'$ on Calabi-Yau manifolds, are discussed: the spirit is that of describing the possible constraints on model-building that are common to this class of models, without making reference to any particular manifold. Section 2.1 will review the main ideas and results about Calabi-Yau compactification, including a discussion of the gauge symmetry breaking at the compactification scale. Section 2.2 will introduce the general problems that are to be faced by superstring-inspired model building. Section 2.3 will discuss the problems associated with supersymmetry breaking in the hidden sector and its transmission to the observable sector in the form of soft SUSY-breaking terms.

Chapter 3 will discuss in detail a 'minimal' low-energy supergravity model, characterized by an extended gauge group $SU(3)_C \times SU(2)_L \times U(1)_Y \times U(1)_E$ and by an enlarged particle content with respect to the usual supersymmetric extension of the standard model, which satisfies the general constraints imposed by Calabi-Yau compactification. Even if no specific manifold is known giving rise to such a model, it is nevertheless representative of the new phenomenological effects that could arise from superstring theories. Section 3.1 will illustrate the ingredients of the model, stressing the assumptions behind them and their motivations. Section 3.2 will examine in great detail the possibility of generating radiatively the breaking of the extended electroweak symmetry in a phenomenologically acceptable way. Sections 3.3, 3.4 and 3.5 will study the particle spectrum of the model, with particular

emphasis on the features that make it different from conventional supersymmetric models. Present limits on the new particles and prospects for their detection at future colliders will be presented.

Chapter 4 will deal with what is probably the most interesting phenomenological possibility suggested by Calabi-Yau compactification: the existence of an extra massive neutral gauge boson, Z', in addition to the Z predicted by the standard model. A general parametrization for flavour-conserving neutral gauge bosons from E_6 will be introduced in section 4.1: popular superstring-inspired models can be recovered as particular cases. The structure of the mass matrix for the $Z - Z'$ system will be explored in section 4.2, and a systematic fit to all the existing neutral-current data will be performed in section 4.3, to extract limits on the mass and on the couplings of this hypothetical Z' in section 4.4. Finally, the prospects for the detection of a new Z' at present at future colliders will be explored in section 4.5.

Chapter 5 will contain some concluding remarks.

Chapter 2

General problems of superstring-inspired models

2.1 Some results on compactification

This section summarizes a number of results on a class of possible compactifications of the heterotic string [6] from $d = 10$ to $d = 4$, which will be used in the following as constraints in the construction of realistic superstring-motivated models. We shall concentrate on the so-called 'Calabi-Yau' [7] compactifications [8], with some comments on alternative possibilities [9]. Orbifold compactifications [10] and direct formulations of string theories in $d = 4$ [11] will not be discussed here: they are promising fields of research, but at the time of this writing the corresponding phenomenological scenarios have not yet been explored in sufficient detail.

2.1.1 Calabi-Yau manifolds

In order to be realistic, the $SO(32)$ or $E_8 \times E_8'$ heterotic string in $d = 10$ must possess a stable vacuum state of the form $\mathcal{M}_4 \times K$, where $\mathcal{M}_4$ is four-dimensional Minkowski space-time and K is some compact six-dimensional space. In principle, that vacuum should be selected by the underlying string dynamics; in practice, the only thing one can do at the moment is to expand the corresponding two-dimensional supersymmetric non-linear sigma-model around a background field configuration of the desired form and to check the consistency of the solution, in

order to derive some conditions that must be satisfied by K and thus constrain the resulting four-dimensional theory. In a famous paper [8], Candelas, Horowitz, Strominger and Witten imposed the following phenomenologically-motivated requirements:

1. the geometry of the background solution must be of the form $\mathcal{M}_4 \times K$, where $\mathcal{M}_4$ is a maximally symmetric space-time and K a compact six-dimensional manifold;

2. there should be unbroken $N = 1$ supersymmetry in four dimensions at the compactification scale, in order to solve the hierarchy problem;

3. the resulting gauge group and fermion spectrum must be realistic, with the gauge group containing $H_o \equiv SU(3)_C \times SU(2)_L \times U(1)_Y$ and the fermions transforming according to chiral representations of it.

Even if the analysis can be conducted at the level of the point-like field theory limit, an essential role in the compactification process is played by the higher-derivative terms of the lagrangian which are induced by the exchange of massive string modes. In the absence of these terms, there are powerful no-go theorems which forbid supersymmetric compactifications of $N = 1$, $d = 10$ supergravity with four-dimensional chiral fermions. For the sake of the present discussion, it is enough to recall the modified form of the field strength H associated to the antisymmetric tensor B:

$$H = dB - (\omega_{3Y} - \omega_{3L}), \tag{2.1}$$

where ω_{3Y} and ω_{3L} are the Yang-Mills and Lorentz Chern-Simon three-forms, respectively, defined as:

$$\omega_{3Y} = \frac{1}{30} Tr(A_\wedge F - \frac{1}{3} A_\wedge A_\wedge A), \tag{2.2}$$

$$\omega_{3L} = tr(\omega_\wedge R - \frac{1}{3} \omega_\wedge \omega_\wedge \omega). \tag{2.3}$$

In eq. (2.2), A is the gauge vector field of $E_8 \times E_8'$ or $SO(32)$, F is the corresponding field strength and the trace Tr is taken over the adjoint representation of the gauge group. In eq. (2.3), ω is the spin connection, R the related curvature tensor and the trace tr is taken over the vector representation of $SO(1,9)$. Note also that eq. (2.1) implies the Bianchi identity:

$$dH = trR_{\wedge}R - \frac{1}{30}TrF_{\wedge}F. \tag{2.4}$$

The requirement of unbroken $N = 1$, $d = 4$ supersymmetry, combined with the constraint of eq. (2.4), turns out to be extremely powerful. Assuming for simplicity that $\Phi = constant$ and $H = 0$, so that eq. (2.4) becomes

$$trR \wedge R = \frac{1}{30}TrF \wedge F, \tag{2.5}$$

one finds the following results:

1. $\mathcal{M}_4$ must be Minkowski space-time (vanishing cosmological constant);
2. K must be a Kähler manifold of $SU(3)$ holonomy, with the spin connection ω identified with the gauge connection A of some $SU(3)$ subgroup of the ten-dimensional gauge group.

Upon compactification on Calabi-Yau manifolds, the quantum numbers of the light fields of the resulting four-dimensional theory are determined by topological invariants of K and of the gauge fields defined on K. The massless gauge non-singlet fields in $d = 4$ originate from the gauge supermultiplet (in the adjoint representation of $E_8 \times E_8'$) of the corresponding ten-dimensional theory. Gauge singlet fields originating from the gravitational supermultiplet will be considered in subsection 2.1.3. If the gauge group is $SO(32)$, then one gets $SO(26)$ as a gauge group in four-dimensions, under which the adjoint representation of $SO(32)$ has only real representations and therefore does not allow for chiral fermions. Much more interesting is the case of $E_8 \times E_8'$. Considering the maximal subgroup $SU(3) \times$

$E_6 \subset E_8$, and embedding the spin connection in the $SU(3)$ factor, one obtains $E_6 \times E_8'$ as a gauge group in $d = 4$. In particular, the only fields transforming non-trivially under E_8' are the corresponding gauge bosons and gauginos. On the other hand, the adjoint 278 representation of E_8 decomposes under $SU(3) \times E_6$ as:

$$278 \rightarrow (1,78) \oplus (3,27) \oplus (\overline{3},\overline{27}) \oplus (8,1). \tag{2.6}$$

The first term in (2.6) corresponds to the vector supermultiplet in the adjoint representation of E_6; the second and the third terms correspond to chiral supermultiplets in the fundamental representation of E_6 or its conjugate: the numbers of 27 and $\overline{27}$ are given by topological invariants of the manifold K, the Betti-Hodge numbers $b_{1,2}$ and $b_{1,1}$, respectively. In particular, the number of chiral fermion generations, $n_G \equiv \#(27) - \#(\overline{27}) = b_{2,1} - b_{1,1}$, is given by

$$n_G = \frac{|\chi|}{2}, \tag{2.7}$$

where χ is another topological invariant called the Euler characteristic of the Calabi-Yau manifold. Finally, the E_6 singlets corresponding to the (8,1) term are likely to be all superheavy, and will be neglected in the following.

The number of achievements made possible by Calabi-Yau compactifications is impressive: first of all, the four-dimensional gauge group $E_6 \times E_8'$ and the light particle content are suitable for a realistic model, E_6 being an acceptable grand-unification group and E_8' being a natural candidate for the 'hidden sector' of low-energy supergravity models. One can generate chiral fermions and they naturally sit in fundamental 27 representations of E_6. Moreover, the number of chiral fermion generations can be associated to a topological invariant of the compactification manifold, and the Yukawa couplings computed (at least in principle) in terms of the ten-dimensional gauge couplings.

The results described above have been derived at lowest order in an expansion in α'/r^2, where r is the radius of the compact manifold, and are subject to corrections

when higher orders in α'/r^2 are included [12]. However, the qualitative features that will be used in the following analysis are not expected to change [13]: a detailed discussion of this topic goes beyond the scope of the present work.

2.1.2 Gauge symmetry breaking at the compactification scale

Models based on compactifications of the $E_8 \times E_8'$ heterotic string on a simply-connected Calabi-Yau manifold K_o have to face two very severe problems:

1. the number of chiral generations, $n_G^o = |\chi(K_o)|/2$, is in general excessively large;

2. an acceptable Higgs breaking of E_6 down to the standard model group $H_o \equiv SU(3)_C \times SU(2)_L \times U(1)_Y$ is impossible, since the only H_o-singlets contained in the 27 ($\overline{27}$) of E_6 are also singlets under $SU(5)$, so that one would end up with a low-energy group containing $SU(5)$ with unacceptable baryon-number violation.

Both difficulties can be avoided [14] if there is a suitable discrete symmetry group G that acts freely on K_o (for any element $g \in G$ other than the identity, the equation $gx_o = x_c$ has no solution for $x_o \in K_o$ or, in other words, there are no fixed points). In this case one can consider the (non simply-connected) quotient manifold $K = K_o/G$. One has then $\chi(K) = \chi(K_o)/N(G)$, where $N(G)$ is the number of elements of G, so that $n_G = n_G^o/N(G)$ can become acceptably small.

Moreover, a new mechanism for E_6 symmetry breaking becomes available, the so-called Hosotani breaking [15] (flux breaking, Wilson-loop breaking). Single-valued fields $\psi(x)$ on K, and in particular the zero modes of compactification, can be replaced by fields $\psi(x_o)$ on K_o satisfying the following boundary condition:

$$\psi(gx_o) = U_g \psi(x_o) \qquad \forall g \in G, \tag{2.8}$$

where the mapping $g \to U_g$ is a homomorphism of G onto a discrete subgroup $\overline{G}$ of E_6. Therefore the above equation expresses invariance under the direct sum $G \oplus \overline{G}$. The quantities U_g are analogous to Higgs bosons in the adjoint representation of E_6, and can be shown to correspond to vacuum expectation values of Wilson-loop operators of the type

$$U_g = P \exp i \int_{\Gamma_g} A_m^\alpha dx^m, \tag{2.9}$$

where $A_m^\alpha(x)$ are non-trivial gauge configurations on K with vanishing field strength and the path ordered integral is taken along the non-contractible loop Γ_g on K, which is the image of the path from x_0 to gx_o on K_o (the path independence of the integral being guaranteed by the identification of the gauge connection with the spin connection). Since massless gauge bosons of E_6 are invariant under the action of G, the subgroup of E_6 which remains unbroken after compactification is simply the maximal subgroup H which obeys the condition:

$$[H, \overline{G}] = 0. \tag{2.10}$$

Finding out all the possible subgroups H of E_6 which contain H_o is a straightforward exercise [16,17]: it amounts to classify all the possible discrete subgroups $\overline{G}$ of E_6 which commute with H_o. To do this, it is convenient to consider the maximal subgroup $SU(3)_C \times SU(3)_L \times SU(3)_R$ of E_6, under which the 27 representation decomposes as $(3, \overline{3}, 1) + (\overline{3}, 1, 3) + (1, 3, \overline{3})$. In view of the following considerations, it is useful to label the different fields in the 27 as:

$$27 = \begin{pmatrix} u \\ d \\ D \end{pmatrix} + \begin{pmatrix} u^c & d^c & D^c \end{pmatrix} + \begin{pmatrix} H^o & H^+ & e^c \\ \overline{H}^- & \overline{H}^o & \nu^c \\ e & \nu & N \end{pmatrix}, \tag{2.11}$$

where $SU(3)_C$ indices have been omitted, while $SU(3)_L$ indices correspond to different rows and $SU(3)_R$ indices to different columns. On the other hand, since we want to leave $SU(3)_C$ unbroken, it is not restrictive to assume that the U_g are of the form:

$$U_g = 1_C \otimes U_{gL} \otimes U_{gR}, \tag{2.12}$$

where 1_C is the unit $SU(3)_C$ matrix and U_{gL} and U_{gR} are $SU(3)_L$ and $SU(3)_R$ matrices, respectively. In addition, we want to leave $SU(2)_L \times U(1)_Y$ unbroken, where the embedding of the $SU(2)_L$ generators is given by

$$1_C \otimes \begin{pmatrix} SU(2)_L & \begin{matrix} 0 \\ 0 \end{matrix} \\ \begin{matrix} 0 & 0 \end{matrix} & 1 \end{pmatrix} \otimes 1_R \tag{2.13}$$

and the one of the $U(1)_Y$ generator by

$$Y = Y_L + Y_R, \tag{2.14}$$

with

$$Y_L = O_C \oplus \begin{pmatrix} 1/3 & & \\ & 1/3 & \\ & & -2/3 \end{pmatrix}_L \oplus O_R, \tag{2.15}$$

$$Y_R = O_C \oplus O_L \oplus \begin{pmatrix} 4/3 & & \\ & -2/3 & \\ & & -2/3 \end{pmatrix}_R . \tag{2.16}$$

From the above expressions one derives that any matrix U_g commuting with H_o must commute at least with its rank-five extension $\hat{H} \equiv SU(3)_C \times SU(2)_L \times U(1)_L \times U(1)_R$, and therefore the allowed four-dimensional gauge groups H can have only rank six or five. Rank-six groups correspond to abelian discrete groups $\overline{G}$, generated by matrices U_g of the form

$$U_{gL} = \begin{pmatrix} \alpha_g & & \\ & \alpha_g & \\ & & \alpha_g^{-2} \end{pmatrix}, \quad U_{gR} = \begin{pmatrix} \beta_g & & \\ & \gamma_g & \\ & & \delta_g \end{pmatrix}, \tag{2.17}$$

with $\alpha_g, \beta_g, \gamma_g, \delta_g \in C$ and $\beta_g \gamma_g \delta_g = 1$. Rank-five groups correspond to matrices U_g such that

$$U_{gL} = \begin{pmatrix} \alpha_g & & \\ & \alpha_g & \\ & & \alpha_g^{-2} \end{pmatrix}, \quad U_{gR} = \begin{pmatrix} \beta_g & \\ & V_g \end{pmatrix}, \tag{2.18}$$

with $\alpha_g, \beta_g \in C$, the 2×2 matrices $\{V_g\}$ constituting an irreducible representation of G and $\beta_g \det V_g = 1$. A complete list of the different possible groups H is given below. The corresponding form of the matrices U_{gL} and U_{gR} and the decomposition

of the 27 of E_6 into irreducible multiplets of H can be found in the literature [16,17]. Different embeddings of the same H into E_6 are considered as separate cases.

Rank 6:

1. $SU(6)_G \times SU(2)_N$
2. $SU(6)_G \times SU(2)_R$
3. $SU(6)_{CY} \times SU(2)_L$
4. $SU(6)_G \times U(1)$
5. $[SU(6)_G \times U(1)]'$
6. $SO(10)_G \times U(1)$
7. $SO(10) \times U(1)$
8. $SU(5) \times SU(2)_N \times U(1)$
9. $SU(5) \times SU(2)_R \times U(1)$
10. $SU(5) \times SU(2)_L \times U(1)$
11. $[SU(5) \times SU(2)_L \times U(1)]'$
12. $SU(5) \times U(1) \times U(1)$
13. $[SU(5) \times U(1) \times U(1)]'$
14. $SU(4)_C \times SU(2)_L \times SU(2)_N \times U(1)$
15. $SU(4)_C \times SU(2)_L \times SU(2)_R \times U(1)$
16. $SU(4)_C \times SU(2)_L \times U(1) \times U(1)$
17. $[SU(4)_C \times SU(2)_L \times U(1) \times U(1)]'$
18. $SU(3)_C \times SU(3)_L \times SU(2)_R \times U(1)$

19. $SU(3)_C \times SU(3)_L \times SU(2)_N \times U(1)$

20. $SU(3)_C \times SU(2)_L \times SU(3)_R \times U(1)$

21. $SU(3)_C \times SU(2)_L \times SU(2)_R \times U(1) \times U(1)$

22. $SU(3)_C \times SU(2)_L \times SU(2)_N \times U(1) \times U(1)$

23. $SU(3)_C \times SU(3)_L \times SU(3)_R$

24. $SU(3)_C \times SU(3)_L \times U(1) \times U(1)$

25. $SU(3)_C \times SU(2)_L \times U(1) \times U(1) \times U(1)$

Rank 5:

26. $SU(6)$

27. $SU(5) \times U(1)$

28. $SU(4)_C \times SU(2)_L \times U(1)$

29. $SU(3)_C \times SU(3)_L \times U(1)$

30. $SU(3)_C \times SU(2)_L \times U(1) \times U(1)$

As we shall see later, most of the above possibilities do not represent good candidates for a realistic low-energy theory, because of several phenomenological reasons.

To complete the discussion of symmetry breaking at the compactification scale it is also important to understand which components of the $b_{1,1}$ $(27 + \overline{27})$ survive as massless fields on K . The rule for the determination of the light 'survivors' is set by eq. (2.8). Since the index theorem ensures that $n_G = n_G^o/N(G)$ chiral generations, corresponding to n_G 27 superfields, will survive on K, to determine the additional self-conjugate light pairs coming from the $b_{1,1}$ $(27 + \overline{27})$ it is convenient to concentrate on the $b_{1,1}$ $\overline{27}$ on K_o. In general, they will transform as a sum of irreducible representations (IR) R_i of G. On the other hand, each $\overline{27}$ decomposes

under $\overline{G}$ (which is a discrete subgroup of E_6) into a sum of IRs L_j. The survivors on K will correspond, according to (2.8), to the fields invariant under $G \oplus \overline{G}$. Given a multiplet $\overline{\psi}$ of H contained in a $\overline{27}$ of E_6, it will belong to an IR L_j of $\overline{G}$, and therefore it will survive on K, if and only if it also belongs to an IR R_i of G such that the direct product representation $R_i \otimes L_j$ contains a singlet of $G \oplus \overline{G}$. If $\overline{\psi} \in \overline{27}$ is light, then the index theorem ensures that the self-conjugate $\psi \in 27$ will also remain light.

Historically, the first class of manifolds which was considered for model building were the so-called $\mathcal{Y}$-manifolds, with $b_{1,1} = 1$. In this particular case, the single $\overline{27}$ which is present is invariant under G, so that its surviving components on K are simply those invariant under $\overline{G}$. A complete classification of the survivors for the different subgroups H of E_6 can be found in ref.[16,17].

On the manifolds with $b_{1,1} > 1$, however, the situation is radically changed, since it is the general condition (2.8) that determines the survivors. If one is not working with a specific manifold with known discrete symmetries, one can contemplate the possibility that an arbitrary given set of H submultiplets, contained in the $b_{1,1}$ $(27 + \overline{27})$ of E_6, can remain light on K, for an appropriate choice of the manifold K_o and its discrete symmetry G.

Before concluding this section, a peculiar feature of the Hosotani symmetry-breaking mechanism must be stressed. Since the gauge multiplets of H, in the theory formulated on K_o/G, originate from a single multiplet of the theory formulated on K_o (the E_6 adjoint representation), their couplings at the compactification scale will still obey the grand-unification condition, and the standard renormalization group analysis of the gauge coupling constants will be valid also in this context. On the other hand, different chiral multiplets of H in the theory formulated on K_o/G will in general originate from different irreducible representations of E_6 in the theory formulated on K_o, and therefore their superpotential couplings will not obey E_6 Clebsch-Gordan relations: this allows to circumvent some bad predictions

about particle mass ratios that characterize conventional GUTs in their simplest formulations.

Finally, let us remark that we have concentrated on the Hosotani breaking of E_6, which is the gauge group in the observable sector, but a similar mechanism can be operative for breaking the hidden E_8' down to some subgroup of it at the compactification scale.

2.1.3 The effective $N = 1$, $d = 4$ supergravity theory

We describe here the possible form of the effective low-energy $N = 1$, $d = 4$ supergravity theory which would emerge from Calabi-Yau compactifications of the $E_8 \times E_8'$ heterotic superstring (or, more generally, from $N = 1$ supersymmetric compactifications on $\mathcal{M}_4 \times K$, where $\mathcal{M}_4$ is four-dimensional Minkowski space and K is a six-dimensional compact space). A consistent approach would involve integrating out all the massive string and compactification modes, generating in such a way effective interactions among the light fields. This procedure goes beyond our present capabilities. A simplified approach, due to Witten [18], is a truncation of $N = 1$, $d = 10$ supergravity, whose results will be presented here and used in the rest of this work, assuming that they reproduce the essential features of Calabi-Yau compactification. At the end of this subsection we shall also comment about alternative approaches and possible modifications to Witten's results.

As a starting point, one can take the standard form of $N = 1$, $d = 10$ supergravity coupled to $E_8 \times E_8'$ Yang-Mills theory [19], corresponding to a truncation of all the massive string modes. One can then assume that the light fields are invariant under translations of the six compactified coordinates x^m $(m = 4, \ldots, 9)$: this would give rise to an $N = 4$, $d = 4$ supergravity theory. Finally, one can keep only the fields which are singlets under the action of $SU(3)_D \equiv SU(3)_S \oplus SU(3)_G$, where $SU(3)_S$ is a subgroup of the rotation group $O(6) \sim SU(4)$ of the internal coordinates x^m [under which the supersymmetric charges Q^A $(A = 1, 2, 3, 4)$ trans-

form as $1 \oplus 3$ and the coordinates x^m as $3 \oplus \bar{3}$] and $SU(3)_G$ belongs to the maximal subgroup $SU(3)_G \times E_6 \subset E_8$: the residual $N = 1$ supersymmetry corresponds to the generator which is a singlet under $SU(3)_S$. In this way one obtains as surviving light fields in $d = 4$ the gravitational supermultiplet $(g_{\mu\nu}, \psi_\mu)$, the gauge supermultiplet $(A^\alpha_\mu, \chi^\alpha)$ of the unbroken gauge group, one generation of chiral fermions Φ^a (corresponding to a 27-dimensional representation of E_6), plus two chiral gauge-singlet superfields S and T, whose real and imaginary spin–zero components are given by:

$$S = S_R + iS_I, \qquad T = T_R + iT_I, \tag{2.19}$$

$$S_R = e^{3\sigma}\phi^{-3/4}, \quad T_R = e^{\sigma}\phi^{3/4} + \Phi^*_a\Phi^a, \tag{2.20}$$

$$S_I = 3\sqrt{2}D, \qquad T_I = -\sqrt{2}a. \tag{2.21}$$

The real parts of S and T are different combinations of the dilaton ϕ, already present in the $d = 10$ supergravity theory, and of the 'breathing mode' σ which describes the fluctuation of the overall size of the six-dimensional manifold K:

$$g_{mn} \equiv e^{\sigma} g^{(o)}_{mn}, \tag{2.22}$$

where $g^{(o)}_{mn}$ is a reference metric normalized so that:

$$\int_K d^6y [\det g^{(o)}]^{1/2} = M_P^{-6}. \tag{2.23}$$

In the definition of the imaginary parts of S and T, D and a are pseudoscalar fields parametrizing relevant zero modes of the $d = 10$ antisymmetric tensor field B_{MN}:

$$\phi^{-3/2} e^{6\sigma} H_{\mu\nu\rho} = \epsilon_{\mu\nu\rho\sigma}\partial^\sigma D, \tag{2.24}$$

$$B_{mn} = \epsilon_{mn} a. \tag{2.25}$$

The first equation above corresponds to a four-dimensional duality transformation, where $H_{\mu\nu\rho} = \frac{1}{3}(\partial_\mu B_{\nu\rho} + \partial_\nu B_{\rho\mu} + \partial_\rho B_{\mu\nu})$ + Yang-Mills Chern-Simons form (without Lorentz Chern-Simons form, since we are neglecting higher derivative terms in our

truncation procedure). In the second equation, ϵ_{mn} is the $SU(3)_S$-invariant tensor $\epsilon_{45} = \epsilon_{67} = \epsilon_{89} = +1$, $\epsilon_{54} = \epsilon_{76} = \epsilon_{98} = -1$.

Considering terms up to two derivatives in the fields (which should be a good approximation at low energies) the resulting $N = 1$, $d = 4$ supergravity theory [20] is determined by two independent functions of the light chiral superfields: a real function $\mathcal{G}$, called the *Kähler* potential, which determines the kinetic terms for the chiral superfields and contains information about the superpotential, and an analytic function $f_{\alpha\beta}$, transforming as a symmetric product of adjoint representations of the gauge group, which determines the kinetic term for the gauge supermultiplets. According to the truncation procedure outlined above one finds (working in units where $M_P = \sqrt{8\pi/G_N} = 1$):

$$f_{\alpha\beta} = \delta_{\alpha\beta} S, \tag{2.26}$$

$$\mathcal{G} = -\log(S + S^*) - 3\log(T + T^* - 2\Phi_a^*\Phi^a) + \log|W(\Phi)|^2, \tag{2.27}$$

where:

$$W(\Phi) = h_{abc}\Phi^a\Phi^b\Phi^c, \tag{2.28}$$

h_{abc} being proportional to the characteristic third-rank symmetric tensor d_{abc} of E_6. Note that the Kähler potential $\mathcal{G}$ of eq.(2.27) has a remarkable $\frac{SU(1,1)}{U(1)} \times \frac{SU(n,1)}{SU(n)\times U(1)}$ no-scale structure [21], whose consequences will be described in section 2.3.

The truncation procedure of Witten applies to the case of a hypothetical Calabi-Yau manifold with $b_{1,1} = 1$ and $b_{1,2} = 0$, corresponding to only one generation of chiral fermions. That procedure can however be extended [22] to the generic case in which $b_{1,1} \geq 1$, $b_{1,2} \geq 0$, and the no-scale structure of the Kähler potential is still preserved. Although the structure of the supergravity model derived by the truncation procedure is very appealing, there might be corrections to it coming from the massive modes which have been neglected, corresponding to terms suppressed by inverse powers of the heavy masses: this is particularly important in view of the fact that both the string scale M_S and the compactification scale M_C are likely

to be of the order of the Planck scale M_P. It is therefore interesting to compare the previous result with the most general effective lagrangian compatible with the classical symmetries of the underlying $d = 10$ supergravity and superstring theories. These symmetries are, apart from local $d = 10$, $N = 1$ supersymmetry and the Yang-Mills gauge symmetry:

1. 'Axion-type' symmetries, corresponding to the invariance under the change of the antisymmetric tensor B_{MN} by an exact two-form, implying that in the $d = 10$, $N = 1$ supergravity lagrangian B_{MN} has only derivative couplings through its field strength H_{MNP}.

2. 'Scale invariances', related to the fact that the vacuum expectation values of the dilaton field and of the breathing mode (associated to the determination of the gauge coupling constant and of the compactification radius) are not fixed at the classical level.

Using the set of invariances described above, one finds that the resulting $d = 4$, $N = 1$ supergravity model must be characterized by exactly the same gauge kinetic function and the same S-dependent Kähler potential as in the truncated case, while there could be modifications to the part of the Kähler potential depending on the (T, Φ^a) fields. The generality of this result is confirmed by explicit computations in orbifolds [23] and four-dimensional superstring models [24].

Even the last result need not necessarily be the final word. There is still left the logical possibility of corrections to it coming from quantum effects, both at the perturbative and at the non-perturbative level. Speculations have been made about the possible modifications coming from string loop effects, but the literature on the subject is controversial, and a complete computation of the one-loop string corrections is not yet available. Another plausible source of quantum corrections, this time at the non-perturbative level in the effective field theory, is gaugino condensation in the hidden sector, whose effects will be considered in section 2.3.

2.2 First problems for model building

In this section we briefly review some phenomenological problems that must be faced by the various candidate low-energy models allowed by the general rules of Calabi-Yau compactification and Wilson loop symmetry breaking [16,17,25, 26,27,-28]. For the time being, we shall assume the possibility of generating an acceptable supersymmetry breaking in the observable sector: this point will be discussed separately in the following section.

After Wilson loop breaking at the compactification scale, from E_6 to one of the groups H listed in the previous section, the subsequent stages of symmetry breaking, down to the standard model group H_0 and finally to $SU(3)_C \times U(1)_{em}$, are expected to proceed through the conventional Higgs mechanism, with some of the scalar fields in the chiral supermultiplets acquiring non-vanishing VEVs. One must therefore make sure that among the surviving light fields one can find Higgs particles with the appropriate quantum numbers. For example, the only H_0 singlets contained in the 27 or $\overline{27}$ of E_6 are also singlets under $SU(5)$: this implies that most of the models with simple factors of rank $r \geq 4$ in H are ruled out, since the complete breaking of this simple factor must occur at the electroweak scale, and this is phenomenologically unacceptable (among the other things, nucleon decay mediated by $SU(5)$ gauge bosons would occur at a very fast rate). As explained in the previous section, on manifolds with $b_{1,1} = 1$ the condition which determines the light 'survivors' is particularly simple, and strongly reduces the number of acceptable models. Things become more complicated on manifolds with $b_{1,1} > 1$: in this case the identification of the light survivors requires the knowledge of the discrete symmetries of the manifold, and non trivial constraints of this kind can be implemented only in specific models.

Another serious problem of the models under consideration is baryon and lepton number non conservation [29], possibly leading to nucleon decay. Nucleon

decay via gauge interactions is harmless in the models where the corresponding gauge bosons acquire mass in the Wilson loop breaking, since their mass is expected to be close to the Planck mass, giving enough suppression to the relevant four-fermion operators. An additional source of trouble, typical of supersymmetric models, is the possibility of nucleon decay due to renormalizable $|\Delta B = \Delta L| = 1$ combinations of Yukawa couplings in the low-energy superpotential, in the present case those involving the exotic (D, D^c) colour triplet superfields contained in the 27 of E_6. This problem has two possible ways out. One is the existence of an intermediate scale of symmetry breaking, such that the (D, D^c) particles acquire heavy enough masses (of order $10^{16}\ GeV$): some obstacles to the feasibility of such a scenario will be mentioned later. Another solution, exploiting the peculiarities of Hosotani breaking, is the existence of global symmetries that prevent the occurrence of the unwanted combinations of Yukawa couplings. A similar solution (R-parity) characterizes the conventional supersymmetric extensions of the standard model. In the present context, however, the symmetry should follow from the properties of the compactification manifold, but no satisfactory example has been found yet. Of course, the symmetry relations of the surviving gauge group H must be respected.

One more problem is associated to neutrino masses. The existence of a 'right-handed neutrino' state, ν^c, in the 27 of E_6, allows for the presence of superpotential couplings containing $\nu\nu^c H^0$, which generate a Dirac mass for neutrinos when H^0 acquires a non vanishing VEV. Due to the restricted particle content of these models, the elegant 'see saw' mechanism of conventional grand unification is no longer possible at the level of renormalizable couplings. Different solutions to this problem have been proposed. One suggestion [30] is that large Majorana masses for the ν^c state are generated by non-renormalizable operators of the form $\frac{1}{M}\nu^c\nu^c\tilde{\nu}^{c*}\tilde{\nu}^{c*}$ if $\tilde{\nu}^c$ acquires a very large VEV (if $M = M_P$, $m_{\nu^c} \sim$ few TeV requires $< \tilde{\nu}^c > \sim 10^{11}\ GeV$): these operators could be generated in the effective low

energy theory by the exchange of massive Kaluza-Klein or string modes. Another proposal [31], which also assumes $< \tilde{\nu}^c > \neq 0$ and exploits the structure of the resulting neutralino mass matrix, can solve the problem only for one generation. Both these approaches need to assume that $< \tilde{\nu}^c > \neq 0$, but this is likely to be a source of many other problems [32]. A third possibility is to assume that the Yukawa couplings corresponding to Dirac neutrino masses are forbidden by some symmetry of the compactification manifold: in this case the right handed neutrinos can remain massless without particular problems, since they are singlets under the standard model gauge group.

An additional set of constraints that must be satisfied by any acceptable model comes from the conventional renormalization group analysis, starting from unification of the gauge coupling constants at the compactification scale M_C. More precisely, one has to check, for each symmetry breaking pattern and particle spectrum, the resulting values for the Weinberg angle and the unification mass. Moreover, the validity of the analysis is related to the perturbative behaviour of the effective gauge couplings. In particular, many models with excessive light particle content must be discarded because of Landau poles in the gauge couplings evolution. In the absence of intermediate mass scales, the number of generations must be equal to three, and the only acceptable low energy groups are of the form $SU(3) \times SU(2)_L \times T$ [$T = U(1)$ or $U(1) \times U(1)$ or $SU(2)_N \times U(1)$]. If intermediate mass scales can be consistently generated, four generation models and different gauge groups can also survive the general tests described above.

Taking into account the previous discussion, it is very important to understand if models with intermediate mass scales (IMS) of symmetry breaking, between the electroweak scale m_W and the Planck scale M_P, are phenomenologically viable. In order to preserve the supersymmetric solution of the gauge hierarchy problem, any acceptable IMS breaking must correspond to an approximate flat direction of the scalar potential.Therefore, the scalar gauge-non-singlet fields which acquire large

VEVs must be self-conjugate multiplets contained in the $b_{1,1}$ $(27+\overline{27})$ pairs, and their VEVs must be approximately equal, to avoid a large D-term contribution to the scalar potential. Since one wants to break H to a subgroup containing H_0, the only candidates are $(N,\overline{N})$ and $(\tilde{\nu}^c,\overline{\tilde{\nu}}^c)$, which will be simply denoted here by (x,y). Moreover, the superpotential couplings which could induce a large F-term contribution to the potential must also be absent. Another necessary condition for the generation of IMS is supersymmetry breaking, in the form of soft SUSY breaking terms characterized by a common scale $O(1TeV)$: without these terms the degeneracy along the flat directions of the scalar potential cannot be lifted by radiative corrections. In summary, the relevant part of the effective potential can be written in the form:

$$\begin{aligned} V &= m_x^2|x|^2+m_y^2|y|^2+cg^2(|x|^2-|y|^2)^2 \\ &+ \left[(n+1)^2\frac{|f_n|^2}{M_P^{4n-2}}|x|^{2n}|y|^{2n}(|x|^2+|y|^2)+\ldots\right] \\ &+ 1-loop\ \ contributions, \end{aligned} \tag{2.29}$$

where c and f_n are numerical factors of order 1. Note that we have included possible non renormalizable terms that can be induced by the exchange of massive string or compactification modes: the integer $n \geq 1$ is the smallest value compatible with the symmetries of the theory and the dots stand for possible higher dimensional terms. A detailed study [33] of the potential (2.29) shows that, for reasonable values of the parameters, it is possible to generate radiatively IMS ranging from 10^6 to 10^{14} GeV along the flat directions of the renormalizable interactions. Possible non renormalizable terms in the scalar potential are not necessary for the generation of a stable minimum, but set an upper limit to the allowed IMS: $M_I \leq 10^{10}-10^{11}\ GeV$ for $n=1$, $M_I \leq 10^{13}-10^{14}\ GeV$ for $n=2$, and so on ....

Even if radiative generation of IMS is possible, there is still a long way to go [34] to formulate a fully consistent model of this kind. In order to solve the nucleon decay problem, one must have $M_I > 10^{15}\ GeV$. Also the requirement of

perturbative unification tends to push M_I towards very high values. However, this might create cosmological problems because of excessive entropy generation at the IMS phase transition. One has also to check that the effective theory below M_I has the right structure to describe correctly the electroweak symmetry breaking. Even if there is no no-go theorem for IMS models, their consistency is still an open question.

Before concluding this section, a final comment is in order. Many of the problems discussed above could be avoided if the unbroken gauge group emerging from compactification (before Hosotani breaking) were $SO(10)$ or $SU(5)$. Possible compactifications on manifolds of $SU(3)$ holonomy, where the spin connection is no longer identified with the gauge connection, corresponding to $SO(10)$ or $SU(5)$ unification groups, have been suggested by Witten [9]. Unfortunately, these vacua are generically unstable with respect to non perturbative effects at the level of the two-dimensional sigma model [35], and they might also have some phenomenological drawbacks [36]. Effective unification in $SU(5)$ or $SO(10)$ still remains, phenomenologically, the most attractive possibility, but its implementation should probably rely on orbifolds [10] or four-dimensional superstring models [11].

2.3 Problems with supersymmetry breaking

In this section we describe the problem of supersymmetry breaking in the context of the effective $N = 1$, $d = 4$ supergravity theory abstracted from the superstring. Our starting point will be the modified no-scale model introduced in section 2.1.3, characterized by a gauge group $H \times H' \subset E_6 \times E_8'$, by the chiral multiplets (S, T, Φ^a) and by the gauge kinetic function, Kähler potential and superpotential:

$$f_{\alpha\beta} = \delta_{\alpha\beta} S, \tag{2.30}$$

$$\mathcal{G} = -\log(S + S^*) - 3\log(T + T^* - 2\Phi_a^* \Phi^a) + \log|P(\Phi)|^2, \tag{2.31}$$

$$P(\Phi) = h_{abc} \Phi^a \Phi^b \Phi^c. \tag{2.32}$$

2.3.1 The origin of supersymmetry breaking

The most interesting compactifications of the $E_8 \times E_8'$ heterotic superstring are those corresponding to an unbroken $N = 1$ local supersymmetry in four dimensions, both because they have good chances of being quantum mechanically stable and because they can lead to a solution of the hierarchy problem. However, one has eventually to break the remnant supersymmetry in order to get a realistic model. In the phenomenological supergravity models developed before the superstring era, the most satisfactory mechanisms for SUSY breaking required the introduction of a so-called 'hidden sector', constituted by superfields which had only gravitational interactions with the 'observable' sector, to which the ordinary particles belong. In particular, one of the possible sources of supersymmetry breaking had been identified as gaugino condensation [37], in which case another crucial ingredient was the existence of a non-trivial gauge kinetic function. All these features seem to emerge naturally from the superstring framework.

At the grand unification scale M_{GUT}, to be identified with the compactification scale M_C:

$$M_C = < e^{-2\sigma} > = \frac{1}{< S_R >^{1/2} < T_R >^{1/2}}, \tag{2.33}$$

the effective four-dimensional gauge coupling constant is connected to the vacuum expectation value of the S_R field:

$$g^2_{GUT} = \frac{1}{< S_R >}. \tag{2.34}$$

Let us consider the largest non-abelian factor $\hat{H}'$ of the gauge group $H' \subset E_8'$ left unbroken after compactification. Since the only light fields transforming non-trivially under $\hat{H}'$ are the members of its gauge vector supermultiplet, they will become strongly interacting at the scale

$$\Lambda_{cond} \sim M_C e^{-\frac{<S_R>}{2b_o}}, \tag{2.35}$$

where $b_o = 3C_2(\hat{H}')/16\pi^2$ is the coefficient of the one-loop beta function of $\hat{H}'$. This

can plausibly trigger gaugino condensation, with $< Tr\bar{\chi}\chi > \sim \Lambda_{cond}^3$. Inspecting the supersymmetry transformations of the different fields, one can show [38] that gaugino condensation can induce supersymmetry breaking, thus generating a non-vanishing gravitino mass. However, this also induces a non-vanishing cosmological constant at tree level. One possibility to improve the situation is to introduce a constant term c in the superpotential, whose origin was initially attributed to a non-vanishing VEV for the field strength H of the antisymmetric tensor B. In this case, after integrating out the gauge superfields in the hidden sector, one obtains for the field S the following effective superpotential:

$$\omega(S) = c + he^{-\beta S}, \tag{2.36}$$

where $\beta = -3/2b_o$ and h is expected to be of order 1, so that the full superpotential below the condensation scale is now given by

$$W(\Phi, S) = P(\Phi) + \omega(S). \tag{2.37}$$

The corresponding tree-level scalar potential can be easily calculated using the standard formulas of supergravity:

$$\begin{aligned} V_o &= e^{\mathcal{G}}(\mathcal{G}'^k \mathcal{G}''^{-1l}_k \mathcal{G}'_l - 3) \\ &+ \frac{1}{2} Ref^{-1}_{\alpha\beta}(\mathcal{G}'_a T^{\alpha a}_b \Phi^b)(\mathcal{G}'_c T^{\beta c}_d \Phi^d) \\ &= \frac{1}{(S+S^*)(T+T^*-2\Phi^*_a\Phi^a)^3}|P + \omega - \omega_S(S+S^*)|^2 \\ &+ \frac{1}{6}\frac{P^*_a P^a}{(S+S^*)(T+T^*-2\Phi^*_a\Phi^a)^3} \\ &+ \frac{(6\Phi^*_a T^{\alpha a}_b \Phi^b)^2}{(S+S^*)(T+T^*-2\Phi^*_c\Phi^c)^2}. \end{aligned} \tag{2.38}$$

Each of the three terms in the above equation is positive semidefinite, so that a tree level minimum with vanishing vacuum energy must correspond to their separate vanishing. Neglecting the possibility of flat directions for the gauge non-singlet fields (which would not modify the conclusion of our analysis), one obtains that

$< \Phi^a >= 0$: to simplify the notation, from now on we shall omit the Φ dependence wherever there is no risk of confusion, putting all the Φ fields to zero. The tree level vacuum expectation value of S is in turn determined by $< \mathcal{G}_S >= 0$, corresponding to

$$< \omega - \omega_S(S + S^*) > \;=\; 0. \tag{2.39}$$

Introducing the variable $z = \beta S_R$, and denoting by z_0 its tree-level VEV, one obtains:

$$\cos \beta S_I = -1, \tag{2.40}$$

$$(1 + 2z_0)e^{-z_0} = c/h. \tag{2.41}$$

On the other hand, the VEV of T is left undetermined, and the same holds true for the gravitino mass

$$m_{3/2}^2 = e^{\mathcal{G}} =< \frac{1}{(2S_R)(2T_R)^3}|c + he^{-\beta S}|^2 > . \tag{2.42}$$

It is also important to note that all the possible soft supersymmetry breaking parameters in the observable sector remain zero at the tree level, despite the fact that supersymmetry is broken with a non-vanishing gravitino mass. This can be easily checked using the standard supergravity formula for the gaugino masses:

$$\begin{aligned} (m_{1/2})_{\alpha\beta} &= < \frac{1}{2} f'^{*k}_{\alpha\beta} e^{\mathcal{G}/2} \mathcal{G}'_l \mathcal{G}''^{-1l}_{\;\;k} > \\ &= \delta_{\alpha\beta} < \frac{1}{2S_R} e^{\mathcal{G}/2} \mathcal{G}'_S (\mathcal{G}''^{-1})^S_S >= 0 \end{aligned} \tag{2.43}$$

and the explicit expression of V_o given above, since

$$(m_o^2)^a_b = \frac{\partial^2 V}{\partial \Phi^*_a \partial \Phi^b} \tag{2.44}$$

and

$$A h_{abc} = \frac{\partial^3 V}{\partial \Phi^a \partial \Phi^b \partial \Phi^c}. \tag{2.45}$$

In summary, the tree level analysis leaves at least two unanswered questions. What fixes the VEV of T (and therefore the gravitino mass $m_{3/2}$ and the compactification scale M_C)? How is supersymmetry breaking transmitted from the hidden

to the observable sector? One might hope that one-loop radiative corrections can provide a satisfactory answer to both questions. However, explicit calculations [39] of the one loop effective potential show that the T direction is destabilized, so that the VEV of T cannot be computed in perturbation theory. One has therefore to assume, as a working hypothesis, that some other effect (string loop corrections? non-perturbative effects on the world sheet?) does the job.

2.3.2 Supersymmetry breaking in the observable sector

Even assuming that the 'true' potential has a minimum at a finite value of $< T >$, it can be shown that soft susy breaking scalar masses in the observable sector are not generated even at one loop [40]. The conventional proof makes use of the fact that the T-dependence of the $\mathcal{G}$ function always occur in the combination $T + T^* - 2\Phi_a^*\Phi^a$, so that $(m_0^2)_b^a = \partial^2 V/(\partial\Phi_a^*\partial\Phi^b) = \partial V/\partial T = 0$ at the minimum also at the one loop level.

Even if soft masses for the gauge-non-singlet scalars are not generated at the one loop level, this does not mean that the observable sector cannot feel the effects of supersymmetry breaking. There is still the possibility that non-zero gaugino masses and/or trilinear scalar couplings are generated by radiative corrections in the hidden sector [41,42,43,44]. While, contrary to early expectations [41], loops involving gravitons and gravitinos do not contribute to gaugino masses [42,43], loops involving the components of the S chiral superfield give in general non vanishing contributions [42,44]. The magnitude of these contributions depends on the model dependent parameters h and c, but in principle allows for the hierarchy $m_{1/2} << m_{3/2} << M_P$. Trilinear scalar couplings can also be generated at the one loop level, but their magnitude is negligible when compared to gaugino masses. Once the seed of supersymmetry breaking is introduced into the observable sector in the form of gaugino masses, all the other kinds of soft SUSY breaking parameters are naturally generated by radiative corrections in the observable sector, as

will be seen in a specific example in the following chapter.

Even if there are some indications on how supersymmetry breaking is transmitted from the hidden to the observable sector, the problem of supersymmetry breaking still presents many obscure points. The origin and the form of the superpotential (2.36) for the S field could be different [45]; the effect which eventually fixes the VEV of T and generates the desired hierarchy $m_{3/2} << M_P$ is unknown; the tree level vanishing of the cosmological constant is in general destroyed by radiative corrections. Qualitatively new ideas [46,47] are probably required for further progress.

Chapter 3

A 'minimal' model

3.1 Generalities

This chapter contains a detailed phenomenological study [26,48,49] of a 'minimal' low-energy model [14] which is compatible with the generic constraints imposed by Calabi-Yau compactification. Even if an explicit example of manifold giving rise to such a model is not known, a complete classification of all Calabi-Yau spaces is still lacking, leaving open the possibility that in future such a manifold can be found. Moreover, this minimal model can be viewed as the most economical representative example of the new phenomenological possibilities allowed by the superstring scenario: light exotic fermions and scalars originating from 27-dimensional representations of E_6, an additional light Z' boson, etc., which could also be present in non-minimal Calabi-Yau models. It might also be that alternative compactifications, e.g. the ones on orbifolds, can give rise to realistic models with very similar features [50].

3.1.1 The low-energy group

As explained in section 2.1, compactification of the $E_8 \times E_8'$ heterotic superstring on a non simply-connected Calabi-Yau manifold can yield, as possible four-dimensional gauge groups in the observable sector, many different subgroups H of E_6 containing the standard H_0, all of them having rank r greater than four.

As reviewed in section 2.2, many of the possible models associated with the different groups suffer from fatal diseases when faced with simple phenomenological constraints: neutrino masses, proton decay, the measured value of $\sin^2\theta_W$, etc.. Among the surviving models, there are several ones which can work only if there are intermediate symmetry-breaking scales between the compactification scale M_C and the electroweak breaking scale m_W: even if they may present some advantages for solving the problems with neutrino masses and proton decay, they have also to face a series of phenomenological problems [32,34]. Here we consider those models which can be acceptable also in the absence of intermediate mass scales (i.e., the 'minimal' ones as far as the number of relevant mass scales is concerned). The analysis of gauge couplings renormalization restricts then the choice of the gauge group among the unique $r = 5$ candidate $SU(3)_C \times SU(2)_L \times U(1)^2$ and the $r = 6$ candidates $SU(3)_C \times SU(2)_L \times U(1)^3$, $SU(3)_C \times SU(2)_L \times SU(2)_R \times U(1)^2$.

For either of the rank-6 groups to be acceptable, one must be able to break them down to the standard model group H_0, i.e. to reduce their rank by two. Each 27 of E_6 makes available to us two H_0-singlets: one, denoted here by N, is the $SO(10)$-singlet contained in the decomposition $[27]_{E_6} \rightarrow [16+10+1]_{SO(10)}$, and the other one is the $SU(5)$-singlet contained in the decomposition $[16]_{SO(10)} \rightarrow [10+\overline{5}+1]_{SU(5)}$, denoted here by ν^c and conjugate to the 'right-handed neutrino' of conventional grand unification. To get from $r = 6$ to $r = 4$, at least one representative of each of these types of fields must acquire a vacuum expectation value, and they must be larger than the VEVs of the $SU(2)_L$-doublets giving masses to the W and the Z, since the extra gauge bosons must be heavier than the standard model ones in order to be phenomenologically acceptable. However, a non-vanishing VEV for the scalar partner of the right-handed neutrino, $\tilde{\nu^c}$, is disfavoured by various phenomenological considerations [32,34]. Even if with some special construction it might be possible to build an acceptable model, we discard here the possibility that $< 0|\tilde{\nu^c}|0 > \neq 0$. Under this assumption, the only remaining possibility for the

gauge group is the rank-5 candidate:

$$\hat{H} = SU(3)_C \times SU(2)_L \times U(1)_Y \times U(1)_{Y'}. \tag{3.1}$$

Note that, as explained in section 2.1, the embedding of the extra $U(1)$ inside E_6 is completely fixed, and therefore the couplings of the different particles to the corresponding extra neutral gauge boson are also completely fixed.

3.1.2 The light matter fields

We now seek to specify the matter content of our model, in terms of light chiral superfields, after compactification and Wilson-loop symmetry breaking. The sources of ambiguity are in the number of generations n_G, in the possible addition of some pairs of conjugate multiplets from $(27 + \overline{27})$ representations of E_6, and in the presence of additional gauge singlets.

The first of these ambiguities is easily removed, since in the absence of intermediate mass scales a perturbative regime for the gauge coupling constants is only obtained for $n_G = 3$: we therefore assume the existence of a suitable Calabi-Yau manifold with $|\chi| = 6$, so that $n_G = |\chi|/2 = 3$.

To discuss the possibility of surviving split multiplets from the $b_{1,1} \geq 1$ self-conjugate $(27+\overline{27})$ representations of E_6, we have to remember the general analysis of section 2.1, and in particular the generic form of the matrices U_g of the discrete subgroup $\overline{G}$ of E_6 which corresponds to the four-dimensional gauge group $\hat{H}$:

$$1_C \otimes \begin{pmatrix} \alpha_g & & \\ & \alpha_g & \\ & & \alpha_g^{-2} \end{pmatrix} \otimes \begin{pmatrix} \beta_g & \\ & V_g \end{pmatrix}, \tag{3.2}$$

with $\alpha_g, \beta_g \in C$, the 2×2 matrices $\{V_g\}$ constituting an irreducible representation of a non-abelian discrete group G, and $\beta_g \det V_g = 1$. Let us consider first the case in which $b_{1,1} = 1$, or $b_{1,1} > 1$ with the $(27 + \overline{27})$s singlets under the action of G. Then for generic values of α_g, β_g and V_g there are no light survivors. Only under particular circumstances one can have either $(e^c + h.c.)$ [if $\alpha_g^{-2} = \beta_g$] or $(H + h.c.)$

[if $\alpha_g = \beta_g$] invariant under $\overline{G}$ and thus in the spectrum of light particles. The situation is different if the $b_{1,1}$ copies of the $(27+\overline{27})$ transform non-trivially under the group G: in this case, as previously discussed, no definite statement about the light survivors can be made on general grounds. In any case, in a model without intermediate mass scales we do not see any compelling reason for introducing these additional fields: in fact, the job of low-energy symmetry breaking, with acceptable values for the particle masses and $\sin^2\theta_W$, can be performed with the fields in the conventional 27 representations. On the other hand, since the $\overline{27}$s do not couple to pairs of 27 representations, an acceptable mass spectrum for the survivors could be difficult to obtain, and many additional parameters should be introduced. We therefore regard as the most natural and attractive possibility the one in which there are no light self-conjugate chiral multiplets.

In the Calabi-Yau compactifications under consideration (where $\omega = A$ and $H = 0$), gauge singlet superfields like S and T do not mix in the superpotential with gauge non-singlet superfields. Even if they are essential in the discussion of issues such as supersymmetry breaking, they do not play a rôle in the low-energy considerations of the present chapter, since they are likely to have only very weak couplings to matter $O(1/M_P)$ and superheavy masses $O(M_P)$. Therefore they will be neglected in the following.

Summarizing, the matter content of our model is: $n_G = 3$ generations of 27 chiral superfields with the quantum numbers of the fundamental representation of E_6, no light split multiplets from $(27+\overline{27})$s and no light gauge singlets. Note that this is the most economical ('minimal') choice that is possible in Calabi-Yau compactification.

With respect to the gauge group $\hat{H} \equiv SU(3)_C \times SU(2)_L \times U(1)_Y \times U(1)_{Y'}$, the 27 left-handed chiral superfields contained in the fundamental representation of E_6 have the following transformation properties:

$$Q \equiv (u,d) \sim (3,2,+1/6,+1/3),$$

$$u^c \sim (\overline{3}, 1, -2/3, +1/3),$$
$$e^c \sim (1, 1, +1, +1/3),$$
$$D \sim (3, 1, -1/3, -2/3),$$
$$H \equiv (H^+, H^o) \sim (1, 2, +1/2, -2/3); \tag{3.3}$$
$$d^c, D^c \sim (\overline{3}, 1, +1/3, -1/6),$$
$$L \equiv (\nu, e), \overline{H} \equiv (\overline{H^0}, \overline{H^-}) \sim (1, 2, -1/2, -1/6),$$
$$N, \nu^c \sim (1, 1, 0, +5/6). \tag{3.4}$$

Group and generation indices are understood. The first two numbers in brackets denote the dimensions of the $SU(3)_C$ and $SU(2)_L$ representations, respectively; the third and the fourth one the Y and Y' hypercharges, respectively, with conventional normalizations: the properly normalized quantities $\hat{Y}$ and $\hat{Y}'$, such as $TrT_{3L}^2 = Tr\hat{Y}^2 = Tr\hat{Y}'^2$ over the 27, are given by $\hat{Y} = \sqrt{3/5}Y$ and $\hat{Y}' = \sqrt{3/5}Y'$. We can identify eq. (3.3) and (3.4) with different representations of the maximal $SU(6) \times SU(2)_N$ subgroup of E_6: (3.3) corresponds to a $(15, 1)$, (3.4) to a $(6, 2)$; under $SU(5) \times U(1)_{Y'} \subset SU(6)$ one has $15 \to (10, +1/3) + (5, -2/3)$ and $6 \to (\overline{5}, -1/6) + (1, +5/6)$. The fact that the components of the 27 which fall into $SU(2)_N$ doublets [eq.(3.4)] have the same transformation properties under $SU(6)$, and therefore under $\hat{H}$, makes the identification of the ordinary charge-$(-1/3)$ quarks and charged leptons a non-trivial problem: in the minimal model, however, the solution is straightforward, and will be presented in the following subsection, after introducing the superpotential.

3.1.3 The superpotential

The states introduced in the previous section have, besides the usual gauge couplings, also generalized Yukawa interactions. The most general superpotential couplings allowed by the original E_6 invariance, followed by the Hosotani symmetry-

breaking mechanism, are:

$$
\begin{aligned}
f &= h_U Q u^c H + h_E L e^c \overline{H} && (3.5)\\
&+ h_\nu H L \nu^c + \lambda H \overline{H} N && (3.6)\\
&+ \lambda_\nu D d^c \nu^c + k D D^c N && (3.7)\\
&+ \lambda_L Q D^c L + h_D Q d^c \overline{H} && (3.8)\\
&+ \lambda_Q D Q Q + \lambda_C D^c u^c d^c && (3.9)\\
&+ \lambda_E D e^c u^c. && (3.10)
\end{aligned}
$$

Group and generation indices are understood for simplicity, but the different coupling constants should be interpreted as $3 \times 3 \times 3$ tensors. Two important points are also worth stressing. First, that as a consequence of the Wilson-loop mechanism the different superpotential couplings need not be linked by the usual E_6 Clebsch-Gordan relations: this is to be contrasted with what occurs in conventional grand unification. Second, that consideration of the most general superpotential couplings allowed by $\hat{H}$ gauge invariance (like $H\overline{H}$, HL, $\overline{H}e^c\overline{H}$, Le^cL, $H\overline{H}\nu^c$, HLN, $DD^c\nu^c$, Dd^cN, Qd^cN, Qd^cL, $QD^c\overline{H}$, $D^cu^cD^c$, $d^cu^cd^c$) would be misleading, because couplings other than those in (3.5)-(3.10) would not be allowed by the underlying E_6 structure.

Note also that, treating the superpotential couplings as phenomenological parameters, as a consequence of the fact that $\hat{H}$ commutes with $SU(2)_N$ there is an overall ambiguity corresponding to arbitrary rotations between the two sets of fields $(D^c, \overline{H}, N)$ and (d^c, L, ν^c). To remove this ambiguity, we may without loss of generality identify L with the standard lepton doublet, in which case lepton number conservation requires $< 0|\tilde{\nu}|0 >= 0$. In order to identify the mass eigenstates corresponding to the ordinary charge-$(-1/3)$ quarks and charged leptons, we must examine the corresponding mass matrices, which take the forms

$$
\begin{pmatrix} d & D \end{pmatrix} M_{1/3} \begin{pmatrix} d^c \\ D^c \end{pmatrix}: \qquad M_{1/3} = \begin{pmatrix} h_D < 0|\overline{H^o}|0 > & 0 \\ \lambda_\nu < 0|\tilde{\nu^c}|0 > & k < 0|N|0 > \end{pmatrix} \qquad (3.11)
$$

and

$$\left(\begin{array}{cc} e^c & H^+ \end{array} \right) M_1 \left(\begin{array}{c} e \\ \overline{H^-} \end{array} \right) : \quad M_1 = \left(\begin{array}{cc} h_E < 0|\overline{H^o}|0 > & 0 \\ h_\nu < 0|\tilde{\nu^c}|0 > & \lambda < 0|N|0 > \end{array} \right). \quad (3.12)$$

The physical squared masses are given by the eigenvalues of the matrices $M_{1/3}^\dagger M_{1/3}$ and $M_1^\dagger M_1$, respectively. We assume for simplicity real Yukawa couplings and VEVs. Note that, in order to avoid unacceptable zero mass eigenvalues in (3.11) and (3.12), it must be that $< 0|N|0 > \neq 0$. On the other hand, the possibilities that $\lambda_D < 0|\tilde{\nu^c}|0 >$, $\lambda_L < 0|\tilde{\nu^c}|0 > \neq 0$ have potential phenomenological problems [32] with flavour-changing neutral currents and the physical values of m_d, m_e. Thus we will assume in the following that $< 0|\tilde{\nu^c}|0 > = 0$, which implies $< 0|\overline{H^o}|0 > \neq 0$ to avoid zero eigenvalues in (3.11) and (3.12). It must also be that $< 0|H^o|0 > \neq 0$ to give masses to the quarks of charge $+2/3$. We are then led to a situation where we can identify (d, d^c) with the ordinary quarks of charge $-1/3$, (D, D^c) with some new exotic particles, and there is no mixing between the two sectors. Similarly, we will identify (e, e^c) with the ordinary charged leptons, and $(H^+, \overline{H^-})$ with some new states having the quantum numbers of the charged Higgses in the standard supersymmetric model. The identification of the fields (u, u^c) with the ordinary quarks of charge $+2/3$ is unambiguous. In addition, to complete each 27 of E_6 there are the two standard model singlets N and ν^c previously introduced. Note finally that the extension of the above considerations to arbitrary E_6 superstring-inspired models is not trivial, since for many of the possible symmetry breaking patterns different members of the $SU(2)_N$ doublets have different transformation properties under the low-energy gauge group: for a more general discussion see ref.[51].

Now that we have identified the different physical fields inside the 27 of E_6, we can comment on the different possible couplings in the superpotential. Some of them (h_U, h_E, h_D) are nothing else than the usual Yukawa couplings that are used to give masses to the ordinary quarks and leptons, via the VEVs of H

and $\overline{H}$, in the standard supersymmetric model. Some other couplings (λ, k) are necessary to give masses to the exotic particles D, D^c, H, $\overline{H}$, N contained in the 27 of E_6. Moreover, as we are going to see later, λ and k play an essential role in the radiative breaking of the gauge symmetry, through their contributions to the one-loop renormalization group equations. The coupling λ is also needed to avoid the appearance of a massless Higgs field in the particle spectrum. When, as shown in the next section, $< 0|N|0 > \neq 0$, one obtains an effective $\mu H\overline{H}$ coupling as in the supersymmetric standard model, with the additional bonus that now the phenomenologically desirable scale of $\mu = \lambda < 0|N|0 > \leq O(1)TeV$ has a natural explanation and does not need to be introduced by hand. There is no renormalizable coupling which could give a Majorana mass to the right-handed neutrino ν^c. In absence of intermediate mass scales non-renormalizable effective couplings would also not be able to generate large enough Majorana masses for ν^c. Therefore couplings of type h_ν become extremely dangerous, since they would generate, after H acquires a VEV, Dirac mass terms for neutrinos. In a realistic model they must be vanishing or extremely small, and the same must be true for the masses of the right-handed neutrinos. Another possible source of trouble is the simultaneous presence of the two sets of couplings $(i) \equiv (\lambda_\nu, \lambda_L, \lambda_E)$ and $(ii) \equiv (\lambda_Q, \lambda_C)$. In the absence of intermediate mass scales, the scalar components of the (d, D^c) supermultiplets cannot be superheavy, and therefore the explicit baryon- and lepton- number violation associated to the simultaneous presence of (i) and (ii) would lead to unacceptably fast nucleon decay. On the other hand, at least one coupling from the sets (i) or (ii) is needed to make the (D, D^c) particles unstable. Fortunately set (i) conserves both B and L if we assign $B(D) = +1/3$, $L(D) = +1$, $B(D^c) = -1/3$, $L(D^c) = -1$: in this case (D, D^c) have the quantum numbers of leptoquarks; set (ii) does the same if we assign $B(D) = -2/3$, $L(D) = 0$, $B(D^c) = +2/3$, $L(D^c) = 0$: in this case (D, D^c) have the quantum numbers of diquarks. The existence of non-vanishing couplings either in (i) or in (ii) is

phenomenologically acceptable.

In summary, the constraints coming from neutrino masses and nucleon decay require that the couplings λ_ν and [(i) or (ii)] be vanishingly small. How plausible is this possibility? The superstring offers two mechanisms for setting Yukawa couplings naturally to zero: the first is topological, and has to do with the non-intersection of complex hypersurfaces in the manifold of compactification; the second one is the possible existence of discrete symmetries. The topological mechanism seems very powerful: ref.[52] gives an example where only 111 out of 8436 possible Yukawa couplings are in fact non-zero. Though no one has an example of Calabi-Yau manifold which gives one of the patterns postulated above, discrete symmetries may be unnecessary eventually. In the mean time, it is encouraging that one can postulate relatively simple discrete symmetries to obtain the desired result. We consider here three possible cases, all corresponding to an invariance under $Z_2 \otimes Z_2'$:

1.

$$\begin{aligned} Z_2 &: [3,\overline{3}]_{SU(3)} \to (-1)[3,\overline{3}]_{SU(3)}, \\ Z_2' &: \nu^c \to (-1)\nu^c. \end{aligned} \tag{3.13}$$

This forbids the couplings characterized by λ_Q, λ_C and λ_ν, leaving the ones corresponding to h_U, h_E, h_D, λ, k, λ_L and λ_E.

2.

$$\begin{aligned} Z_2 &: [3,\overline{3}]_{SU(3)} \to (-1)[3,\overline{3}]_{SU(3)}, \\ Z_2' &: [L,e^c] \to (-1)[L,e^c]. \end{aligned} \tag{3.14}$$

This forbids the couplings characterized by λ_Q, λ_C, λ_L and λ_E, leaving the ones corresponding to h_U, h_E, h_D, λ, k and λ_ν.

3.

$$Z_2 \;:\; [L, e^c, \nu^c] \to (-1)[L, e^c, \nu^c],$$
$$Z_2' \;:\; \nu^c \to (-1)\nu^c. \tag{3.15}$$

This forbids the couplings characterized by λ_ν, λ_L and λ_E, leaving the ones corresponding to h_U, h_E, h_D, λ, k, λ_Q and λ_C.

Each of the three possibilities above is acceptable and could give rise to interesting phenomenology, as will be discussed in section 3.5. More complicated possibilities, involving for example the generational structure of the couplings, could also occur, but we regard the ones given above as the most natural. It should be stressed that each of our choices (3.13), (3.14) or (3.15) of Yukawa couplings automatically evades several kinds of nasty problems with flavour-changing neutral currents and weak universality. With respect to flavour-changing neutral currents, box diagrams could be of some importance but, as we will see later, our spectrum is relatively 'heavy', so their contribution is of no great concern. Similar arguments apply to CP-violating effects, $(g-2)_{e,\mu}$, the electric dipole moment of the neutron, etc. [32].

3.2 Radiative breaking of the gauge symmetry

3.2.1 The structure of the scalar potential

Given the ingredients of the minimal model introduced in the previous section, we want now to investigate how the extended electroweak symmetry can be broken as an effect of radiative corrections, generalizing a procedure already applied to conventional supergravity models. As usual, we will parametrize the effects of supersymmetry breaking on the observable sector with a set of soft SUSY-breaking parameters: gaugino masses, scalar masses and trilinear scalar couplings.

In the study of low-energy gauge symmetry breaking, all the parameters in the effective potential must be evolved from the superheavy scale $M_C \equiv M_{GUT} \sim M_P$

down to the electroweak scale $O(m_W)$, according to the corresponding renormalization group equations (RGE). In order to express the corresponding boundary conditions in terms of only one unknown, we will assume here that the dominant seed of supersymmetry breaking in the observable sector (at the compactification scale) is a universal gaugino mass $m_{1/2}$: this choice is motivated by the considerations of section 2.3, but could have more general validity. One-loop radiative corrections will then generate scalar masses and trilinear scalar couplings of comparable magnitude when evaluated at the electroweak scale.

As in conventional supergravity models, for a certain range of superpotential couplings some neutral scalar fields can develop a negative $(mass)^2$ at some renormalization scale $Q \sim M_P e^{-1/Y}$, where $Y = h^2/4\pi$ and h is a typical Yukawa coupling: this will destabilize the origin of the effective potential and produce gauge symmetry breaking with non-vanishing VEVs of order Q. In the discussion of radiative symmetry breaking, therefore, the Yukawa interactions play an important role: in the following we will consider the case in which the dominant ones (influencing the RGE in a way comparable to the gauge couplings) correspond to the following superpotential terms:

$$f = hQ_3 u_3^c H_3 + \lambda H_3 \overline{H}_3 N_3 + k D_3 D_3^c N_3, \tag{3.16}$$

with obvious contractions of group indices.

Some comments on the 'reduced' superpotential (3.16) are in order. First of all, in the model under consideration the only fields which are allowed to develop non-vanishing VEVs are H_a, $\overline{H}_a$ and N_a $(a = 1, 2, 3)$. We can therefore neglect, to simplify the discussion, the superpotential couplings which do not contain any of these fields [λ_ν or (λ_E, λ_L) or (λ_Q, λ_C)], assuming that they are small enough not to perturb the RGE and generate unwanted VEVs. In addition, we assume that the dominant couplings in the matrices λ_{abc} and k_{abc} are the diagonal ones

corresponding to the third generation:

$$\lambda \equiv \lambda_{333} \quad and \quad k \equiv k_{333}. \tag{3.17}$$

This simplifies considerably the RGE analysis and evades some problems with unwanted minima and/or flavour-changing neutral currents. Finally, we assume that among the Yukawa couplings of ordinary quarks and leptons (h_U, h_E and h_D) the only non-negligible one is

$$h \equiv h_{U_{333}}, \tag{3.18}$$

associated to the top quark mass. We will see in the following that this assumption can be justified a posteriori. A more general form of the superpotential (and of the associated scalar potential) will be considered in sections 3.3, 3.4 and 3.5 for the discussion of the particle spectrum.

Given the superpotential (3.16), the low-energy lagrangian at scales $Q < M_C$ will include a soft supersymmetry breaking part of the general form:

$$\begin{aligned} -\mathcal{L}_{soft} &= \frac{1}{2}\Sigma_A M_A(\lambda_A\lambda_A + h.c.) + \Sigma_i \tilde{m}_i^2 |z^i|^2 \\ &+ [(hA_h Q_3 u_3^c H_3 + \lambda A_\lambda \overline{H}_3 H_3 N_3 + kA_k D_3 D_3^c N_3) + h.c.], \end{aligned} \tag{3.19}$$

where the z^i are all the scalar fields, the λ_A are the gaugino fields associated to the different factors of the gauge group ($A = 3, 2, 1, 1'$) and the A parameters have the dimension of a mass.

With the structure of Yukawa couplings introduced above, it will be possible to consider situations in which only $H_3 \equiv H$, $\overline{H}_3 \equiv \overline{H}$ and $N_3 \equiv N$ acquire non-vanishing VEVs, while

$$< 0|H_a|0 >=< 0|\overline{H}_a|0 >=< 0|N_a|0 >= 0 \quad (a = 1, 2). \tag{3.20}$$

Therefore the part of the scalar potential relevant to our analysis will be that containing the Higgs fields H, $\overline{H}$ and N only:

$$V_{Higgs} = \tilde{m}_H^2|H|^2 + \tilde{m}_{\overline{H}}^2|\overline{H}|^2 + \tilde{m}_N^2|N|^2 + (\lambda A_\lambda H\overline{H}N + h.c.)$$

$$+ \quad \lambda^2(|H|^2|N|^2 + |\overline{H}|^2|N|^2 + |H\overline{H}|^2) + \frac{1}{2}g_2^2[H^\dagger(\frac{\vec{\tau}}{2})H + \overline{H}^\dagger(\frac{\vec{\tau}}{2})\overline{H}]^2$$
$$+ \quad \frac{1}{2}\frac{3}{5}g_1^2(\frac{1}{2}|H|^2 - \frac{1}{2}|\overline{H}|^2)^2 + \frac{1}{2}\frac{3}{5}g_{1'}^2(\frac{5}{6}|N|^2 - \frac{2}{3}|H|^2 - \frac{1}{6}|\overline{H}|^2)^2. \quad (3.21)$$

Of course, in restricting ourselves to the simplified potential (3.21), we implicitly assumed that all the scalar fields different from H, $\overline{H}$ and N have vanishing VEVs. To prove such an assumption would require the minimization of the full scalar potential, which is clearly a fool's errand. Nevertheless, previous studies suggest that no other VEVs arise if all the soft masses $\tilde{m}_i^2$ (apart from $\tilde{m}_H^2$, $\tilde{m}_{\overline{H}}^2$ and $\tilde{m}_N^2$) are positive and the following conditions are satisfied:

$$A_h^2 \leq 3(\tilde{m}_{Q_3}^2 + \tilde{m}_{u_3^c}^2 + \tilde{m}_H^2), \quad (3.22)$$

$$A_k^2 \leq 3(\tilde{m}_{D_3}^2 + \tilde{m}_{D_3^c}^2 + \tilde{m}_N^2). \quad (3.23)$$

Given now the potential (3.21), to discuss its minimization it is convenient to set, by definition:

$$< 0|H|0 > \equiv \begin{pmatrix} v^+ \\ v \end{pmatrix}, \quad < 0|\overline{H}|0 > \equiv \begin{pmatrix} \overline{v} \\ v^- \end{pmatrix}, \quad < 0|N|0 > \equiv x. \quad (3.24)$$

In general, one expects all the entries in (3.24) to be non-zero and complex. Making use of gauge invariance, one can make $v^+ = 0$ and v, x real and non-negative. Taking this into account, one can write instead of (3.24):

$$\begin{aligned} V_{Higgs} &= \tilde{m}_H^2 v^2 + \tilde{m}_{\overline{H}}^2 \overline{v}^2 + \tilde{m}_N^2 x^2 + \lambda A_\lambda x v(\overline{v} + \overline{v}^*) \\ &+ \lambda(v^2x^2 + |\overline{v}|^2x^2 + |\overline{v}|^2v^2) + \frac{1}{8}(g_2^2 + \frac{3}{5}g_1^2)(v^2 - |\overline{v}|^2)^2 \\ &+ \frac{1}{120}g_{1'}^2(5x^2 - 4v^2 - |\overline{v}|^2)^2 + [\frac{1}{8}(g_2^2 + \frac{3}{5}g_1^2) + \frac{1}{120}g_{1'}^2]|\overline{v^-}|^4 \\ &+ [\tilde{m}_{\overline{H}}^2 + \lambda^2x^2 + \frac{1}{4}g_2^2(v^2 + |\overline{v}|^2) - \frac{1}{4}\frac{3}{5}g_1^2(v^2 - |\overline{v}|^2) \\ &- \frac{1}{60}g_{1'}^2(5x^2 - 4v^2 - |\overline{v}|^2)]|v^-|^2. \end{aligned} \quad (3.25)$$

One can immediately note that in (3.25) the only term where the phase of $\overline{v}$ is relevant is $\lambda A_\lambda x v(\overline{v} + \overline{v}^*)$, which is clearly minimized for $\overline{v} \in R$: in particular, $\overline{v}$

will have the opposite sign to λA_λ. One can therefore write $V_{Higgs} = V_{neutral} + V_{charged}$, with:

$$\begin{aligned} V_{neutral} &= \tilde{m}_H^2 v^2 + \tilde{m}_{\overline{H}}^2 + \tilde{m}_N^2 x^2 + 2\lambda A_\lambda x v \overline{v} + \lambda^2 (v^2 x^2 + \overline{v}^2 x^2 + v^2 \overline{v}^2) \\ &+ \frac{1}{8}(g_2^2 + \frac{3}{5} g_1^2)(v^2 - \overline{v}^2)^2 + \frac{1}{120} g_{1'}^2 (5x^2 - 4v^2 - \overline{v}^2)^2, \end{aligned} \tag{3.26}$$

$$\begin{aligned} V_{charged} &= [\frac{1}{8}(g_2^2 + \frac{3}{5} g_1^2) + \frac{1}{120} g_{1'}^2] |\overline{v}^-|^4 \\ &+ [\tilde{m}_{\overline{H}}^2 + (\lambda^2 + \frac{1}{12} g_{1'}^2) x^2 + (\frac{1}{4} g_2^2 - \frac{3}{20} g_1^2 + \frac{1}{15} g_{1'}^2) v^2 \\ &+ (\frac{1}{4} g_2^2 + \frac{3}{20} g_1^2 + \frac{1}{60} g_{1'}^2) \overline{v}^2] |\overline{v}^-|^2. \end{aligned} \tag{3.27}$$

Let $(x, v, \overline{v})$ be the global minimum of $V_{neutral}$. Then $(x, v, \overline{v}, \overline{v}^- = 0)$ will be a *local* minimum of V_{Higgs} if and only if

$$\tilde{m}_{\overline{H}}^2 + (\lambda - \frac{1}{12} g_{1'}^2) x^2 + (\frac{1}{4} g_2^2 - \frac{3}{20} g_1^2 + \frac{1}{15} g_{1'}^2) v^2 + (\frac{1}{4} g_2^2 + \frac{3}{20} g_1^2 + \frac{1}{60} g_{1'}^2) \overline{v}^2 > 0. \tag{3.28}$$

In particular, if all the addenda in (3.28) are separately positive, one can be sure that it is also a *global* minimum: in all cases of interest $g_1^2 = g_{1'}^2 < g_2^2$ and $\tilde{m}_{\overline{H}}^2 > 0$, so that the mentioned sufficient condition simply amounts to:

$$\lambda^2 - \frac{1}{12} g_{1'}^2 > 0. \tag{3.29}$$

In the following, therefore, we shall restrict ourselves to the minimization of $V_{neutral}$, checking a posteriori if conditions (3.22),(3.23) and (3.29) are satisfied.

Let us discuss finally the minimization of $V_{neutral}$: one can easily see that if $\lambda \neq 0$ it is automatically bounded from below and the symmetric minimum $x = v = \overline{v} = 0$ becomes unstable when at least one of the masses $\tilde{m}_H^2$, $\tilde{m}_{\overline{H}}^2$, $\tilde{m}_N^2$ becomes negative. The precise determination of the minimum of the potential and of x, v and $\overline{v}$ is too difficult to be done analytically, so that a dedicated computer program has been devoted to it in the present work.

3.2.2 The renormalization group equations

The parameters appearing in the low-energy lagrangian (and in particular in the scalar potential) depend on the energy scale Q according to the renormalization group equations: we have derived them according to well-known techniques, in the supersymmetric one-loop approximation, and they are listed below for the different types of couplings.

Gauge couplings and gaugino masses:

$$\frac{dg_A^2}{dt} = \frac{b_A}{8\pi^2} g_A^4, \tag{3.30}$$

$$\frac{dM_A}{dt} = \frac{b_A g_A^2}{8\pi^2} M_A, \tag{3.31}$$

where $t = \log Q$, $A = 3, 2, 1, 1'$ and $b_3 = 0$, $b_2 = 3$, $b_1 = b_{1'} = 9$.

Yukawa couplings:

$$\frac{dh}{dt} = \frac{h}{8\pi^2}(-\frac{8}{3}g_3^2 - \frac{3}{2}g_2^2 - \frac{13}{30}g_1^2 - \frac{2}{5}g_{1'}^2 + 3h^2 + \frac{1}{2}\lambda^2), \tag{3.32}$$

$$\frac{d\lambda}{dt} = \frac{\lambda}{8\pi^2}(-\frac{3}{2}g_2^2 - \frac{3}{10}g_1^2 - \frac{7}{10}g_{1'}^2 + \frac{3}{2}h^2 + 2\lambda^2 + \frac{3}{2}k^2), \tag{3.33}$$

$$\frac{dk}{dt} = \frac{k}{8\pi^2}(-\frac{8}{3}g_3^2 - \frac{2}{15}g_1^2 - \frac{7}{10}g_{1'}^2 + \lambda^2 + \frac{5}{2}k^2). \tag{3.34}$$

Trilinear scalar couplings:

$$\frac{dA_h}{dt} = \frac{1}{8\pi^2}(\frac{16}{3}M_3 g_3^2 + 3M_2 g_2^2 + \frac{13}{15}M_1 g_1^2 + \frac{4}{5}M_{1'} g_{1'}^2 + 6A_h h^2 + A_\lambda \lambda^2), \tag{3.35}$$

$$\frac{dA_\lambda}{dt} = \frac{1}{8\pi^2}(3M_2 g_2^2 + \frac{3}{5}M_1 g_1^2 + \frac{7}{5}M_{1'} g_{1'}^2 + 3A_h h^2 + 4A_\lambda \lambda^2 + 3A_k k^2), \tag{3.36}$$

$$\frac{dA_k}{dt} = \frac{1}{8\pi^2}(\frac{16}{3}M_3 g_3^2 + \frac{4}{15}M_1 g_1^2 + \frac{7}{5}M_{1'} g_{1'}^2 + 2A_\lambda \lambda^2 + 5A_k k^2). \tag{3.37}$$

Scalar masses:

$$\frac{d\tilde{m}_{Q_a}^2}{dt} = \frac{1}{8\pi^2}(-\frac{16}{3}M_3^2 g_3^2 - 3M_2^2 g_2^2 - \frac{1}{15}M_1^2 g_1^2 - \frac{4}{15}M_{1'}^2 g_{1'}^2 + \delta_{a3} h^2 F_h), \tag{3.38}$$

$$\frac{d\tilde{m}^2_{u^c_a}}{dt} = \frac{1}{8\pi^2}(-\frac{16}{3}M_3^2g_3^2 - \frac{16}{15}M_1^2g_1^2 - \frac{4}{15}M_{1'}^2g_{1'}^2 + \delta_{a3}2h^2F_h), \quad (3.39)$$

$$\frac{d\tilde{m}^2_{d^c_a}}{dt} = \frac{1}{8\pi^2}(-\frac{16}{3}M_3^2g_3^2 - \frac{4}{15}M_1^2g_1^2 - \frac{1}{15}M_{1'}^2g_{1'}^2), \quad (3.40)$$

$$\frac{d\tilde{m}^2_{L_a}}{dt} = \frac{1}{8\pi^2}(-3M_2^2g_2^2 - \frac{3}{5}M_1^2g_1^2 - \frac{1}{15}M_{1'}^2g_{1'}^2), \quad (3.41)$$

$$\frac{d\tilde{m}^2_{e^c_a}}{dt} = \frac{1}{8\pi^2}(-\frac{12}{5}M_1^2g_1^2 - \frac{4}{15}M_{1'}^2g_{1'}^2), \quad (3.42)$$

$$\frac{d\tilde{m}^2_{\nu^c_a}}{dt} = \frac{1}{8\pi^2}(-\frac{5}{3}M_{1'}^2g_{1'}^2), \quad (3.43)$$

$$\frac{d\tilde{m}^2_{H_a}}{dt} = \frac{1}{8\pi^2}(-3M_2^2g_2^2 - \frac{3}{5}M_1^2g_1^2 - \frac{16}{15}M_{1'}^2g_{1'}^2$$
$$+ \delta_{a3}3h^2F_h + \delta_{a3}\lambda^2F_\lambda), \quad (3.44)$$

$$\frac{d\tilde{m}^2_{\overline{H}_a}}{dt} = \frac{1}{8\pi^2}(-3M_2^2g_2^2 - \frac{3}{5}M_1^2g_1^2 - \frac{1}{15}M_{1'}^2g_{1'}^2 + \delta_{a3}\lambda^2F_\lambda), \quad (3.45)$$

$$\frac{d\tilde{m}^2_{N_a}}{dt} = \frac{1}{8\pi^2}(-\frac{5}{3}M_{1'}^2g_{1'}^2 + \delta_{a3}2\lambda^2F_\lambda + \delta_{a3}3k^2F_k), \quad (3.46)$$

$$\frac{d\tilde{m}^2_{D_a}}{dt} = \frac{1}{8\pi^2}(-\frac{16}{3}M_3^2g_3^2 - \frac{4}{15}M_1^2g_1^2 - \frac{16}{15}M_{1'}^2g_{1'}^2 + \delta_{a3}k^2F_k), \quad (3.47)$$

$$\frac{d\tilde{m}^2_{D^c_a}}{dt} = \frac{1}{8\pi^2}(-\frac{16}{3}M_3^2g_3^2 - \frac{4}{15}M_1^2g_1^2 - \frac{1}{15}M_{1'}^2g_{1'}^2 + \delta_{a3}k^2F_k). \quad (3.48)$$

The functions F_h, F_λ and F_k are defined by:

$$F_k \equiv \tilde{m}^2_{Q_3} + \tilde{m}^2_{u^c_3} + \tilde{m}^2_H + A_h^2, \quad (3.49)$$

$$F_\lambda \equiv \tilde{m}^2_H + \tilde{m}^2_{\overline{H}} + \tilde{m}^2_N + A_\lambda^2, \quad (3.50)$$

$$F_k \equiv \tilde{m}^2_{D_3} + \tilde{m}^2_{D^c_3} + \tilde{m}^2_N + A_k^2. \quad (3.51)$$

Note that, as long as they do not involve the Yukawa couplings h, λ and k, which have been assumed to be the only non-negligible ones, the RGE for scalar masses assume the simple form:

$$\frac{d\tilde{m}_i^2}{dt} = -\frac{1}{8\pi^2}\Sigma_A c_A(i)M_A^2g_A^2, \quad (3.52)$$

where i is an index running over all the scalar fields and the coefficients $c_A(i)$ can be read off from eqs. (3.38) to (3.51).

To solve the RGE, one must also specify the boundary conditions at the unifi-

cation scale $Q = M_{GUT}$. According to what stated before, we shall assume:

$$g_3(M_{GUT}) = g_2(M_{GUT}) = g_1(M_{GUT}) = g_{1'}(M_{GUT}) = g_{GUT}, \tag{3.53}$$

$$M_3(M_{GUT}) = M_2(M_{GUT}) = M_1(M_{GUT}) = M_{1'}(M_{GUT}) = m_{1/2}, \tag{3.54}$$

$$h(M_{GUT}) = h_{GUT}, \quad \lambda(M_{GUT}) = \lambda_{GUT}, \quad k(M_{GUT}) = k_{GUT}, \tag{3.55}$$

$$\tilde{m}_i^2(M_{GUT}) = 0, \qquad A_h(M_{GUT}) = A_\lambda(M_{GUT}) = A_k(M_{GUT}) = 0. \tag{3.56}$$

In words, we have, as required by the superstring, unification of the properly normalized gauge coupling constants at $Q = M_{GUT}$. The values of the Yukawa couplings h, λ and k at the unification scale M_{GUT} are, together with the universal gaugino mass $m_{1/2}$, the free parameters of our model. All the soft supersymmetry breaking parameters in the scalar sector are assumed to be vanishing at $Q = M_{GUT}$: trilinear couplings and non-vanishing physical values of the masses will however be generated as effects of radiative corrections.

Given the boundary conditions (3.53) to (3.56), we have all the tools to solve the corresponding RGE. For example, the equations for the gauge couplings and the gaugino masses are trivially solved to give:

$$g_A^2(Q) = \frac{g_{GUT}^2}{1 + \frac{b_A}{8\pi^2} g_{GUT}^2 \log(M_{GUT}/Q)}, \tag{3.57}$$

$$M_A(Q) = \frac{g_A^2(Q)}{g_{GUT}^2} m_{1/2}. \tag{3.58}$$

Note that, with our boundary conditions and particle content, the gauge coupling constants and the gaugino masses associated to the two $U(1)$ factors evolve in exactly the same way. This leads to considerable simplifications in the RGE for the Yukawa couplings and the other SUSY-breaking parameters, which have however been written in the general case.

A first simple exercise is the computation of the grand unification scale M_{GUT} and of the weak mixing angle $\sin^2\theta_W(m_W)$. Assuming the validity of the supersymmetric one-loop approximation for the gauge couplings in the whole energy range

$m_W \leq Q \leq M_{GUT}$, and taking as physical inputs $\alpha_3(m_W) = 0.11$, $\alpha(m_W) = 1/128$, one finds:

$$M_{GUT} \simeq 4.4 \times 10^{17}\ GeV, \tag{3.59}$$

$$\sin^2\theta_W(m_W) \simeq 0.21. \tag{3.60}$$

Note also that, within the above approximation, the $SU(3)$ β-function vanishes, so that $\alpha_{GUT} = \alpha_3(m_W)$. Taking into account the possible correction to our approximation (higher-loop and threshold effects), the above results are satisfactory: M_{GUT} is not far from M_P and $\sin^2\theta_W$ is reasonably close to its experimental value.

Passing now to the RGE involving the Yukawa couplings and the trilinear scalar couplings, we note that they constitute a system of coupled nonlinear ordinary differential equations, whose exact analytic solutions is not possible: we shall therefore adopt in the following numerical methods. The same holds true for the RGE for scalar masses which involve the couplings h, λ and k; for the other scalar masses, however, the analytic solution can be easily found:

$$\begin{aligned}
\hat{m}_i^2(Q) \;=\; \frac{\tilde{m}_i^2(Q)}{m_{1/2}^2} \;=\; & \{c_3(i)\frac{g_{GUT}^2}{8\pi^2}\log(M_{GUT}/Q) \\
& + \frac{1}{6}c_2(i)[1 - \frac{1}{[1+3(g_{GUT}^2/8\pi^2)\log(M_{GUT}/Q)]^2}] \\
& + \frac{1}{18}c_1(i)[1 - \frac{1}{[1+9(g_{GUT}^2/8\pi^2)\log(M_{GUT}/Q)]^2}] \\
& + \frac{1}{18}c_{1'}(i)[1 - \frac{1}{[1+9(g_{GUT}^2/8\pi^2)\log(M_{GUT}/Q)]^2}]\},
\end{aligned} \tag{3.61}$$

where the coefficients $c_A(i)$ have been defined in (3.52).

3.2.3 Numerical results

Now that we have displayed all the necessary tools to analyse low-energy gauge symmetry breaking, it is clear how to proceed. Given a set of Yukawa couplings (h_{GUT}, λ_{GUT}, k_{GUT}) at the scale M_{GUT}, one must evolve the relevant parameters, solving the corresponding RGE, down to the symmetry breaking scale $\overline{Q}$. Here one should minimize the effective potential (for a given value of $m_{1/2}$), determining v, $\overline{v}$

and x. What fixes the scale $\overline{Q}$ at we should stop the RGE clock? As seen in section 2.3, in the absence of flat directions the complete one-loop effective potential can be approximated by the renormalization group improved tree level potential only at a scale $\overline{Q}$ of the same order of the field VEVs, where the finite logarithms in the one-loop corrections are small. Since the mass scale in the tree level potential is set by the gaugino mass $m_{1/2}$, it is natural to expect (and can be checked a posteriori) that the vacuum expectation values x, v and $\overline{v}$ scatter around the value of $m_{1/2}$: therefore in the following we will make the identification

$$\overline{Q} \equiv m_{1/2}. \tag{3.62}$$

Both the solution of the RGE and the minimization of the Higgs potential can be performed factorizing out the gaugino mass $m_{1/2}$, whose only role is that of fixing the scale of gauge and SUSY breaking. For this reason, it is convenient to express all dimensional quantities in units of $m_{1/2}$, denoting them by a hat ($\hat{}$): e.g., the VEVs of the neutral scalar fields, in units of $m_{1/2}$, will be denoted by $\hat{v}$, $\hat{\overline{v}}$ and $\hat{x}$.

What are the constraints to be satisfied by a given solution, characterized by a set $(m_{1/2}, \hat{v}, \hat{\overline{v}}, \hat{x})$ and corresponding to some boundary conditions ($m_{1/2}$, h_{GUT}, λ_{GUT}, k_{GUT}), to be considered acceptable? First of all, one needs $m_{1/2} \leq O(1)TeV$, in order for low-energy supersymmetry to solve the hierarchy problem. Second, one has to impose that all the VEVs $(v, \overline{v}, x)$ be different from zero, to obtain a satisfactory mass spectrum for quarks, leptons and gauge bosons. In particular, the experimental value of the electroweak breaking scale must be reproduced, and this corresponds to the constraint:

$$m_W = g_2(m_W)\sqrt{\frac{v^2 + \overline{v}^2}{2}} \simeq 82GeV, \tag{3.63}$$

while the top quark mass (at the scale m_W) is given by

$$m_{top}(m_W) = h(m_W)v. \tag{3.64}$$

Other phenomenological constraints will be considered soon.

The crucial parameters in the study of the scalar potential are the soft masses $\tilde{m}_H^2$, $\tilde{m}_{\overline{H}}^2$ and $\tilde{m}_N^2$, for the symmetric minimum $v = \overline{v} = x = 0$ becomes unstable whenever at least one of them acquires a negative value. The typical Q-dependence of these masses is illustrated in fig. 3.1: (a) shows the evolution of $\hat{m}_H^2 \equiv \tilde{m}_H^2/m_{1/2}^2$ for $h_{GUT} = 0.025$, 0.035 and 0.045 (when $\lambda_{GUT} = 0.1$ and $k_{GUT} = 0.05$); (b) shows the evolution of $\hat{m}_{\overline{H}}^2 \equiv \tilde{m}_{\overline{H}}^2/m_{1/2}^2$ for $\lambda_{GUT} = 0$, 0.1 and 0.3 (when $h_{GUT} = 0.035$ and $k_{GUT} = 0.05$); (c) shows the evolution of $\hat{m}_N^2 \equiv \tilde{m}_N^2/m_{1/2}^2$ for $k_{GUT} = 0$, 0.05 and 0.1 (when $h_{GUT} = 0.035$ and $\lambda_{GUT} = 0.1$). As can be easily understood by looking at the corresponding RGE, the behaviour of $\tilde{m}_H^2$ is mainly determined by the top Yukawa coupling h, $\tilde{m}_{\overline{H}}^2$ has only a very slight dependence on λ, and the evolution of $\tilde{m}_N^2$ depends heavily on k and to a lesser extent on λ. In particular, for reasonably small values of h_{GUT}, λ_{GUT} and k_{GUT} the only masses that can be driven to negative values in the TeV region are $\tilde{m}_H^2$ and $\tilde{m}_N^2$.

The appearance of symmetry breaking in the TeV region as the renormalization scale goes down is illustrated in fig. 3.2. The requirement that v, $\overline{v}$ and x must be all non-zero at the scale $\overline{Q} \equiv m_{1/2} = O(1)TeV$ already selects a limited region of parameter space: for h_{GUT} or k_{GUT} too small, or λ_{GUT} too large, v and $\overline{v}$ cannot become nonzero around the electroweak scale. In the opposite case x and $\overline{v}$ vanish. Restricting ourselves to values of (h_{GUT}, λ_{GUT}, k_{GUT}) which give $v, \overline{v}, x \neq 0$, two qualitatively different scenarios emerge, as can be seen from fig. 3.2, corresponding to which soft mass becomes negative first. For larger values of h_{GUT} and/or very small values of k_{GUT} and λ_{GUT}, one has the situation represented in fig. 3.2a (corresponding to $h_{GUT} = 0.035$, $\lambda_{GUT} = 0.17$ and $k_{GUT} = 0$): at scales $Q >> m_W$ both $\tilde{m}_H^2$ and $\tilde{m}_N^2$ are positive, so that $v = \overline{v} = x = 0$. At a certain scale Q', $\tilde{m}_H^2$ becomes negative and at the minimum it is now $v \neq 0$. At a lower scale Q'', also $\overline{v}$ and x become non-zero simultaneously, due to the presence of the trilinear term $\lambda A_\lambda v \overline{v} x$ in the potential. The above possibility presents the general feature

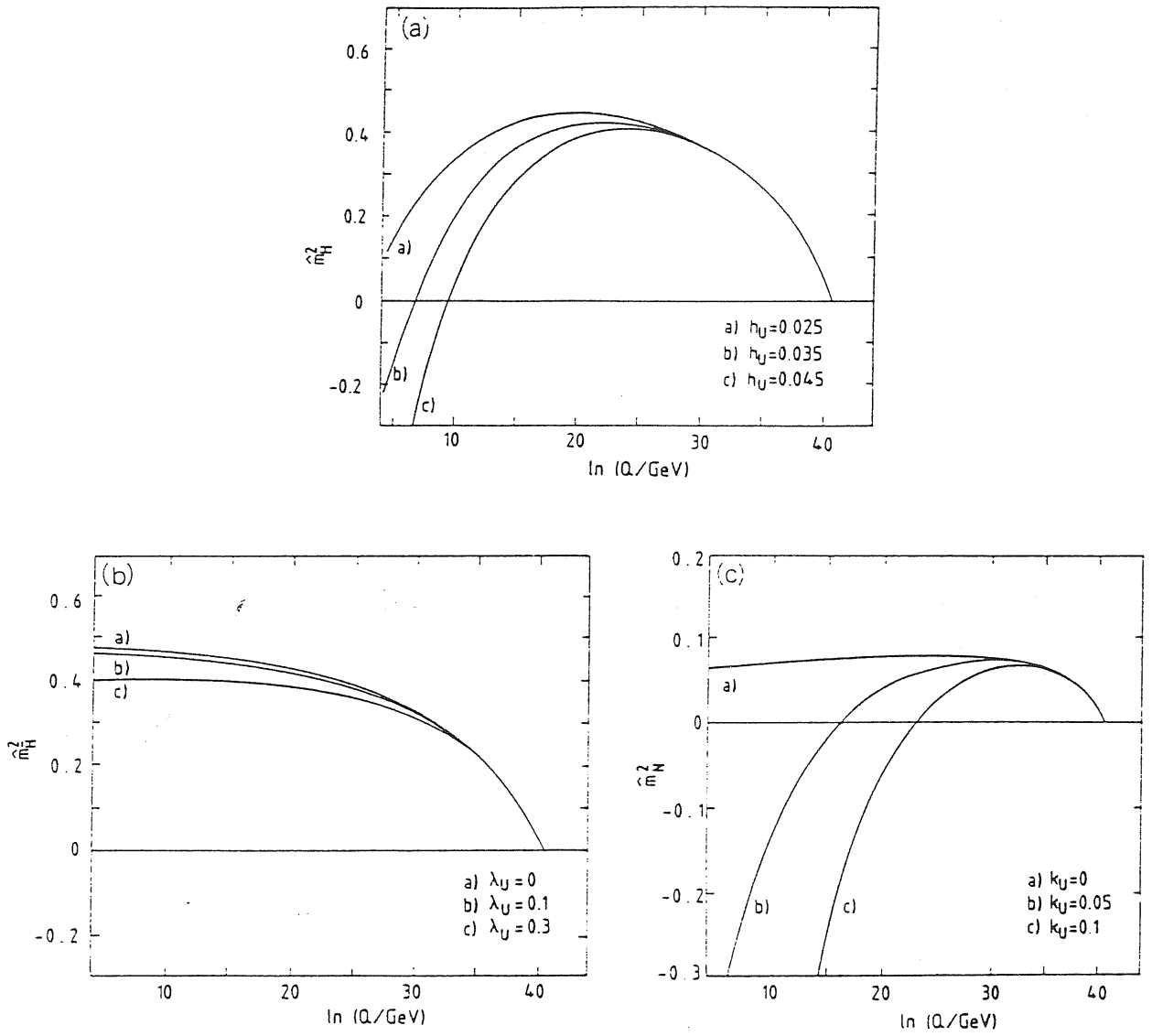

Figure 3.1: Typical Q-dependence of the soft scalar masses $\hat{m}_H^2$, $\hat{m}_{\overline{H}}^2$ and $\hat{m}_N^2$.

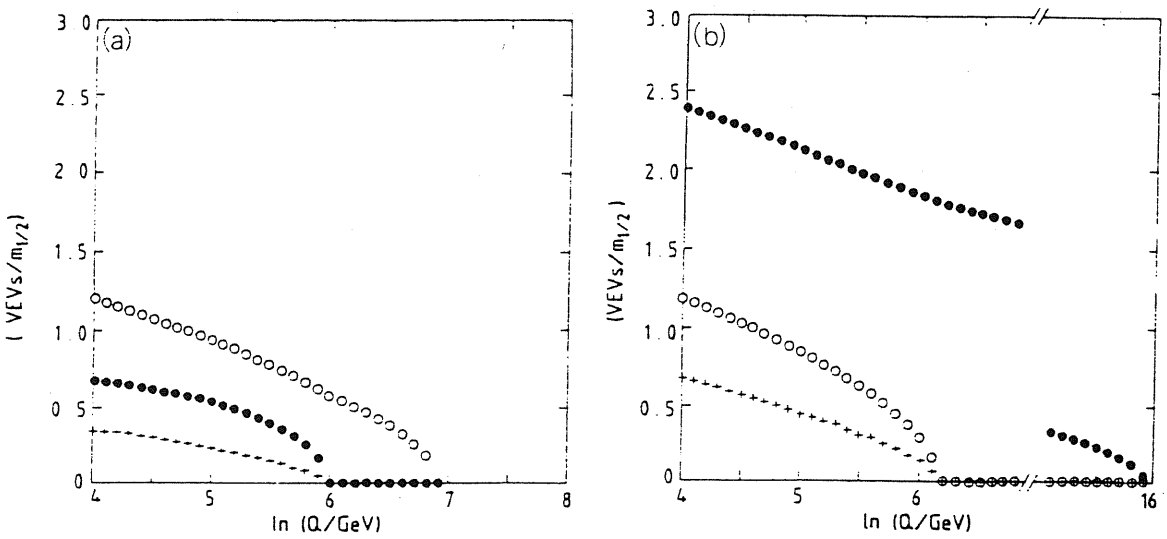

Figure 3.2: Dependence of the VEVs v, $\bar{v}$ and x on the renormalization scale Q.

that $v > x$, and is therefore incompatible with neutral current phenomenology, as will be discussed in subsection 3.3.1. Much more intriguing is the opposite situation, which occurs for non-negligible k_{GUT} - which is also necessary to give phenomenologically acceptable masses to the D-particles - and/or relatively big values of λ_{GUT} and/or relatively small values of h_{GUT}, corresponding to values of the top mass around $40GeV$. In this case, illustrated in fig. 3.2b (corresponding to $h_{GUT} = 0.025$, $\lambda_{GUT} = 0.1$ and $k_{GUT} = 0.05$), it is $\tilde{m}_N^2$ that becomes negative first, and this allows solutions with $x > v$, in accordance with phenomenological requirements. In particular, when we calculate renormalization effects fore values of h_{GUT} corresponding to $m_{top} \sim 40GeV$ and even relatively small values of k_{GUT} (e.g. $k_{GUT} \sim 0.05$), we find that one can naturally obtain at low energy situations in which $\tilde{m}_N^2 < 0$ and $\tilde{m}_H^2, \tilde{m}_{\bar{H}}^2 > 0$, with all these $(mass)^2$ being of order $m_{1/2}^2$. Conspiring with the other terms in the potential, this pattern is able to produce, without fine-tuning, ratios x/v of order of several units, which are enough to satisfy all the phenomenological constraints of subsection 3.3.1. Note also that, due to the presence of the top Yukawa coupling h, in general one has $\tilde{m}_H^2 < \tilde{m}_{\bar{H}}^2$: a consequence of this fact is that one always ends up with $v > \bar{v}$: typical values

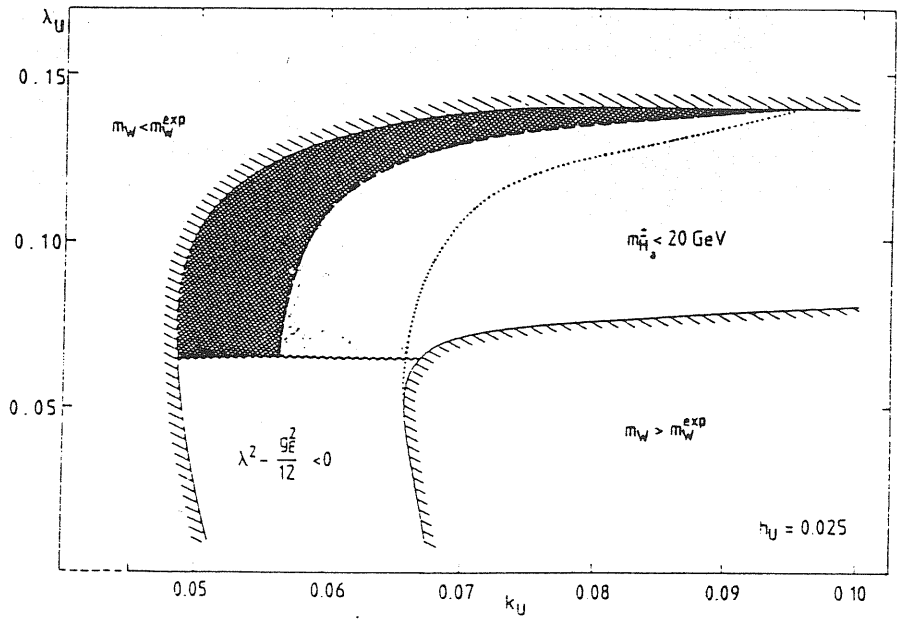

Figure 3.3: Allowed region in the (k_{GUT}, λ_{GUT}) plane for $h_{GUT} = 0.025$, corresponding to $m_{top} \sim 40\, GeV$.

of the parameter $\overline{v}/v$ range from 0.4 to 0.6. Our neglect of the b-quark Yukawa coupling with respect to the t-quark one is therefore justified a posteriori.

To proceed further in the analysis, it is convenient to reduce the number of free parameters, by fixing the top Yukawa coupling h_{GUT}: as an illustrative example we take $h_{GUT} \sim 0.025$, which roughly corresponds to the representative value $m_{top} \sim 40 GeV$. At the end of this subsection, however, we shall also consider the possibility of higher top masses. For fixed h_{GUT}, the residual parameter space can be graphically represented in the (k_{GUT}, λ_{GUT})-plane, as done in fig. 3.3: we shall see in the following how different phenomenological constraints lead us to discard most of these points, leaving however a finite region (the shaded area of fig. 3.3) corresponding to solutions fully consistent with phenomenology.

A very stringent constraint is given by the correct fitting of the electroweak breaking scale. Requiring formula (3.63) to reproduce the experimental value of the W-mass, together with the condition $v, \overline{v}, x \neq 0$ and a gaugino mass in the range $50 GeV - 3 TeV$, is enough to forbid a considerable region of the $(k_{GUT},$

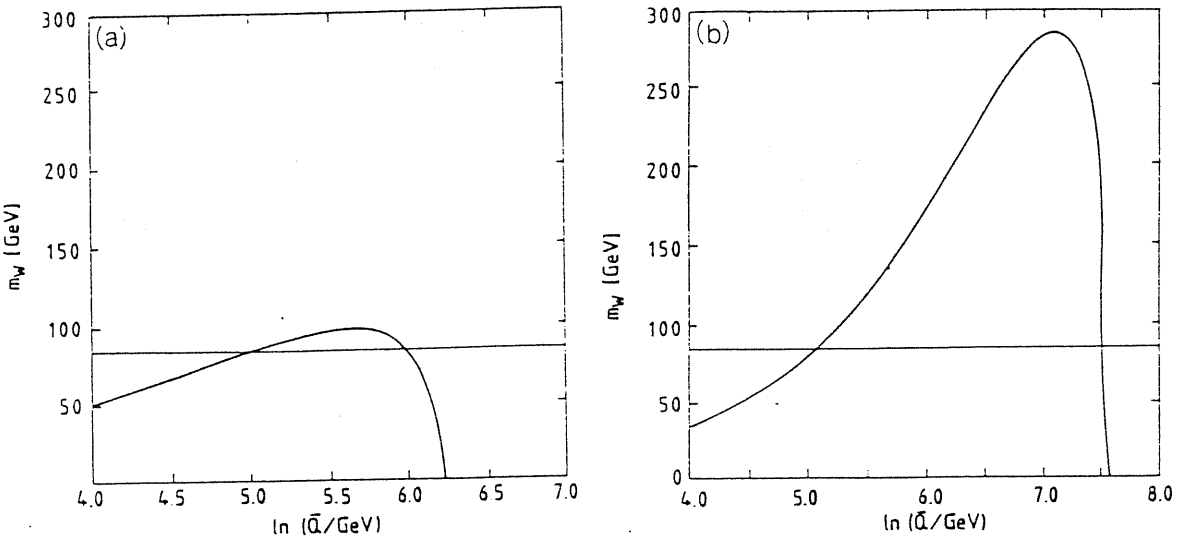

Figure 3.4: Relation between the symmetry breaking scale $\overline{Q} \equiv m_{1/2}$ and the corresponding value of m_W. Case (a) corresponds to $h_{GUT} = 0.025$, $\lambda_{GUT} = 0.07$ and $k_{GUT} = 0.05$; case (b) to $h_{GUT} = 0.025$, $\lambda_{GUT} = 0.12$ and $k_{GUT} = 0.07$.

λ_{GUT}) plane, the one outside the solid lines in fig. 3.3: too high values of λ_{GUT} and/or too small values of k_{GUT} give $v = \overline{v} = 0$ or $m_W < m_W^{exp} \simeq 82GeV$; values of λ_{GUT} and/or k_{GUT} in the opposite direction give $m_W > m_W^{exp}$. The role played by the m_W-fit in determining the value of $\overline{Q} \equiv m_{1/2}$ can be understood by looking at fig. 3.4.

Another important constraint is given by the requirement of an acceptable mass spectrum for the many exotic particles which are present in the model, combined with the consistency of our minimization procedure for the scalar potential:

1. From e^+e^- collider data we know that all charged particles which have not been seen up to now must weigh more than $O(20)GeV$ [53]. Moreover, from the CERN $p\bar{p}$ collider limits on monojets we can infer that $m_{\tilde{q}}, m_{\tilde{g}} \geq O(50)GeV$ [54]. This limit will be considered in more detail in section 3.3.

2. All the $(mass)^2$ of the physical neutral scalar particles must be positive.

3. Conditions (3.28) and (3.29) must be satisfied, for the consistency of our minimization procedure.

4. Conditions (3.22) and (3.23) must be also be satisfied, to avoid charge and colour breaking minima.

5. The lightest supersymmetric particle must be neutral and weakly interacting, to satisfy stringent astrophysical bounds [55] .

The region of the (k_{GUT}, λ_{GUT}) plane that satisfies all the above constraints corresponds to the shaded area in fig. 3.3. Note that a big region (on the right of the dotted line) could give, as an effect of negative D-term contributions, negative or too small squared-masses for the 'unhiggses' $H_a^{\pm}$ $(a = 1, 2)$: the exact location of the dotted line depends on the Yukawa couplings of the unhiggses, which have been neglected here; a more detailed discussion of this constraint can be found in section 3.4. The region of fig. 3.3 under the wavy line might also be excluded, because there the sufficient condition (3.29) for the consistency of our minimization procedure is not satisfied. To decide if these points are acceptable or not, a more detailed study of the scalar potential is needed, which goes beyond the scope of the present work.

Let us now comment on the general features of the solutions corresponding to points of the surviving region. The two parameters of greatest phenomenological interest are the ratio x/v and the gaugino mass $m_{1/2}$: the first (combined with $\overline{v}/v$) determines all the neutral current phenomenology, beginning with the masses of the neutral gauge bosons. The second gives the scale of the spectrum of all the supersymmetric particles. Depending on the values of λ_{GUT} and k_{GUT}, one can obtain values of x/v from ~ 2 to ~ 20 and values of $m_{1/2}$ from $\sim 100\, GeV$ to our upper limit of $3TeV$. The values of x/v and of $m_{1/2}$ are not unrelated, for the following reason. Because the allowed range of variation of k_{GUT} is rather restricted, the magnitude of $\hat{x}$ is essentially fixed. On the other hand, the magnitude of $\hat{v}$ and the value of $m_{1/2}$ must combine in such a way to give the right value of the W-mass. Therefore high values of x/v correspond in general to high

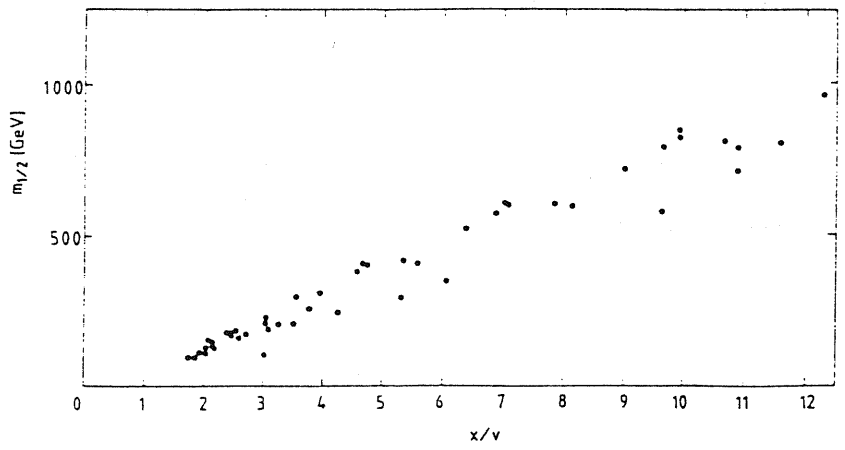

Figure 3.5: Theoretical 'scatter plot' showing the correlation between x/v and $m_{1/2}$ for some representative cases corresponding to $h_{GUT} = 0.025$ ($m_{top} \sim 40$ GeV).

gaugino masses, and viceversa. The points of the $(x/v, m_{1/2})$ plane corresponding to some allowed points in the (k_{GUT}, λ_{GUT}) plane are presented in fig. 3.5. The corresponding points in the $(x/v, \overline{v}/v)$ plane are shown in fig. 3.6. The region of very high x/v and $m_{1/2}$ poses some problems of naturalness: if $m_{1/2} >> m_W$, radiative corrections to the scalar potential are large compared to m_W, and the corresponding minimum with $x >> v, \overline{v}$, which is related to approximate cancellations of certain terms, becomes less stable. A related effect is that the dependence of m_W on $\overline{Q} \equiv m_{1/2}$ is very strong, as in the r.h.s. of fig. 3.4b, requiring a sort of fine-tuning of parameters to obtain the correct m_W. This is no longer true, however, for smaller values of x/v and $m_{1/2}$, as shown in fig. 3.4a and in the l.h.s. of fig. 3.4b.

This requirement of 'naturalness' is difficult to quantify exactly, and largely a matter of taste; as an empirical rule, we asked that small variations in the input parameters λ_{GUT}, k_{GUT} do not produce too large variations in the ratio x/v (related, as explained before to the ratio $m_{1/2}/m_W$):

$$\left| \frac{\partial[\log(x/v)]}{\partial[\log k_{GUT}, \lambda_{GUT}]} \right| \leq 10. \tag{3.65}$$

If the constraint (3.65) is to be satisfied, one can obtain values of x/v up to ~ 10,

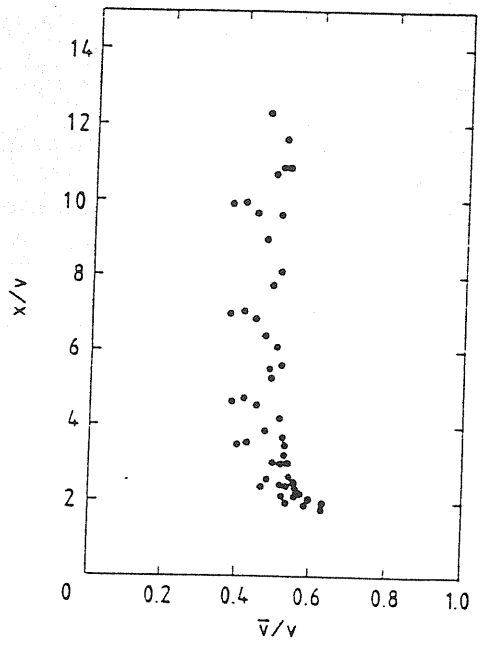

Figure 3.6: Theoretical 'scatter plot' showing the points of the $(\bar{v}/v, x/v)$plane corresponding to some representative cases for $h_{GUT} = 0.025$ ($m_{top} \sim 40\,GeV$).

corresponding to gaugino masses $m_{1/2}$ up to $\sim 500GeV$. In the remainder of this chapter we shall consider only this more natural class of solutions, corresponding to the darker region of the shaded area in fig. 3.3. The general features of the resulting particle spectrum will be discussed in sections 3.3, 3.4 and 3.5.

Let us comment finally, for the sake of completeness, on the possibility of a top quark mass significantly heavier than 40 GeV. A different value of h_{GUT} will correspond, in general, to a different allowed region in the (λ_{GUT}, k_{GUT}) plane. A general result is that, as long as the top Yukawa coupling increases, $\tilde{m}_H^2$ tends to acquire lower and lower values around the electroweak scale, making less and less natural the desired hierarchy $x > v$: the phenomenological success of the model considered in this work tends therefore to ask for a relatively light top mass. Increasing h_{GUT} has the effect of shrinking the region of the (λ_{GUT}, k_{GUT}) plane compatible with the naturalness constraint (3.65): this region disappears for values of h_{GUT} around 0.045, corresponding to a top quark mass $\sim 70GeV$. Higher values of the top quark mass can be permitted if one relaxes the condition (3.65).

In view of the considerations of the following sections, the main results of our numerical investigations have been summarized in table 3.1, which gives the preferred values of some relevant model parameters at the electroweak breaking scale $\overline{Q} \equiv m_{1/2}$. A few remarks on the origin of the different limits are in order. The range of variation of $\overline{v}/v$ is just the result of an extensive numerical search in the parameter space and is strictly related to the allowed range of variation for the top quark Yukawa coupling: higher values of the top quark mass generically lead to smaller values of $\overline{v}/v$, and viceversa. The lower limit on x/v is enforced by the constraints on the $Z - Z'$ mass matrix, to be discussed in detail in subsection 3.3.1 and, in a more general context, in chapter 4. The lower limit on $m_{1/2}$ comes from the requirement of a positive $(mass)^2$ for the left-handed sneutrinos, to be discussed in subsection 3.3.2; it can be slightly improved by enforcing the constraints on the unhiggs masses, to be discussed in section 3.4, but this kind of limit is much more model-dependent than the previous one. The upper limits on x/v and $m_{1/2}$ are more subjective, being related to the naturalness constraint, and must be taken with a grain of salt. We have already commented on the strong correlation between $m_{1/2}$ and x/v, and further comments will be given in section 3.4. The limits on the other parameters are obtained just taking the allowed region in the (h_{GUT}, λ_{GUT}, k_{GUT}, $m_{1/2}$) parameter space and solving the RGE to obtain the corresponding values at the electroweak breaking scale. Even in this case there are correlations, which can be easily guessed looking at the form of the RGE and which will be taken into account in the analysis of sections 3.4 and 3.5.

3.3 The particle spectrum

In the rest of this chapter we examine in detail the interesting zoo of still unobserved particles that are predicted to exist, with masses within the TeV region, by the model under consideration. After writing down the relevant mass matrices, we discuss the model predictions deriving from our analysis of supersymmetry and

$$
\begin{array}{ccccc}
0.2 & \leq & \frac{\bar{v}}{v} & \leq & 0.6 \\
2.8 & \leq & \frac{\bar{u}}{v} & \leq & 10 \\
100GeV & \leq & m_{1/2} & \leq & 500GeV \\
0.15 & \leq & \lambda & \leq & 0.35 \\
-0.65 & \leq & \hat{A}_\lambda & \leq & -0.35 \\
0.25 & \leq & k & \leq & 0.55 \\
3.00 & \leq & \hat{m}^2_{D_3} & \leq & 3.35 \\
2.95 & \leq & \hat{m}^2_{D^c_3} & \leq & 3.30 \\
-3.5 & \leq & \hat{A}_k & \leq & -3.0
\end{array}
$$

Table 3.1: Typical values of the model parameters at the electroweak symmetry-breaking scale.

gauge symmetry breaking, as well as constraints on the model parameters coming from the existing experimental data. Furthermore, working in a less model-dependent framework, we try to point out the possible signals that should be looked for at present and future colliders, when they differ significantly from the ones of the standard supersymmetric model.

3.3.1 The extra Z' boson

One of the cleanest features of the minimal model is the existence of a second Z' boson, associated to the $U(1)_{Y'}$ factor of the gauge group: this possibility is discussed in great detail and in a general context in chapter 4. We collect here some more model-dependent considerations that follow from the previous numerical results on gauge symmetry breaking and from some cosmological arguments.

The mass matrix for the massive neutral gauge bosons (Z, Z') in the minimal model is given by:

$$
\mathcal{M}^2_{Z,Z'} = m_Z^2 \begin{pmatrix} 1 & \sin\theta_W \frac{4v^2-\bar{v}^2}{3(v^2+\bar{v}^2)} \\ \sin\theta_W \frac{4v^2-\bar{v}^2}{3(v^2+\bar{v}^2)} & \sin^2\theta_W \frac{25x^2+16v^2+\bar{v}^2}{9(v^2+\bar{v}^2)} \end{pmatrix} \equiv m_Z^2 \begin{pmatrix} 1 & a \\ a & b \end{pmatrix}, \quad (3.66)
$$

where $m_Z^2 = \frac{(g_2^2+\frac{3}{5}g_1^2)}{2}(v^2+\bar{v}^2) = \frac{m_W^2}{\cos^2\theta_W}$ is the unmixed Z mass, corresponding to the standard model prediction. The eigenvalues of the matrix (3.66) are given by

$$m_{Z_{1,2}}^2 = \frac{1}{2}[(1+b) \mp \sqrt{(1-b)^2+4a^2}]m_Z^2 \tag{3.67}$$

and the corresponding eigenstates by

$$\begin{aligned} Z_1 &= Z\cos\theta + Z'\sin\theta, \\ Z_2 &= -Z\sin\theta + Z'\cos\theta, \end{aligned} \tag{3.68}$$

where

$$\tan 2\theta = \frac{2a}{1-b}. \tag{3.69}$$

For a given value of m_W (or $\sin^2\theta_W$), the mass matrix (3.66) depends only on the two parameters x/v and $v/\bar{v}$: contours corresponding to different values of the mass of the heaviest eigenstate Z_2 are displayed in fig. 3.7. An important fact to note is that, for the preferred range of parameters given in table 3.1, the off-diagonal term in (3.66) is never negligible, and it has the effect of lowering the mass m_{Z_1} of the lightest mass eigenstate Z_1 with respect to the unmixed value m_Z. This introduces a stronger constraint than the ones considered in chapter 4 (where we do not make any model-dependent assumption on the relative magnitude of the different VEVs). Two different definitions of the weak angle,

$$\sin^2\theta_W \equiv \frac{g_1^2}{g_2^2+\frac{5}{3}g_1^2} \quad and \quad \sin^2\overline{\theta_W} \equiv 1 - \frac{m_W^2}{m_{Z_1}^2}, \tag{3.70}$$

which are equivalent in the standard model limit, correspond now to different quantities, and the relation

$$\Delta \equiv \sin^2\theta_W - \sin^2\overline{\theta_W} < 0 \tag{3.71}$$

must be fulfilled. Contours of Δ in the relevant part of the $(x/v, \bar{v}/v)$ plane are also plotted in fig. 3.7. Recent UA1 and UA2 data on the W and Z_1 masses, combined with the relation

$$m_W = \frac{38.65GeV}{\sin\theta_W}, \tag{3.72}$$

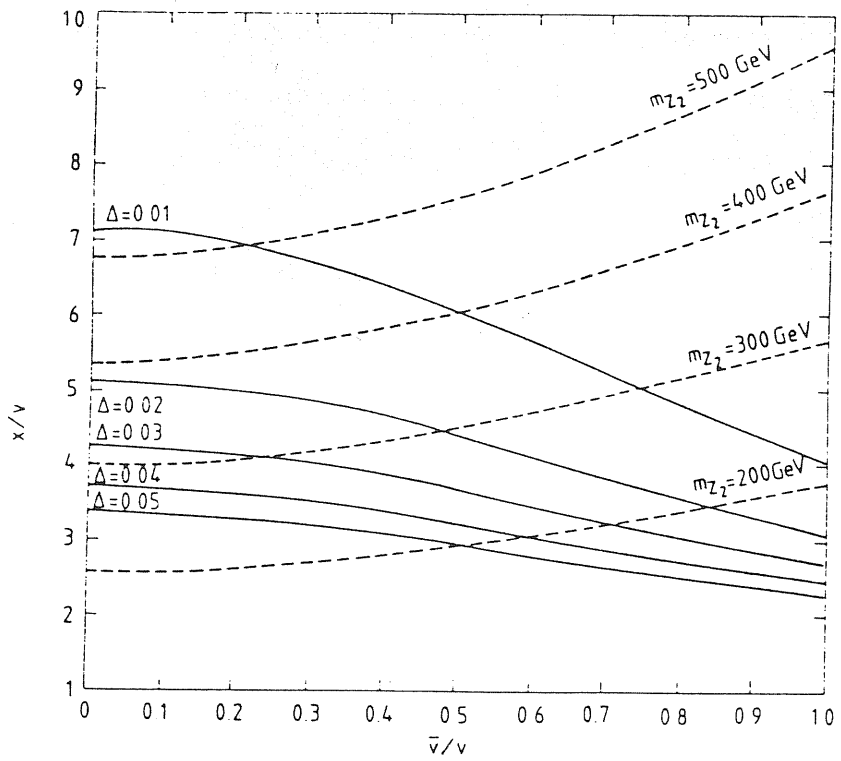

Figure 3.7: Contours of $\Delta \equiv \sin^2\theta_W - \sin^2\overline{\theta_W}$ (solid lines) and m_{Z_2} (dashed lines) in the $(x/v, \overline{v}/v)$ plane, calculated for the input values $m_W = 82GeV$ and $\sin^2\theta_W \doteq 0.224$.

which includes standard model radiative corrections, yield $\sin^2\theta_W = 0.224 \pm 0.011$ and $\sin^2\overline{\theta_W} = 0.212 \pm 0.022$, corresponding to

$$\Delta = 0.012 \pm 0.023. \tag{3.73}$$

Taking the representative bound $\Delta < 0.05$ and fixing the values of m_W and of $\sin^2\theta_W$ to their preferred values $\sin^2\theta_W = 0.224$ and $m_W = 82GeV$, we infer from fig. 3.7 that, for $0.2 \leq \overline{v}/v \leq 0.6$ as suggested by our numerical searches, it must be

$$x/v > 2.8, \qquad m_{Z_2} > 185GeV. \tag{3.74}$$

Cosmology has the potential to provide a more stringent constraint on the model parameters. As discussed in subsection 3.1.3, the right handed neutrino ν^c is essentially massless, and could therefore affect primordial nucleosynthesis. The

presence of a total of 6 left- and right-handed neutrinos seems to conflict with the conventionally quoted upper bound $N_\nu < 4$ on the total number of equivalent left-handed neutrinos [56]. However, even if one accepts this bound, it can be reconciled with the presence of 3 right-handed neutrinos because their cosmological density will be suppressed if $m_{Z_2} >> m_Z$ and the ν^c decouple early. Requiring that the ν^c decouple at a temperature $T_d > 300MeV$ before hadron annihilation, one finds [57]:

$$m_{Z_2} \geq 400GeV \quad for \quad \overline{v}/v = 0.4. \tag{3.75}$$

However, there are claims in the literature [58] that the nucleosynthesis constraint can be relaxed to $N_\nu < 5.5$ or even 6, in which case the cosmological lower bound (3.75) becomes much weaker or even disappears. Due to the many uncertainties that still affect nucleosynthesis calculations, we regard the bound (3.75) as less firm than the bounds from particle physics experiments, and we neglect it in the following considerations.

3.3.2 Squarks, sleptons and gluinos

We turn now to the discussion of the sparticle masses, starting with those which have a counterpart in the supersymmetric standard model.

Since the one-loop coefficient of the $SU(3)_C$ β-function vanishes in our model, from the RGE (3.31) we deduce that the gluino mass $m_{\tilde{g}}$ is just equal to the primordial gaugino mass $m_{1/2}$:

$$m_{\tilde{g}} = m_{1/2}. \tag{3.76}$$

The other gauginos, associated to $SU(2)_L \times U(1)_Y \times U(1)_{Y'}$, mix with the higgsinos in the neutralino and chargino mass matrices, to be discussed in the following section. The entry in the neutralino mass matrix corresponding to the photino is associated to a mass

$$m_{\tilde{\gamma}} \sim \frac{1}{7} m_{1/2}. \tag{3.77}$$

In general, however, the lightest eigenstate $\tilde{\chi}$ in the neutralino mass matrix is a mixture of photino, other gauginos and higgsinos, with a mass

$$m_{\tilde{\chi}} \sim (\frac{1}{5} \ to \ \frac{1}{7}) m_{1/2}. \tag{3.78}$$

Usually this state corresponds to the lightest supersymmetric particle (apart from a very small region of parameter space where the lightest supersymmetric particle is a left-handed sneutrino) and has mainly gaugino components.

Passing now to spin-0 particles, when their Yukawa couplings are negligible (which is the case for the partners of all ordinary quarks and leptons, apart from the top) their masses are the sum of a soft contribution (depending only on $m_{1/2}$) and a D-term contribution (depending only on x/v and $\overline{v}/v$):

$$m_i^2 = \tilde{m}_i^2(m_{1/2}) + m_i^{D^2}(\frac{x}{v}, \frac{\overline{v}}{v}). \tag{3.79}$$

In the case of the top squarks one has a mass matrix of the form

$$\begin{array}{ccc} & \tilde{u}_L^* & \tilde{u}_R^* \\ \tilde{u}_L & m_{LL}^2 & m_{LR}^2 \\ \tilde{u}_R & m_{LR}^2 & m_{RR}^2 \end{array} \tag{3.80}$$

with

$$\begin{aligned} m_{LL}^2 &= \tilde{m}_{Q_3}^2 + h^2 v^2 + m_Q^{D^2} \\ m_{LR}^2 &= \tilde{m}_{u_3^c}^2 + h^2 v^2 + m_{u^c}^{D^2} \\ m_{LR}^2 &= h A_h v + h \lambda x \overline{v}. \end{aligned} \tag{3.81}$$

The off-diagonal term increases the splitting of the degeneracy between the two mass eigenstates. For the allowed range of parameters, however, the masses of the top squarks are of the same order of those of the other squarks, and therefore relatively heavy. The only coloured scalars which can be light enough to be of present experimental interest are the spin-0 D-particles, to which section 3.5 is entirely devoted.

The soft contributions $\tilde{m}_i^2(m_{1/2})$ can be easily calculated using eq. (3.62). One finds for example that:

$$m_{\tilde{q}} : m_{\tilde{l}} : m_{\tilde{e^c}} : m_{\tilde{g}} = 2 : 0.7 : 0.4 : 1. \tag{3.82}$$

However, one must not forget the D-term contributions, which are important for the lightest states, and whose general expression is:

$$\begin{aligned} m_i^{D^2}(\frac{x}{v},\frac{\overline{v}}{v}) &= \frac{1}{2}g_2^2 T_{3L}^i(v^2-\overline{v}^2) \\ &+ \frac{1}{2}\frac{3}{5}g_1^2 Y^i(v^2-\overline{v}^2) \\ &+ \frac{1}{2}\frac{3}{5}g_{1'}^2 Y'^i(\frac{5}{3}x^2-\frac{4}{3}v^2-\frac{1}{3}\overline{v}^2) \\ &= m_W^2\{-T_{3L}^i[\frac{1-(\overline{v}/v)^2}{1+(\overline{v}/v)^2}] \\ &+ Y^i\tan^2\theta_W[\frac{1-(\overline{v}/v)^2}{1+(\overline{v}/v)^2}] \\ &+ Y'^i\tan^2\theta_W[\frac{5(x/v)^2-4-(\overline{v}/v)^2}{3(1+(\overline{v}/v)^2)}]\}, \end{aligned} \tag{3.83}$$

where the numerical values of T_{3L}^i, Y^i and Y'^i can be read off from eqs. (3.3) and (3.4). One can then try to put bounds on the SUSY breaking parameter $m_{1/2}$ using the negative results of the low-energy SUSY-search experiments. Since one finds $x/v > 1 > \overline{v}/v$, it is clear from eq. (3.83) that the D-terms are most negative if $T_{3L}^i > 0$, $Y^i < 0$, $Y'^i < 0$, and the quantum numbers in eqs. (3.3) and (3.4) therefore indicate that the $\tilde{\nu}$, $\overline{H}^0$ and H^+ have the largest negative contributions to their mass squared. One does not expect large supersymmetric masses for the $\tilde{\nu}$, while for the $\overline{H}^0$ and H^+ this possibility cannot be excluded. One must require $m_{\tilde{\nu}}^2 > 0$ in the physical vacuum, and this is shown in fig. 3.8 as a constraint in the $(x/v, m_{1/2})$ plane for the two typical values $\overline{v}/v = 0.2$ and $\overline{v}/v = 0.6$. The vertical line in figure 3.8 corresponds to the bound $\Delta < 0.05$ discussed in the previous subsection. The discussion of the limits coming from the $\overline{H}^0$ and H^+ masses is more complicated. In addition to the Higgs doublets $H, \overline{H}$ whose neutral components develop non-zero VEVs, our model contains also the unhiggses $H_a, \overline{H}_a$

$(a = 1, 2)$ with the same quantum numbers but no VEVs. To give to the fermionic partners of their charged components, $\tilde{H}_a^+$ and $\tilde{\overline{H}}_a^-$, masses greater than $20GeV$, there must be in the superpotential couplings of the form $\lambda_{ab3} H_a \overline{H}_b N$, which were assumed in section 3.2 to be small compared to $\lambda H \overline{H} N$. In general, therefore, the unhiggs mass matrices will contain additional contributions proportional to these other Yukawa couplings: if these contributions can be neglected (which need not be the case, since the validity of our approximation depends on the unknown value of the λ_{ab3}), then we are left with eq. (3.81), and in this case $m_{H_a^+} > 20GeV$ would give the more stringent constraint on $m_{1/2}$ shown in fig. 3.8 as a dashed line. Because of the lower bound on x/v corresponding to the vertical line, we can derive an absolute lower bound on $m_{1/2}$:

$$m_{1/2} \geq 140\ (210)\ GeV \quad for \quad \overline{v}/v = 0.2, \tag{3.84}$$

$$m_{1/2} \geq 100\ (150)\ GeV \quad for \quad \overline{v}/v = 0.6, \tag{3.85}$$

if we use $m_{\tilde{\nu}}^2 > 0$ $(m_{H_a^+} > 20GeV)$. We reemphasize that the $m_{H_a^+}$ constraint is more model-dependent because of the unknown Yukawa couplings λ_{ab3}: this pint is discussed further in the next section.

These constraints (3.84),(3.85) are much more severe than those arising from unsuccessful sparticle searches. The $p\overline{p}$ collider bound on $m_{\tilde{g}}$ just translates, via eq. (3.76), into

$$m_{1/2} \geq 45GeV \tag{3.86}$$

which is also shown in fig. 3.8. The $p\overline{p}$ collider bound $m_{\tilde{q}} \geq 50GeV$ is even less interesting, since eq. (3.82) tells us that $m_{\tilde{q}} \geq 2m_{\tilde{g}}$ before the inclusion of the D-terms, which do not change the situation drastically. In the relevant range of x/v and $m_{1/2}$, $m_{\tilde{e}_L} < m_{\tilde{e}_R}$ and the e^+e^- constraint $m_{\tilde{e}_L} < 22GeV$ is also shown in fig. 3.8. The UA1 bound [59] on $(m_{\tilde{e}_L}, m_{\tilde{\nu}})$ from the absence of $W \to \tilde{e}\tilde{\nu}$ decay is not interesting in our model, because eqs. (3.81) and (3.83) tell us

$$m_{\tilde{e}_L}^2 = m_{\tilde{\nu}}^2 + m_W^2 [\frac{1 - (\overline{v}/v)^2}{1 + (\overline{v}/v)^2}], \tag{3.87}$$

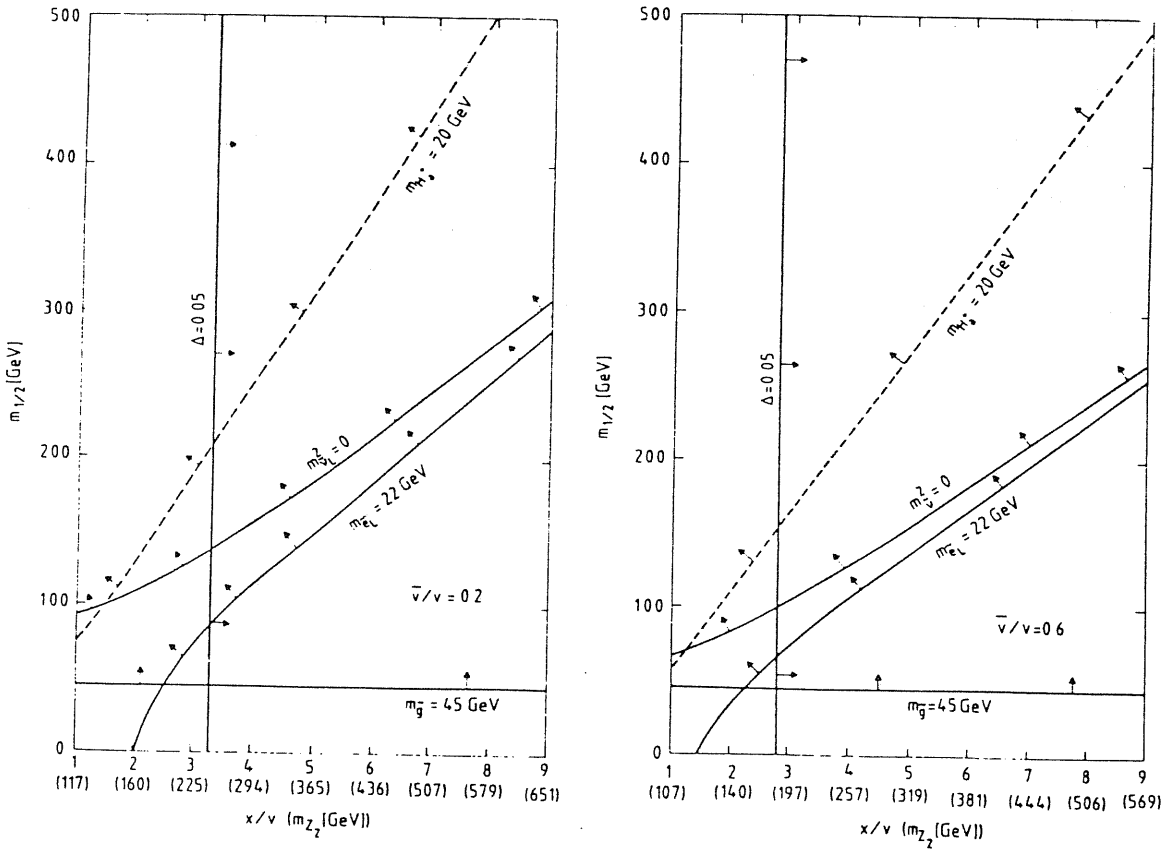

Figure 3.8: Bounds in the $(x/v, m_{1/2})$ plane coming from various phenomenological constraints for (a) $\bar{v}/v = 0.2$ and $\bar{v}/v = 0.6$. On the horizontal axis the values of m_{Z_2} (in GeV) associated to the different values of x/v are also shown.

so that $m^2_{\tilde{\nu}} > 0$ provides a lower bound on $m_{\tilde{e}_L}$ which is greater than the UA1 lower bound of $33GeV$ if $\bar{v}/v < 0.85$, as expected in our model. The ASP bound [60] on $(m_{\tilde{e}}, m_{\tilde{\chi}})$ is also uninteresting, since the constraint (3.84),(3.85) due to $m^2_{\tilde{\nu}} > 0$ and the relation (3.78) tell us

$$m_{\tilde{\chi}} \geq 15GeV, \tag{3.88}$$

whereas the ASP experiment is only sensitive to $m_{\tilde{\chi}} \leq 13GeV$.

Summarizing, if one leaves aside the constraints coming from the unhiggs masses, the tightest constraint actually comes from the theoretical requirement that $m^2_{\tilde{\nu}} > 0$, which corresponds in turn to the following lower bounds on sparticle

masses:

$$m_{\tilde{g}} \geq 100GeV, \;\; m_{\tilde{\chi}} \geq 15GeV, \;\; m_{\tilde{e}_L} \geq 55GeV, \;\; m_{\tilde{e}_R} \geq 90GeV, \;\; m_{\tilde{q}} \geq 180GeV. \tag{3.89}$$

The model therefore predicts a rather heavy spectrum of squarks, sleptons and gluinos, although the naturalness criterion forbids pushing the sparticle masses beyond the TeV range.

3.4 Gauginos and Higgs particles

According to the postulated structure of the superpotential, in the minimal model under consideration baryon and lepton number are exactly conserved by the renormalizable interactions among the light fields, so that we can consistently assign $B = L = 0$ to the chiral supermultiplets H_a, $\overline{H}_a$ and N_a $(a = 1, 2, 3)$. As an effect of gauge symmetry breaking, the fermionic members of these superfields can mix with the gauginos of $SU(2)_L \times U(1)_Y \times U(1)_{Y'}$, while four Goldstone bosons are 'eaten' to give masses to the W, Z and Z'. We examine here in detail [48] this sector of the particle spectrum, which contains additional states with respect to the corresponding sector of the supersymmetric standard model[1]. We investigate the structure of the mass matrices for charged fermions, neutral fermions, charged scalars and neutral scalars, commenting on their eigenvalues, their eigenstates and the corresponding couplings. We explore the constraints on the model parameters imposed by the experimental non-observation of charginos and charged Higgs bosons, as well as by the numerical calculations of section 3.2. We find that the mass of the lightest charged fermion depends on unknown Yukawa couplings, and could be anywhere above the present experimental limit of $\sim 20\, GeV$. The lightest neutral fermion is expected to be stable, apart from a tiny region of parameter space which gives a left-handed sneutrino as the lightest supersymmetric particle.

[1] For related work, see ref. [61].

The lightest charged scalar could well be lighter than the $W^{\pm}$, in contrast with the minimal supersymmetric standard model. We identify one neutral scalar which generally weighs between 45 and 105 GeV, and there could be other neutral spin-zero particles as light as 70 GeV. For the latter particles, which could be light enough to be produced at LEP, production mechanisms are also discussed.

3.4.1 General framework

We introduce here a slightly more general framework than that of the previous sections, in order to perform the following analysis in a less model-dependent way.

In the minimal model, the chargino mass matrix is 4×4 [for $(\tilde{W}^-, \overline{\tilde{H}}^-_{1,2,3})$ $\times$ $(\tilde{W}^+, \tilde{H}^+_{1,2,3})$], the neutralino mass matrix is 12×12 [for $(\tilde{W}_3,\ \tilde{B},\ \tilde{B}',\ \tilde{H}^o_{1,2,3},$ $\overline{\tilde{H}}^0_{1,2,3},\ \tilde{N}_{1,2,3})^2$], the charged scalar mass matrix is 6×6 [for $(H^+_{1,2,3}, (\overline{H^-})^*_{1,2,3})$ $\times$ $((H^+)^*_{1,2,3}, \overline{H}^-_{1,2,3})$], and the neutral scalar mass matrix is 18×18 [for $(ReH^0_{1,2,3},$ $ImH^0_{1,2,3},\ Re\overline{H}^0_{1,2,3},\ Im\overline{H}^0_{1,2,3},\ ReN^0_{1,2,3},\ ImN^0_{1,2,3})^2$]. Short cuts are evidently necessary if we are to extract useful information from these large matrices. We exploit two such short cuts.

The most useful is to note that we can always choose to work in a basis for the matter superfields in which only one of the neutral superfields with each set of quantum numbers has a non-zero VEV [2] for its scalar component. These we denote by

$$< 0|H^0_3|0 > \equiv v, \quad < 0|\overline{H}^0_3|0 > \equiv \overline{v}, \quad < 0|N|0 > \equiv x, \tag{3.90}$$

so that

$$< 0|H^0_{1,2}|0 > = < 0|\overline{H}^0_{1,2}|0 > = < 0|N_{1,2}|0 > = 0. \tag{3.91}$$

In this basis, consideration of the effective scalar potential shows that it is techni-

[2] We assume that the physical vacuum does not violate charge or colour conservation. The numerical results of section 3.2 show that, at least for a specific range of parameters, this is consistent with our theoretical framework. A more detailed investigation in a generalized context might provide interesting constraints on the parameters of the model, but is beyond the scope of this work.

cally "natural" for the Yukawa coupling constants λ_{ijk} of the H_i, $\overline{H}_j$ and N_k superfields to take a particularly simple form. Including soft supersymmetry breaking trilinear interactions of the spin-zero components of the H_i, $\overline{H}_j$ and N_k superfields,

$$V_{soft} = A_{\lambda_{ijk}} \lambda_{ijk} H_i \overline{H}_i N_k + h.c. + \ldots, \tag{3.92}$$

and the soft supersymmetry breaking squared mass matrix m_{ij}^2 for the N_i scalar fields, the condition that the potential be extremized when $< 0|N_{i=1,2}|0 >= 0$ is

$$\frac{\partial V}{\partial x_i} = 2m_{3i}^2 x + 2\lambda_{33i} A_{\lambda_{33i}} v\overline{v} + 2\lambda_{33i}(v^2 + \overline{v}^2)\lambda_{333} x = 0. \tag{3.93}$$

This is obeyed if $\lambda_{jki}\lambda_{jk3} = 0$ when $i = 1, 2$ and analogously for the $D_i D_j^c N_k$ couplings. The leading order renormalization group equations for small λ_{ijk}, etc. then guarantee $m_{3i}^2 = 0$ and the second and third terms in (3.93) vanish as $\lambda_{33i} = 0$ if $\lambda_{333} \neq 0$. Similar considerations for $< 0|H_{1,2}, \overline{H}_{1,2}|0 >$ suggest that it is natural that in the basis (3.90),(3.91):

$$\lambda_{i33} = \lambda_{3i3} = \lambda_{33k} = 0, \quad for\ i, j, k = 1, 2, \tag{3.94}$$

whilst

$$\lambda_{ij3}, \lambda_{i3k}, \lambda_{3jk}, \lambda_{ijk} \neq 0 \tag{3.95}$$

in general. Assuming (3.94) greatly simplifies our mixing analysis: the 4×4 chargino matrix becomes $(2 \times 2) + (1 \times 1) + (1 \times 1)$, the 12×12 neutralino matrix becomes $(6 \times 6) + (6 \times 6)$, the 6×6 charged scalar matrix becomes $(2 \times 2) + (2 \times 2) + (2 \times 2)$, and the 18×18 neutral scalar matrix becomes $(6 \times 6) + (12 \times 12)$. Note also that one of the 2×2 submatrices of the charged scalar matrix has a massless unphysical Goldstone boson eigenstate, whereas the 6×6 neutral scalar submatrix includes two such Goldstone bosons.

As a second short cut, we can assume that the Yukawa couplings of the matrix λ_{ijk} are all relatively real, so that CP violation in this sector is negligible and the VEVs $v, \overline{v}$ and x are also real. Then the (12×12) neutral scalar submatrix further

breaks up to become $(6 \times 6) + (6 \times 6)$, whilst the forms of the other matrices are not changed qualitatively. We are now in a position to discuss the different mass matrices.

In doing so, we shall work in the framework in which the only seed of soft supersymmetry breaking in the observable sector at the compactification scale is a universal gaugino mass $m_{1/2}$, as assumed in section 3.2. Moreover, it is not restrictive to work with areal and positive λ_{333}, so that, since the renormalization group equations drive $A_{\lambda_{333}} < 0$, also the VEVs $v, \overline{v}$ and x will be all real and positive. When making numerical estimates, we shall restrict the ranges of variation of our parameters according to table 3.1.

3.4.2 Charginos

We start with the chargino mass term, which in the basis introduced above becomes

$$\mathcal{L}_c = -(\tilde{W}^- \; \tilde{\overline{H}}_3^- \; \tilde{\overline{H}}_1^- \; \tilde{\overline{H}}_2^-) \begin{pmatrix} M_2 & -g_2 v & 0 & 0 \\ -g_2 \overline{v} & -\lambda_{333} x & 0 & 0 \\ 0 & & -\lambda_{113} x & 0 \\ 0 & 0 & 0 & -\lambda_{223} x \end{pmatrix} \begin{pmatrix} \tilde{W}^+ \\ \tilde{H}_3^+ \\ \tilde{H}_1^+ \\ \tilde{H}_2^+ \end{pmatrix} + h.c.. \tag{3.96}$$

Two eigenvalues associated with (3.96) are trivial, namely

$$m_{1,2}^{\pm} = |\lambda_{113,223}| x = |\lambda_{113,223}| \left(\frac{x}{v}\right) \sqrt{\frac{\sqrt{2}}{4 G_F [1 + (\overline{v}/v)^2]}}. \tag{3.97}$$

The condition $m_{1,2}^{\pm} \geq 20 GeV$ from PEP and PETRA corresponds to a region of the $(|\lambda_{113,223}|, x/v)$ plane which depends only slightly on $\overline{v}/v$ in the dynamically preferred range $0.2 \leq \overline{v}/v \leq 0.6$, as seen in figure 3.9. The input values $m_W = 82\, GeV$, $\sin^2 \theta_W = 0.222$, $\alpha_{em}(m_W) = 1/128$ and $\alpha_3(m_W) = 0.11$ are used in calculating this and the following figures. These lower bounds on $|\lambda_{113,223}|$ are much smaller than typical values of λ_{333} found in the dynamical calculations of section 3.2. The eigenvalues of the non-trivial (2×2) submatrix in (3.96) are given

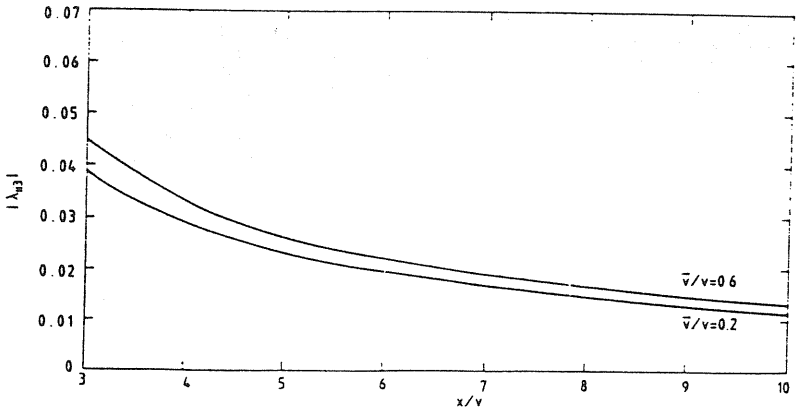

Figure 3.9: Contours in the $(|\lambda_{113,223}|, x/v)$ plane corresponding to the constraint $m^{\pm}_{1,2} \geq 20GeV$, for the cases $\bar{v}/v = 0.2$ and $\bar{v}/v = 0.6$.

by

$$m^{\pm}_{3,4} = \frac{1}{2}((m^2_{LL} + m^2_{RR}) \pm \sqrt{(m^2_{LL} - m^2_{RR})^2 + 4m^2_{LR}}), \tag{3.98}$$

where

$$m^2_{LL} = M_2^2 + (g_2\bar{v})^2, \qquad m^2_{RR} = (\lambda_{333}x)^2 + (g_2v)^2, \tag{3.99}$$

$$m^2_{LR} = -M_2(g_2v) + (\lambda_{333}x)(g_2\bar{v}), \qquad M_2 = \frac{\alpha_{em}m_{1/2}}{\alpha_3 \sin^2\theta_W}. \tag{3.100}$$

We have studied (3.98)-(3.100), varying λ_{333}, $m_{1/2}$, x/v and $\bar{v}/v$ over the dynamically preferred ranges shown in table 3.1 and taking into account the correlation between $m_{1/2}$ and x/v. The lowest values of $m^{\pm}_3$ that we found are shown in fig. 3.10. We see that an absolute lower bound is

$$m^{\pm}_3 \geq 43\, GeV, \tag{3.101}$$

that there could be as many as three charginos lighter than $m_Z/2$, and that two of them could have masses close to the present e^+e^- experimental lower limit.

3.4.3 Neutralinos

We now turn to the *neutralino* mass matrix. As in the case of the charginos (3.96), the $(\tilde{W}_3, \tilde{B}, \tilde{B}', \tilde{H}^0_3, \bar{\tilde{H}}^0_3, \tilde{N}_3)$ sector decouples from the $(\tilde{H}^0_2, \bar{\tilde{H}}^0_2, \tilde{N}_2, \tilde{H}^0_1, \bar{\tilde{H}}^0_1, \tilde{N}_1)$ sector.

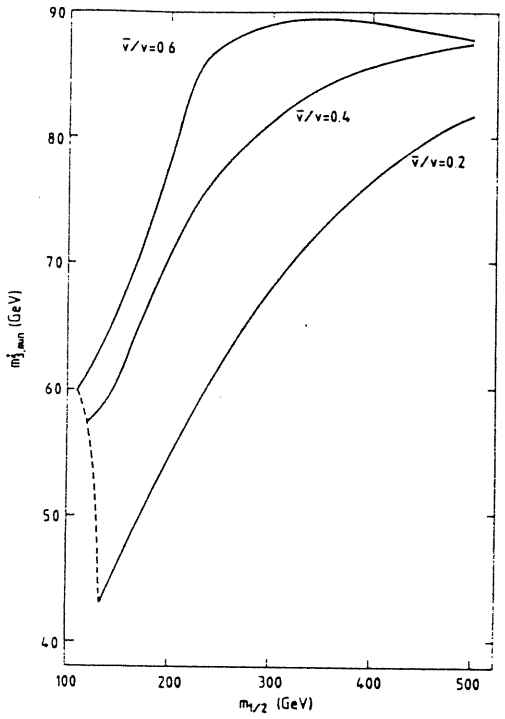

Figure 3.10: The lightest attainable value of the chargino mass $m_3^{\pm}$ as a function of $m_{1/2}$, for some discrete values of $\bar{v}/v$, with x/v and λ_{333} both free to vary inside the ranges given in table 3.1.

The sector containing the neutral gauginos has the rather complicated mass matrix

$$\begin{pmatrix} M_2 & 0 & 0 & -\sqrt{\frac{1}{2}}g_2 v & \sqrt{\frac{1}{2}}g_2\overline{v} & 0 \\ 0 & M_1 & 0 & \sqrt{\frac{3}{10}}g_1 v & -\sqrt{\frac{3}{10}}g_1\overline{v} & 0 \\ 0 & 0 & M_{1'} & -\sqrt{\frac{8}{15}}g_{1'}v & -\sqrt{\frac{1}{30}}g_{1'}\overline{v} & \sqrt{\frac{5}{6}}g_{1'}x \\ & & & 0 & \lambda_{333}x & \lambda_{333}\overline{v} \\ SYMMETRIC & & & \lambda_{333}x & 0 & \lambda_{333}v \\ & & & \lambda_{333}\overline{v} & \lambda_{333}v & 0 \end{pmatrix} \tag{3.102}$$

Using the region of parameter space allowed by our previous numerical searches, we find that the lightest neutralino $\tilde{\chi}$ in this sector most likely has large gaugino components, and a mass obeying eqs. (3.78) and (3.88). Indeed, if the lightest neutralino were predominantly a higgsino, its annihilation rate in the early universe would have been so small that its present relic density would be unacceptably high.

The second neutralino sector has the mass matrix

$$\begin{pmatrix} 0 & \lambda_{223}x & \lambda_{232}\overline{v} & 0 & 0 & \lambda_{231}\overline{v} \\ & 0 & \lambda_{322}v & 0 & 0 & \lambda_{321}v \\ & & 0 & \lambda_{132}\overline{v} & \lambda_{312}v & 0 \\ & & & 0 & \lambda_{113}x & \lambda_{131}\overline{v} \\ SYMMETRIC & & & & 0 & \lambda_{311}v \\ & & & & & 0 \end{pmatrix} \tag{3.103}$$

In order to understand its eigenvalues, a convenient limit of (3.103) to study is when $x/v \to \infty$ with $\overline{v}/v$ fixed. In this case there are $2+2$ heavy Majorana neutralinos with masses $\sim |\lambda_{113,223}|x$ which almost make two neutral Dirac fermions, as well as two light Majorana particles with masses

$$m_{\tilde{\chi}_L} \sim \frac{(\lambda_{i3j}, \lambda_{3ij})^2}{|\lambda_{ii3}, \lambda_{jj3}|}\frac{v^2}{x}, \quad (i,j = 1,2). \tag{3.104}$$

As already mentioned, consistency with cosmology requires $m_{\tilde{\chi}_L} > m_{\tilde{\chi}}$. This is not difficult to arrange, given all the uncertainties in the couplings λ_{ijk}. We do not explore in detail the bounds on the λ_{i3j}, λ_{3ij} and λ_{ij3} that come from requiring $m_{\tilde{\chi}} < m_{\tilde{\chi}_L}$ (3.104), as they would be complicated and difficult to interpret. As an example, if we take $\lambda_{i3j} \sim \lambda_{3ij} \sim 0.15$, $\lambda_{ii3} \sim 0.05$ and $x/v = 3, \overline{v}/v = 0.5$, the estimate (3.104) yields $m_{\tilde{\chi}_L} \sim 23GeV$, which is comfortably above the comparable minimum value of $m_{\tilde{\chi}}$.

3.4.4 Charged scalars

Next we examine the charged Higgs mass matrix, which breaks up into three independent 2×2 submatrices, as already noted. The 2×2 submatrix $\mathcal{M}_3^2$ mixing the 'true' charged Higgses $H_3^{\pm}$ whose neutral partners have VEVs is

$$\mathcal{L}_{\pm} = -\left(\begin{array}{cc} H_3^{+*} & \overline{H}_3^{-} \end{array} \right) \mathcal{M}_3^2 \left(\begin{array}{c} H_3^{+} \\ \overline{H}_3^{-*} \end{array} \right), \tag{3.105}$$

where we use the minimization condition on the potential to eliminate the soft supersymmetry-breaking mass terms in favour of the model parameters λ_{333}, $A_{\lambda_{333}}$:

$$\mathcal{M}_3^2 = \left(\begin{array}{cc} -\lambda_{333}A_{\lambda_{333}}\frac{x\overline{v}}{v} + (\frac{1}{2}g_2^2 - \lambda_{333}^2)\overline{v}^2 & -\lambda_{333}A_{\lambda_{333}}x + (\frac{1}{2}g_2^2 - \lambda_{333}^2)v\overline{v} \\ -\lambda_{333}A_{\lambda_{333}}x + (\frac{1}{2}g_2^2 - \lambda_{333}^2)v\overline{v} & -\lambda_{333}A_{\lambda_{333}}\frac{xv}{\overline{v}} + (\frac{1}{2}g_2^2 - \lambda_{333}^2)v^2 \end{array} \right). \tag{3.106}$$

Solving the eigenvalue problem, one finds a zero mass Goldstone boson which is eaten by the $W^{\pm}$, and a physical field of mass $m_{H^{\pm}}$:

$$m_{H^{\pm}}^2 = m_W^2 + \left[-\lambda_{333}A_{\lambda_{333}}x\left(\frac{\overline{v}}{v} + \frac{v}{\overline{v}}\right) - \lambda_{333}^2(v^2 + \overline{v}^2) \right]. \tag{3.107}$$

Using the dynamically preferred values of table 3.1 we find that the square bracket in (3.107) is always positive, and indeed

$$[\ldots]_{(3.107)} \geq 1700\, GeV^2, \tag{3.108}$$

implying

$$m_{H^{\pm}} \geq 90\, GeV \tag{3.109}$$

for $m_W = 82GeV$. It is more difficult to analyse the eigenvalues of the charged unHiggs mass matrices $\mathcal{M}_{1,2}^2$, i.e. those whose neutral partners do not have VEVs. They take the forms

$$\mathcal{M}_i^2 = \left(\begin{array}{cc} \tilde{m}_{H_i}^2 + m_{H^+}^{D^2} + \lambda_{ii3}^2x^2 & -\lambda_{ii3}\lambda_{333}v\overline{v} - \lambda_{ii3}A_{\lambda_{ii3}}x \\ -\lambda_{ii3}\lambda_{333}v\overline{v} - \lambda_{ii3}A_{\lambda_{ii3}}x & \tilde{m}_{\overline{H}_i}^2 + m_{\overline{H}^-}^{D^2} + \lambda_{ii3}^2x^2 \end{array} \right), \quad (i = 1, 2), \tag{3.110}$$

where $\tilde{m}_{H_i,\overline{H}_i}^2$ are the soft supersymmetry breaking masses that are calculable using the renormalization group equations, and the D-term contributions are

$$m_{H^+}^{D^2} = -\frac{1}{4}(g_2^2 - \frac{3}{5}g_1^2)(v^2 - \overline{v}^2) - \frac{1}{15}g_{1'}^2(5x^2 - 4v^2 - \overline{v}^2), \tag{3.111}$$

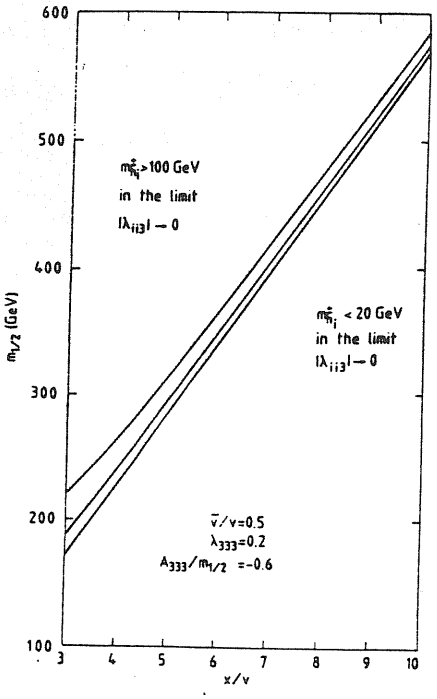

Figure 3.11: Dependence of the lighter charged unhiggs mass $m^{\pm}_{h_i}$ on $m_{1/2}$ and x/v, for the representative values $\overline{v}/v = 0.5$, $\lambda_{333} = 0.2$ and $A^{\lambda}_{333}/m_{1/2} = -0.6$. Lines corresponding to $m^{\pm}_{h_i} = 20, 60$ and $100\ GeV$ in the limit $|\lambda_{ii3}| \to 0$ are shown.

$$m^2_{\overline{H}^-} = \frac{1}{4}(g_2^2 - \frac{3}{5}g_1^2)(v^2 - \overline{v}^2) - \frac{1}{60}g_{1'}^2(5x^2 - 4v^2 - \overline{v}^2). \tag{3.112}$$

Since the D-terms (3.121),(3.122) are negative for $x > v > \overline{v}$ as expected, it is possible for charged unhiggses to be relatively light, even close to the e^+e^- experimental lower limit of about $20GeV$. A full analysis of this possibility is complicated by the large number of unknown parameters in $\mathcal{M}^2_i$: $m_{1/2}$, $\frac{x}{v}$, $\frac{\overline{v}}{v}$, λ_{ii3}, λ_{333}, $A_{\lambda_{ii3}}$. We use the parameter values in table 3.1, which are valid if $|\lambda_{ii3}| < \lambda_{333}$. We present in figure 3.11 results for the lighter charged unhiggs mass $m^{\pm}_{h_i}$ over the $(m_{1/2}, x/v)$ plane in the limit $\lambda_{ii3} \to 0$: larger values of λ_{ii3} give larger values of $m^{\pm}_{h_i}$. On the right of the lowest diagonal solid line in fig. 3.11 which corresponds to

$$m_{1/2} \sim (57GeV)\frac{x}{v} \tag{3.113}$$

for the representative choice $A_{\lambda_{ii3}}/m_{1/2} = -0.6$, $\lambda_{333} = 0.2$, $\overline{v}/v = 0.5$, we find $m^{\pm}_{h_i} < 20GeV$ in the limit $\lambda_{ii3} \to 0$. In this domain, whilst $m^{\pm}_{h_i}$ is generically

$O(x)$ for larger values of λ_{ii3}, there is for any value of $(m_{1/2}, x/v)$ a restricted range of λ_{ii3} values which give $20Gev < m^{\pm}_{h_i} < 100GeV$. On the left of the line corresponding to $m_{h_i^{\pm}} = 20GeV$ in the limit $\lambda_{ii3} \to 0$ there is a somewhat larger domain of $(m_{1/2}, x/v)$ plane for which $20GeV < m^{\pm}_{h_i} < 100GeV$ in the same limit: lines corresponding to $m_{h_i^{\pm}} = 60$ and $100GeV$ for $\lambda_{ii3} \to 0$ are also given. Values of λ_{ii3} up to 0.1 give $m^{\pm}_{h_i}$ only slightly heavier. Finally, the region to the left of the three lines corresponds to $m_{h_i^{\pm}} > 100GeV$ in the limit $\lambda_{ii3} \to 0$.

3.4.5 Neutral scalars

We now turn to the neutral Higgs bosons. As mentioned earlier, their mixing matrix breaks into two 3×3 and two 6×6 submatrices, in our basis in which only H_3, $\overline{H}_3$ and N_3 are the 'true' Higgses with VEVs, and if one assumes that the λ_{ijk} are real. The mass term for the real and imaginary components of the neutral true higgses, defined by $\Phi \equiv (\Phi_R + i\Phi_I)/\sqrt{2}$, $(\Phi \equiv H, \overline{H}, N)$, are:

$$\mathcal{L}_{R,I} = -\frac{1}{2}\begin{pmatrix} H^0_{R,I} & \overline{H}^0_{R,I} & N_{R,I} \end{pmatrix} \mathcal{M}^2_{R,I} \begin{pmatrix} H^0_{R,I} \\ \overline{H}^0_{R,I} \\ N_{R,I} \end{pmatrix}, \tag{3.114}$$

with

$$\mathcal{M}^2_R = \frac{1}{2}\begin{pmatrix} (g^2 + \frac{25}{9}g'^2)v^2 & (4\lambda^2_{333} - g^2 - \frac{5}{9}g'^2)\overline{v}v & (4\lambda^2_{333} - \frac{20}{9}g'^2)vx \\ -2\lambda_{333}A_{\lambda_{333}}\frac{\overline{v}x}{v} & +2\lambda_{333}A_{\lambda_{333}}x & +2\lambda_{333}A_{\lambda_{333}}\overline{v} \\ & (g^2 + \frac{10}{9}g'^2)\overline{v}^2 & (4\lambda^2_{333} - \frac{5}{9}g'^2)\overline{v}x \\ SYM & -2\lambda_{333}A_{\lambda_{333}}\frac{vx}{\overline{v}} & +2\lambda_{333}A_{\lambda_{333}}v \\ & & \frac{25}{9}g'^2x^2 \\ MET & RIC & -2\lambda_{333}A_{\lambda_{333}}\frac{v\overline{v}}{x} \end{pmatrix}, \tag{3.115}$$

where for notational convenience we have put $g \equiv g_2$ and $g' \equiv \sqrt{3/5}g_1 = \sqrt{3/5}g_{1'}$. In the limit of large x/v and $m_{1/2}$ the lightest mass eigenstate of $\mathcal{M}^2_R$ (3.115) is $H^0_L = (vH^0_R + \overline{v}\overline{H}^0_R)/\sqrt{v^2 + \overline{v}^2}$. It is easy to check that $m^0_{H_L} = O(v, \overline{v})$, not $O(x)$. This is to be expected since for large $m_{1/2}$ and x the low-energy effective theory reduces to the standard model, which must contain at least one real neutral true

Higgs boson with mass $O(m_W)$. We find in this limit that

$$m^2_{H^0_L} \simeq \frac{1}{v^2+\overline{v}^2}\{\frac{1}{2}(g^2+g'^2)(v^2-\overline{v}^2)^2+\frac{1}{18}g'^2(4v^2+\overline{v}^2)^2+4\lambda^2_{333}v^2\overline{v}^2\}-\frac{\epsilon}{2C}, \quad (3.116)$$

where

$$\begin{aligned} \epsilon &= \frac{1}{\sqrt{v^2+\overline{v}^2}}[(4\lambda^2_{333}-\frac{20}{9}g'^2v^2+4\lambda_{333}A_{\lambda_{333}}\frac{v\overline{v}}{x}+(4\lambda^2_{333}-\frac{5}{9}g'^2)\overline{v}^2], \\ C &= \frac{25}{9}g'^2. \end{aligned} \quad (3.117)$$

The dominant term in (3.116) is the first one, whilst $\epsilon^2/2C$ makes less than a 10% change in $m_{H^0_L}$ for small $\overline{v}/v$, and a larger one for $\overline{v}/v = 0.6$. Varying only the parameters λ_{333} and $A_{\lambda_{333}}$, one obtains an interval of values of $m^2_{H^0_L}$ which are possible for a given set of values of x/v, $m_{1/2}$ and $\overline{v}/v$. For $x/v \sim 3$ and $m_{1/2} \sim 100GeV$ the approximate expression (3.116) gives a lower bound for $m^2_{H^0_L}$ which is larger than the more precise numerical calculations by 10% for $\overline{v}/v = 0.2$ and by 30% for $\overline{v}/v = 0.6$, whilst the corresponding upper bound is reproduced with a few percent accuracy. We have verified numerically that (3.116) and (3.117) give a good approximation to $m_{H^0_L}$ (i.e. are accurate to within a few percent) when $x/v \geq 4$ and $m_{1/2} \geq 200GeV$.

In general,we find that

$$45GeV \leq m_{H^0_L} \leq 105GeV \quad (3.118)$$

for values of the parameters in the usual ranges. Fig. 3.12 shows contours of $m_{H^0_L}$ in the $(x/v, \overline{v}/v)$ plane for typical values of λ_{333}, $A_{\lambda_{333}}$ and $m_{1/2}$. The other two real neutral true Higgses with masses $O(x)$ are too heavy to be detectable at LEP.

Next we turn to the *imaginary neutral true higgses*, whose mixing matrix is $\mathcal{M}^2_I$:

$$\mathcal{M}^2_I = (-\lambda_{333}A_{\lambda_{333}}x)\begin{pmatrix} \overline{v}/v & 1 & \overline{v}x \\ 1 & v/\overline{v} & v/x \\ \overline{v}/x & v/x & \overline{v}v/x \end{pmatrix}. \quad (3.119)$$

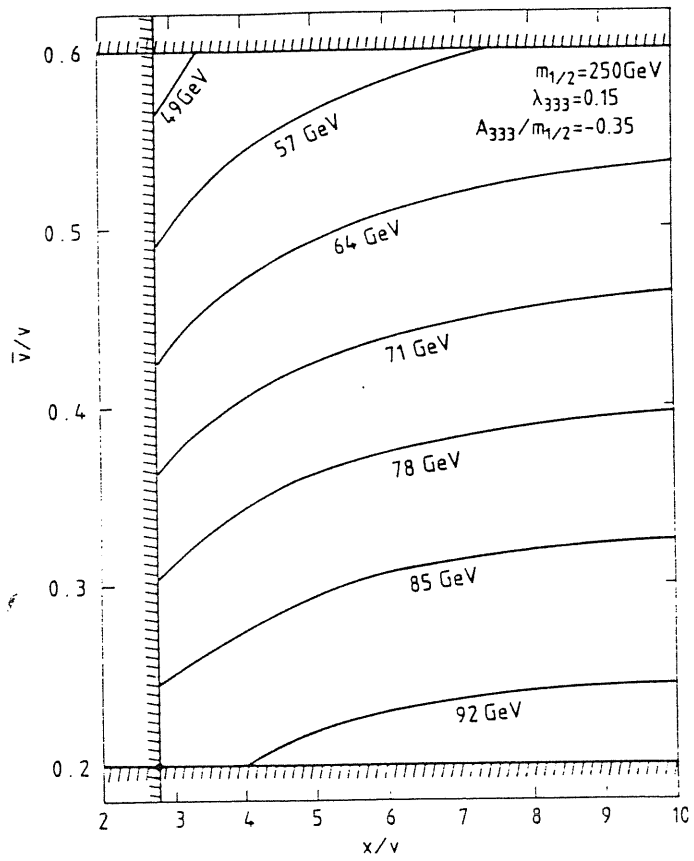

Figure 3.12: Contours of $m_{\tilde{\chi}^0_1}$ in the $(x/v, \overline{v}/v)$ plane corresponding to the representative values $m_{1/2} = 250GeV$, $\lambda_{333} = 0.15$ and $A_{\lambda_{333}}/m_{1/2} = -0.35$; the dependence on $m_{1/2}$ is very slight.

This has two massless eigenstates which are the Goldstone bosons, eaten by the massive neutral gauge bosons Z and Z', and one massive state

$$a = \frac{1}{\sqrt{\overline{v}/v + v/\overline{v} + v\overline{v}/x^2}}[\sqrt{\overline{v}/v}H_I^0 + \sqrt{v/\overline{v}}\overline{H}_I^0 + \sqrt{v\overline{v}/x}N_I], \tag{3.120}$$

with

$$m_a^2 = (-\lambda_{333}A_{\lambda_{333}}x)(\overline{v}/v + v/\overline{v} + v\overline{v}/x^2). \tag{3.121}$$

This state is also very heavy in the limit $x \to \infty$, but can be interestingly light. Taking the minimum values of λ_{333}, $A_{\lambda_{333}}$ and x/v from table 3.1, we find

$$m_a \geq 70GeV, \tag{3.122}$$

which could be even lighter than the real neutral true Higgs (3.118). Figure 3.13 shows contours of m_a in the $(x/v, m_{1/2})$ plane for typical values of λ_{333}, $A_{\lambda_{333}}$ and $\overline{v}/v$.

The final bosons tc be analysed are the neutral unhiggses, i.e. those in multiplets without VEVs, whose real and imaginary components are associated to two 6×6 mixing matrices. These matrices are rather complicated to analyze and depend on several parameters: their explicit form can be found in ref. [48]. A generic feature of both of them is that, in the limit as $x, m_{1/2} \to \infty$, all six eigenstates have masses $O(x)$, as one might expect since none of them have any reason to weigh $O(v, \overline{v})$. It is of course possible to obtain a light-mass eigenstate by playing the positive and negative $O(x^2)$ contributions off against each other, a game which is easier for smaller values of x and $m_{1/2}$, but this is not a generic feature.

3.4.6 Production in e^+e^- collisions

Reviewing our results, we see that there could be as many as three charginos with masses below $\frac{1}{2}m_Z$, additional neutralinos not much heavier than the lightest one having mainly a gaugino component, a charged Higgs boson with $m_{H^\pm} \geq 90Gev$, two charged unhiggses as light as $20GeV$, a real neutral Higgs boson H_L^0 as light

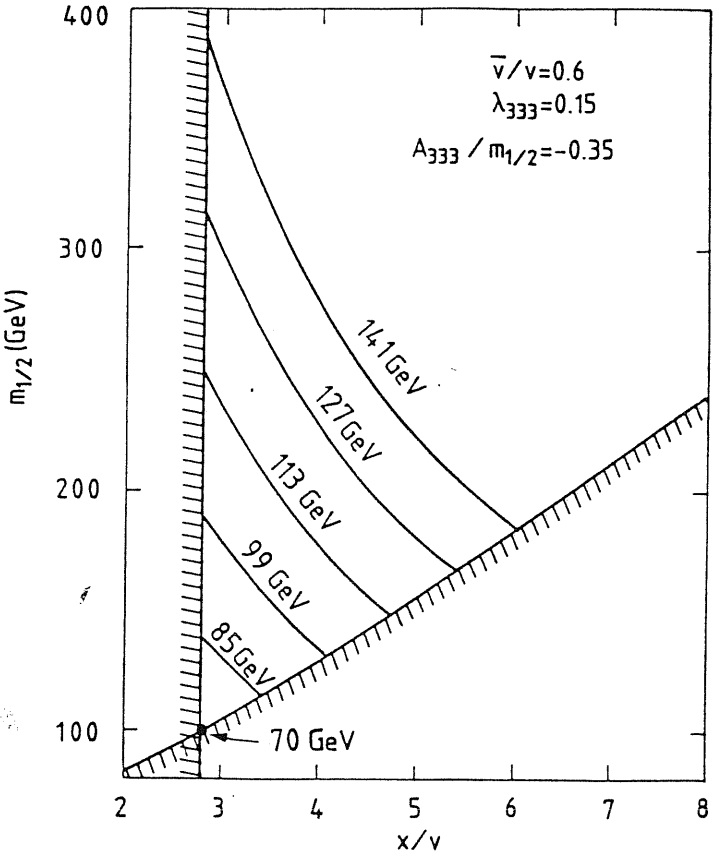

Figure 3.13: Contours of m_a in the $(x/v, m_{1/2})$ plane corresponding to the representative values $\overline{v}/v = 0.6$, $\lambda_{333} = 0.15$ and $A_{\lambda_{333}}/m_{1/2} = -0.35$: m_a increases by ~ 1.5 if $\overline{v}/v$ is decreased to 0.2.

as $45GeV$, and an imaginary neutral Higgs boson a as light as $70GeV$. Searches for light charginos and charged Higgs bosons are sufficiently straightforward (for a recent review, see ref. [62]) that we do not discuss them here.

The neutral Higgs boson H_L^0 could be produced at LEP via the reaction $e^+e^- \to Z^0 + H_L^0$ with a cross section

$$\frac{\sigma(e^+e^- \to Z^0 + H_L^0)}{\sigma(e^+e^- \to Z^0 + H^0)|_{standard\ model}} = \frac{g^2_{H_L^0 ZZ}}{g^2_{H^0 ZZ}}, \tag{3.123}$$

where

$$\begin{aligned} \frac{g_{H_L^0 ZZ}}{g_{H^0 ZZ}} &= \frac{1}{\sqrt{v^2+\overline{v}^2}}\{(\alpha v + \beta \overline{v})\cos^2\theta + \frac{2}{3}\sin\theta_W \sin\theta\cos\theta \\ &\times \ (4v\alpha - \overline{v}\beta) + \frac{1}{9}\sin^2\theta_W \sin^2\theta(25x\gamma + 16v\alpha + \overline{v}\beta)\} \end{aligned} \tag{3.124}$$

is the ratio of the $H_L^0 - Z^0 - Z^0$ and the standard model $H^0 - Z_0 - Z^0$ coupling constants. In eq. (3.124), α, β and γ are the coefficients in the decomposition $H_L^0 = \alpha H^0 + \beta \overline{H}^0 + \gamma N$, and θ is the mixing angle of the two neutral weak bosons present in the model we are considering. Since the neutral current phenomenology and the data on the Z^0 mass constrain the mixing angle θ to be small ($|\sin\theta| \leq 0.11$) one can approximate expression (3.124) with

$$\frac{g_{H_L^0 ZZ}}{g_{H^0 ZZ}} \simeq \frac{1}{\sqrt{v^2+\overline{v}^2}}(\alpha v + \beta\overline{v} + 0.6\sin^2\theta x\gamma). \tag{3.125}$$

For values of $m_{H_L^0}$ close to the lower bound of $45GeV$, the H^0 and $\overline{H}^0$ components in H_L^0 are dominant ($|\alpha|, |\beta| > |\gamma|$), and the ratio of cross sections (3.123) is of order unity. For instance, in the case $m_{H_L^0} = 45GeV$, one has $\overline{v}/v = 0.6$, $x/v = 3$, $\alpha = -0.61$, $\beta = -0.78$, $\gamma = -0.11$ and, correspondingly, $(g_{H_L^0 ZZ}/g_{H^0 ZZ}) \simeq (\alpha v + \beta\overline{v})^2/(v^2+\overline{v}^2) \simeq 0.8$, giving a large production rate at LEP. On the other hand, the imaginary neutral Higgs boson a has no $Z^0 - Z^0 - a$ coupling at the tree level and so cannot be produced with an appreciable rate in association with the Z^0 boson in e^+e^- annihilation.

If toponium Θ is heavy enough, it can decay (for a recent review, see ref. [63]) into both H_L^0 and a with the branching ratios

$$\frac{B(\Theta \to H_L^0 + \gamma)}{B(\Theta \to H^0 + \gamma)|_{standard\ model}} = \beta^2(1 + \frac{\overline{v}^2}{v^2}), \tag{3.126}$$

$$\frac{B(\Theta \to a + \gamma)}{B(\Theta \to H^0 + \gamma)|_{standard\ model}} = \frac{1 + \overline{v}^2/v^2}{1 + \overline{v}^2/v^2 + \overline{v}^2/x^2}. \tag{3.127}$$

Both ratios (3.126) and (3.127) can be of order unity when $m_{H_L^0}$ and m_a are close to their lower bounds. In particular, in the cases $m_{H_L^0} = 45GeV$ and $m_a = 70GeV$, which correspond to $\overline{v}/v = 0.6$, $\overline{v}/x = 0.2$ and $\beta = -0.78$, we have 0.8 and 1.0 for the ratios (3.126) and (3.127), respectively.

The phenomenological scenario we have explored here certainly does not exclude plenty of gaugino and Higgs excitement at LEP!

3.5 Exotic colour triplets (D-particles)

In this section we discuss the possible phenomenology [49] of the additional charge $(-1/3)$ colour triplet particles $D_{1/2}$ of spin 1/2 and $D_0, \overline{D_0^c}$ of spin 0 which are contained in each matter generation in the model under consideration[3]. For the range of parameters suggested by our calculations of radiative symmetry breaking, either a spin-1/2 or a spin-0 particle could be the lightest, and either could be as light as the present lower bound from e^+e^- experiments of about $20GeV$. The D particles could behave as leptoquarks coupling to quarks and leptons, in which case the single production process $ep \to D_0(\overline{D_0^c}) + X$ would occur, and $D_0(\overline{D_0^c}) \to lq$, $D_{1/2} \to lq\tilde{\chi}$ decays would dominate. Alternatively, the D particles could behave as diquarks coupling to pairs of antiquarks, in which case the single production process $p(\overline{p}) \to D_0(\overline{D_0^c}, \overline{D_0}, D_0^c) + X$ would occur, and $D_0(\overline{D_0^c}) \to \overline{qq}$, $D_0^c(\overline{D_0}) \to qq$, $D_{1/2} \to \overline{qq}\tilde{\chi}$ decays would dominate. We present cross sections for $ep \to D_0(\overline{D_0^c}) + X$, $p(\overline{p}) \to D_0(\overline{D_0^c}, \overline{D_0}, D_0^c) + X$, $e^+e^- \to D_0\overline{D_0}(D_0^c\overline{D_0^c})$ and $D_{1/2}\overline{D_{1/2}}$,

[3]For related work, see ref. [64].

$p^{(\overline{p})} \to D_0\overline{D_0}(D_0^c\overline{D_0^c})$ and $D_{1/2}\overline{D_{1/2}} + X$. We calculate the experimental signals and estimate backgrounds for D production and decay in these processes. The decays $D_0(\overline{D_0^c}) \to lq$ and $D_{1/2} \to lq\tilde{\chi}$ or $\overline{q}\overline{q}\tilde{\chi}$ would be detectable in most of these reactions, but $D_0(\overline{D_0^c}) \to \overline{q}\overline{q}$ decays may only be detectable in $e^+e^- \to D_0\overline{D_0}(D_0^c\overline{D_0^c})$ collisions.

3.5.1 Constraints on (D_0, D_0^c) and $D_{1/2}$ masses

Here we discuss in detail the mass matrices for the exotic fermions $D_{1/2}$ and bosons $D_0, \overline{D^c}_0$.

In the field basis defined by eq. (3.90) and (3.91), the part of the superpotential contributing to the $D_{1/2}$ masses is simply

$$f_{D_{1/2}}^{mass} = k_{ab3} D_a D_b^c N_3. \tag{3.128}$$

We have not used, up to now, the freedom of redefining the fields D_a and D_a^c by independent rotations in generation space. We can therefore move to a convenient basis where the following relations hold:

$$k_{ab3} = 0 \quad for \quad a \neq b. \tag{3.129}$$

The two-component spinors of each generation contained in the chiral superfields D_a, D_a^c will then combine to form three Dirac spinors $D_{1/2a}$ of masses

$$m_{D_a} = k_{aa3} x \quad (a = 1, 2, 3). \tag{3.130}$$

Note that the masses of the $D_{1/2}$ particles are completely independent of those of ordinary quarks and leptons, being proportional not only to different Yukawa couplings, but also to different VEVs. Moreover, since we need $x > v, \overline{v}$ to agree with the experimental limits on neutral currents, the present non-observation of D particles is naturally explained in our model. This does not exclude, however, that the relevant Yukawa couplings could be small enough to give to the $D_{1/2a}$ masses close to the experimental bounds.

The mass matrix involving the scalar components of D_a and D_a^c has a slightly more complicated structure. Even in the convenient basis we chose above, one has in general a real symmetric 6×6 matrix, with non-trivial intergenerational mixing. The matrix elements are

$$\begin{array}{ll}
M^2_{D_1\overline{D_1}} = \tilde{m}^2_{D_{11}} + m^2_{D_1} + G^2(D), & M^2_{\overline{D_1^c}D_1^c} = \tilde{m}^2_{D^c_{11}} + m^2_{D_1} + G^2(D^c), \\
M^2_{D_2\overline{D_2}} = \tilde{m}^2_{D_{22}} + m^2_{D_2} + G^2(D), & M^2_{\overline{D_2^c}D_2^c} = \tilde{m}^2_{D^c_{22}} + m^2_{D_2} + G^2(D^c), \\
M^2_{D_3\overline{D_3}} = \tilde{m}^2_{D_{33}} + m^2_{D_3} + G^2(D), & M^2_{\overline{D_3^c}D_3^c} = \tilde{m}^2_{D^c_{33}} + m^2_{D_3} + G^2(D^c), \\
M^2_{D_1D_1^c} = \eta_{k_{113}} x + \lambda_{33c} k_{11c} v\overline{v}, & M^2_{D_1\overline{D_2}} = \tilde{m}^2_{D_{12}}, \\
M^2_{D_1D_2^c} = \eta_{k_{123}} x + \lambda_{33c} k_{12c} v\overline{v}, & M^2_{D_1\overline{D_3}} = \tilde{m}^2_{D_{13}}, \\
M^2_{D_1D_3^c} = \eta_{k_{133}} x + \lambda_{33c} k_{13c} v\overline{v}, & \\
M^2_{\overline{D_1^c}D_2} = \eta_{k_{213}} x + \lambda_{33c} k_{21c} v\overline{v}, & M^2_{\overline{D_1^c}D_2^c} = \tilde{m}^2_{D^c_{12}}, \\
M^2_{\overline{D_1^c}D_3} = \eta_{k_{313}} x + \lambda_{33c} k_{31c} v\overline{v}, & M^2_{\overline{D_1^c}D_3^c} = \tilde{m}^2_{D^c_{13}}, \\
M^2_{D_2D_2^c} = \eta_{k_{223}} x + \lambda_{33c} k_{22c} v\overline{v}, & M^2_{D_2\overline{D_3}} = \tilde{m}^2_{D_{23}}, \\
M^2_{D_2D_3^c} = \eta_{k_{233}} x + \lambda_{33c} k_{23c} v\overline{v}, & \\
M^2_{\overline{D_2^c}D_3} = \eta_{k_{323}} x + \lambda_{33c} k_{32c} v\overline{v}, & M^2_{\overline{D_2^c}D_3^c} = \tilde{m}^2_{D^c_{23}}, \\
M^2_{D_3D_3^c} = \eta_{k_{333}} x + \lambda_{33c} k_{33c} v\overline{v}. &
\end{array} \tag{3.131}$$

Symbols appearing in the above formula correspond to the following general expressions for the superpotential and the soft supersymmetry breaking part of the scalar potential:

$$f = \lambda_{abc} H_a \overline{H}_b N_c + k_{abc} D_a D_b^c N_c + \ldots, \tag{3.132}$$

$$\begin{aligned}
V_{soft} &= \tilde{m}^2_{D_{ab}} \overline{D_a} D_b + \tilde{m}^2_{D^c_{ab}} \overline{D_a^c} D_b^c + \ldots \\
&+ \eta_{k_{abc}} (D_a D_b^c N_c + h.c.) + \ldots
\end{aligned} \tag{3.133}$$

where the dots represent terms which do not contribute to (3.131), m_{D_a} are the fermion masses given by eq. (3.130) and $G^2(D)$ and $G^2(D^c)$ are the generation-independent D-term contributions to the scalar masses:

$$G^2(D) = \frac{5}{9} \frac{m_W^2 \tan^2\theta_W}{1 + (\overline{v}/v)^2} [1 + (\overline{v}/v)^2 - 2(x/v)^2], \tag{3.134}$$

$$G^2(D^c) = \frac{5}{9} \frac{m_W^2 \tan^2\theta_W}{1 + (\overline{v}/v)^2} [1 - 1/2(\overline{v}/v)^2 - 1/2(x/v)^2]. \tag{3.135}$$

To bring the discussion at a reasonable level of simplicity, some short cuts are necessary once again. Our first simplification is to assume that the only Yukawa

couplings contributing significantly to the RGE for the soft SUSY breaking parameters are those diagonal in generation space (λ_{aaa}, k_{aaa}, ...). In this case, the soft supersymmetry breaking part of the scalar potential assumes the simplified form

$$\begin{aligned} V_{soft} &= \tilde{m}^2_{D_a}|D_a|^2 + \tilde{m}^2_{D^c_a}|D^c_a|^2 + \ldots \\ &+ k_{abc}A_{k_{abc}}(D_aD^c_bN_c + h.c.) + \ldots . \end{aligned} \tag{3.136}$$

Moreover, the mass matrix (3.131) for the D_0/D^c_0 bosons becomes block-diagonal in generation space, with each 2×2 block given by

$$\mathcal{M}^2_{0a} = \begin{pmatrix} \tilde{m}^2_{D_a} + m^2_{D_a} + G^2(D) & m_{D_a}A_{k_{aa3}} + \lambda_{333}k_{aa3}v\bar{v} \\ m_{D_a}A_{k_{aa3}} + \lambda_{333}k_{aa3}v\bar{v} & \tilde{m}^2_{D^c_a} + m^2_{D_a} + G^2(D^c) \end{pmatrix}. \tag{3.137}$$

Let us examine now the phenomenological constraints on the quantities appearing in eqs. (3.130) and (3.137). These constraints are derived assuming the boundary conditions (3.53)-(3.56) on the soft supersymmetry breaking terms.

As independent parameters in our analysis, it is convenient to take x/v, $\bar{v}/v$, $m_{1/2}$, $(\tilde{m}_{D_a}/m_{1/2})^2$, $(\tilde{m}_{D^c_a}/m_{1/2})^2$, $A_{k_{aa3}}/m_{1/2}$, λ_{333} and k_{333}. To simplify the discussion further, we shall assume that the only non-negligible Yukawa couplings contributing to the RGE are indeed those considered in section 3.2. In this case, indicative ranges of variation for the different parameters are presented in table 3.1. The couplings $k_{113,223}$ are assumed to be smaller than k_{333}, and there are no lower limits on them apart from the experimental limit on m_{D_a}.

Let us see what are the indications on the $D_{1/2}$ and D_0/D^c_0 masses coming from explicit model calculations. To begin with, let us consider the $D_{1/2}$ masses, given by eq. (3.130), which in terms of the parameters of table 3.1 reads

$$m_{D_a} = k_{aa3}x = k_{aa3}(\frac{x}{v})\{2\sqrt{2}G_F[1 + (\bar{v}/v)^2]\}^{-1/2}, \tag{3.138}$$

where $G_F = 1.166 \times 10^{-5}GeV^{-2}$ is the Fermi constant. Using the limits of table 3.1, one finds $m_{D_3} \geq 105GeV$, while for $a = 1, 2$ the lower limit on m_{D_a} is the experimental one:

$$m_{D_a} \geq 20GeV \quad (a = 1, 2). \tag{3.139}$$

An indicative upper limit on the $D_{1/2}$ masses comes from the naturalness constraint, which forbids very large values of x/v, since they would require a fine tuning of the parameters in the scalar potential which would be unstable under radiative corrections. Using the values of table 3.1, one finds:

$$m_{D_1}, m_{D_2} < m_{D_3} \leq 1TeV. \tag{3.140}$$

In summary, model calculations suggest for the $D_{1/2}$ quarks masses ranging from $20GeV$ to $1TeV$. Although the scale of $D_{1/2}$ masses is generally the same as the scale of the extra Z' boson, since both are related to the breaking of the extra $U(1)_{Y'}$ gauge factor, some $D_{1/2}$ particles may be considerably lighter than the Z' if they have small Yukawa couplings to the N field which acquires a VEV.

Let us comment now on the structure of the D_0, D_0^c mass matrices, eq. (3.137). First of all, note that, for the range of parameters given in table 3.1, always $m_{D_a} A^k_{333} >> \lambda_{333} k_{aa3} v\bar{v}$, so that we can neglect this last contribution to the off-diagonal entry. Note also that, for large values of x/v, the D-term contributions of eqs. (3.134) and (3.135) become negative and big. On the other hand, the positive contributions $\tilde{m}^2_{D_a}$ and $\tilde{m}^2_{D^c_a}$ are proportional to $m^2_{1/2}$. This suggests that light D_0/D_0^c masses can be obtained for relatively high values of x/v and relatively small values of $m_{1/2}$; in particular, to avoid $(mass)^2$ for the charged unhiggses which are too small or negative (as seen in the previous section), a relation of the type $m_{1/2} > K_{cr}(x/v)$ must be satisfied, with K_{cr} slightly dependent on the other parameters, and generically in the range $K_{cr} \sim 55 - 65GeV$. Even taking into account this last constraint, together with the correlation between $\tilde{m}^2_{D_a}$, $\tilde{m}^2_{D^c_a}$ and A^k_{aa3}, one finds the following results:

1. Calling D^1_{0a} and D^2_{0a} the two eigenvalues of the mass matrix (3.137), with masses $m_{D^1_{0a}} < m_{D^2_{0a}}$, the following two hierarchies are both possible:

$$m_{D_a} < m_{D^1_{0a}} < m_{D^2_{0a}}, \tag{3.141}$$

$$m_{D^1_{0a}} < m_{D_a} < m_{D^2_{0a}}. \tag{3.142}$$

2. Under our set of assumptions, masses of the D^1_{03} ($D^1_{01,2}$) particles as low as $100GeV$ ($170GeV$) are allowed. These lower limits come from the study of the unhiggs mass spectrum presented in the previous section, and have been derived under some model-dependent assumptions. Relaxing these assumptions, they can be significantly lowered and could be as light as $20GeV$. On the other hand, the addition of a common scalar mass to the primordial soft SUSY breaking terms would generally lead to higher D_{0a}/D^c_{0a} masses, favouring the case of eq (3.141) with respect to the one of eq. (3.142).

3. When the lowest possible value for the D^1_{0a} masses are attained, the mass eigenstate D^1_{0a} is always an admixture, with contributions of almost equal magnitude, of the interaction eigenstates D^a and $\overline{D^c_a}$.

This is essentially all the information on $D_{1/2}$, D_0, D^c_0 masses that one is able to extract from model calculations. Despite all the constraints on the different parameters, there is still a large freedom for the resulting spectrum of $D_{1/2}$, D_0, D^c_0 masses, which is not significantly bounded from below, thus motivating the phenomenological analysis of the following sections.

3.5.2 Single D_0/D^c_0 production and D-particles decays

D/D^c couplings

As was mentioned in section 3.1, the D, D^c supermultiplets may couple directly to ordinary quarks and leptons through the following superpotential terms:

$$f \ni \lambda_Q DQQ + \lambda_C D^c u^c d^c \tag{3.143}$$

$$+ \lambda_L D^c LQ + \lambda_E D u^c e^c \tag{3.144}$$

$$+ \lambda_\nu D d^c \nu^c. \tag{3.145}$$

According to the results of section 3.1.3, we take the sets (3.143), (3.144) and (3.145) as alternative cases to study.

Couplings to quark-quark pairs

As discussed earlier, in the model under consideration no mixing of the D particles with conventional charge $-1/3$ quarks occurs. Single production of the scalar D is possible in hadron-hadron collisions via $\bar{q}+\bar{q} \to D_0/\overline{D_0^c}$ ($q+q \to D_0^c/\overline{D_0}$) followed by $D_0/\overline{D_0^c} \to \bar{q}+\bar{q}$ ($D_0^c/\overline{D_0} \to q+q$). The squared amplitudes $|\mathcal{M}|^2$ for the decays of $\overline{D_0}$ and D_0^c to quark pairs are given by

$$|\mathcal{M}_{D_0}|^2 = 24\lambda_Q^2 m_{D_0}^2, \quad |\mathcal{M}_{D_0^c}|^2 = 6\lambda_C^2 m_{D_0^c}^2, \tag{3.146}$$

and we have no idea what the ratio of the couplings λ_Q and λ_C might be. The differential cross section for the process $h+h \to (D_0^c/\overline{D_0} \to qq)+X$ is given by

$$\begin{aligned} d^2\sigma &= (1/48\pi)\hat{s}\{u(x_1)d(x_2)+u(x_2)d(x_1)+\ldots\}dx_1dx_2\delta(sx_1x_2-\hat{s}) \\ &\times \{\frac{\lambda_Q^4(64/9)}{((\hat{s}-m_{D_0}^2)^2+\Gamma_{D_0}^2 m_{D_0}^2)}+\frac{\lambda_C^4(4/9)}{((\hat{s}-m_{D_0^c}^2)^2+\Gamma_{D_0^c}^2 m_{D_0^c}^2)}, \end{aligned} \tag{3.147}$$

where $\sqrt{\hat{s}}$ is the centre-of-mass energy of the subprocess $qq \to D_0^c/\overline{D_0} \to qq$, x_1 and x_2 are the fractions of the momenta of the incoming hadrons carried by the quarks with distributions $u(x)$, $d(x)$, etc., and Γ_{D_0,D_0^c} are the decay widths of the $\overline{D_0}$ and D_0^c. No mixing between the $\overline{D_0}$ and D_0^c is taken into account in writing (3.146) and (3.147): its effects can be trivially incorporated.

In fig. 3.14 we show the total cross sections for the above process as a function of the mass m_{D_0}, assuming $m_{D_0} = m_{D_0^c}$ and $\lambda_Q = \lambda_C \equiv \lambda'$ for simplicity. The common Yukawa coupling is parametrized by its ratio to the electromagnetic coupling

$$F \equiv \frac{\lambda_Q^2/4\pi}{\alpha_{em}} = \frac{\lambda_C^2/4\pi}{\alpha_{em}}. \tag{3.148}$$

Note that although neutral current constraints impose severe upper bounds on flavour- or generation-changing couplings of the D/D^c supermultiplets, there are no

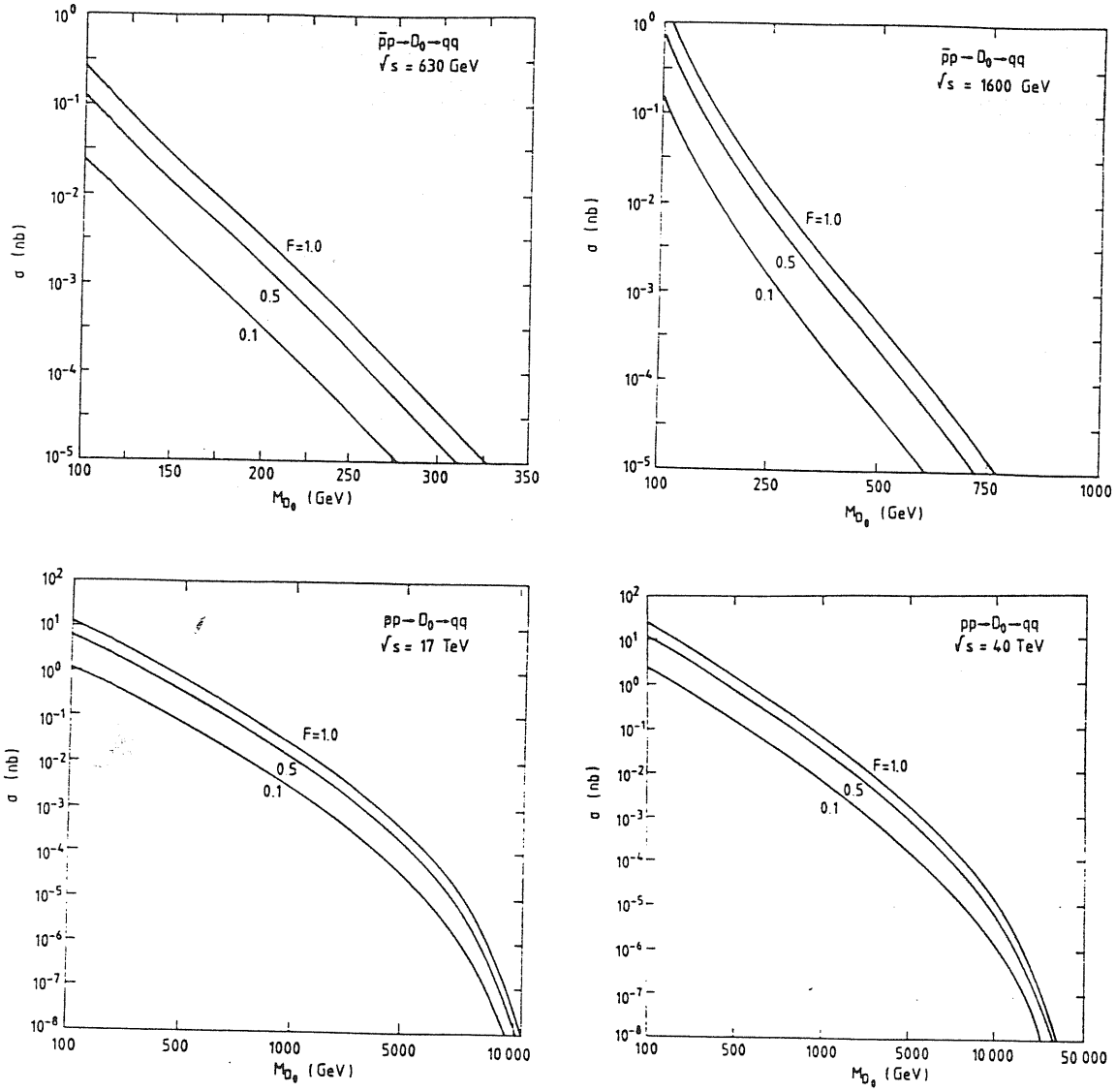

Figure 3.14: Total cross section for $h + h \to (D_0^c/\overline{D_0} \to qq \text{ or } D_0/\overline{D_0^c} \to \overline{qq}) + X$ at different hadronic colliders.

m (GeV)	125	145	168	188	208	228	268	288
δm (GeV)	11.0	12.3	13.7	14.9	16.2	17.3	19.5	20.6
dσ/dm (nb/GeV)	3.10^{-1}	9.10^{-2}	3.10^{-2}	10^{-2}	7.10^{-3}	3.10^{-3}	4.10^{-4}	6.10^{-4}
$\delta\sigma$ (nb)	3.3	1.11	0.41	0.15	0.11	0.05	$7.8.10^{-3}$	12.10^{-3}
σ(nb) F = 1	$0.8.10^{-1}$	$0.3.10^{-1}$	$0.1.10^{-1}$	$0.5.10^{-2}$	$0.2.10^{-2}$	$0.9.10^{-3}$	$0.2.10^{-3}$	$0.6.10^{-4}$

Table 3.2: Signal and background for spin-0 D search at the CERN collider.

severe constraints on their diagonal couplings. Note also that the three generations of scalar D particles could in principle have similar masses, in which case the estimated cross sections should be increased by a factor of 3. Figure 3.14 includes curves for all high-energy hadron-hadron colliders currently envisaged: CERN $p\bar{p}$ at $\sqrt{s} = 630GeV$, FNAL $p\bar{p}$ at $\sqrt{s} = 1600GeV$, LHC pp at $\sqrt{s} = 17TeV$ and SSC at $\sqrt{s} = 40TeV$.

These processes will appear experimentally as two-jet events. We have made a detailed comparison of the signal-to-background ratio at $\sqrt{s} = 630GeV$ using data published by UA2. In table 3.2 we compare their $d\sigma/dM(jet - jet)$ multiplied by the widths δM of the bins they use, corresponding to their mass resolution, with the $\overline{D_0}/D_0^c$ cross section we would expect for $F = 1$. In table 3.2 we have assumed, following UA2, that the mass resolution $\delta m = 0.29[m(GeV)]^{3/4}$ and we have computed $\delta\sigma = \delta m d\sigma/dm$. We see that the QCD jet-jet background is between one and two orders of magnitude larger than our expected $\overline{D_0}/D_0^c$ cross-sections. We expect this state of affairs to be repeated at future colliders, so that it will be difficult to see the scalar D in this way. Nevertheless, it would be useful for theorists if collider experiments could in the future quote directly upper limits on cross-sections for new particles decaying into jet pairs.

We turn now to the decays of the fermions $D_{1/2}$. In fig. 3.15 we show diagrams contributing to their possible decays $D_{1/2} \rightarrow \bar{q} + \bar{q} + \tilde{\chi}$ in leading order. The

squared decay amplitude in the rest frame of the $D_{1/2}$ is given by:

$$
\begin{aligned}
|\mathcal{M}_{D_{1/2}}|^2 &= \lambda_C^2(\sqrt{2}e)^2 4 \\
&\times \{\frac{(1/3)^2 m_{D_{1/2}} E_1 (m_{D_{1/2}} E_1 + \frac{1}{2}m_{D_{1/2}}^2 - \frac{1}{2}m_{\tilde{\gamma}}^2)}{(P^2 - m_{\tilde{d}_R}^2)^2} \\
&+ \frac{(2/3)^2 m_{D_{1/2}} E_2 (m_{D_{1/2}} E_2 + \frac{1}{2}m_{D_{1/2}}^2 - \frac{1}{2}m_{\tilde{\gamma}}^2)}{(P^2 - m_{\tilde{u}_R}^2)^2} \\
&+ \frac{(1/3)^2 m_{D_{1/2}} (m_{D_{1/2}} - E_1 - E_2)(m_{D_{1/2}}(E_1 + E_2) - \frac{1}{2}m_{D_{1/2}}^2 + \frac{1}{2}m_{\tilde{\gamma}}^2)}{(K^2 - m_{D_0^c}^2)^2} \\
&- \frac{(1/3)(-2/3) m_{D_{1/2}}^2 (2E_1 E_2 - m_{D_{1/2}}(E_1 + E_2) + \frac{1}{2}m_{D_{1/2}}^2 - \frac{1}{2}m_{\tilde{\gamma}}^2)}{(P^2 - m_{\tilde{u}_R}^2)(P^2 - m_{\tilde{d}_R}^2)} \\
&- \frac{(1/3)(-1/3) m_{D_{1/2}} (m_{D_{1/2}} - 2E_2)(m_{D_{1/2}}(E_1 + E_2) - \frac{1}{2}m_{D_{1/2}}^2 + \frac{1}{2}m_{\tilde{\gamma}}^2)}{(P^2 - m_{\tilde{d}_R}^2)(K^2 - m_{D_0^c}^2)} \\
&+ \frac{(-2/3)(-1/3) m_{D_{1/2}} (m_{D_{1/2}} - 2E_1)(m_{D_{1/2}}(E_1 + E_2) - \frac{1}{2}m_{D_{1/2}}^2 + \frac{1}{2}m_{\tilde{\gamma}}^2)}{(P^2 - m_{\tilde{u}_R}^2)(K^2 - m_{D_0^c}^2)}\} \\
&+ \lambda_Q^2(\sqrt{2}e)^2 4 \\
&\times \{\frac{(1/3)^2 4 m_{D_{1/2}} (m_{D_{1/2}} - E_1 - E_2)(m_{D_{1/2}}(E_1 + E_2) - \frac{1}{2}m_{D_{1/2}}^2 + \frac{1}{2}m_{\tilde{\gamma}}^2)}{(K^2 - m_{D_0}^2)^2} \\
&+ m_{D_{1/2}} E_1 (m_{D_{1/2}} E_1 + \frac{1}{2}m_{D_{1/2}}^2 - \frac{1}{2}m_{\tilde{\gamma}}^2) \\
&\times [\frac{(2/3)^2}{(P^2 - m_{\tilde{u}_L}^2)^2} + \frac{(-1/3)^2}{P^2 - m_{\tilde{d}_L}^2)^2} + \frac{2(2/3)(-1/3)}{(P^2 - m_{\tilde{u}_L}^2)(P^2 - m_{\tilde{d}_L}^2)}] \\
&+ \frac{(-1/3) m_{D_{1/2}} (m_{D_{1/2}} - 2E_2)(m_{D_{1/2}}(E_1 + E_2) - \frac{1}{2}m_{D_{1/2}}^2 + \frac{1}{2}m_{\tilde{\gamma}}^2)}{(K^2 - m_{D_0}^2)} \\
&\times [\frac{(-2/3)}{(P^2 - m_{\tilde{u}_L}^2)} + \frac{(1/3)}{P^2 - m_{\tilde{d}_L}^2)}]\}, \qquad (3.149)
\end{aligned}
$$

where

$$P^2 = m_{D_{1/2}}(m_{D_{1/2}} - 2E_1), \quad K^2 = 2E_1 E_2(1 - \cos\Phi), \qquad (3.150)$$

Φ is the angle between the two final-state quarks, E_1 and E_2 their energies, we have assumed that the lightest supersymmetric particle $\tilde{\chi}$ is essentially a photino $\tilde{\gamma}$ and we have neglected mixing between left- and right-handed squarks. The partial decay rate $d\Gamma$ of the $D_{1/2}$ is then given by

$$d\Gamma = \frac{1}{(2\pi)^3}\frac{1}{m_{D_{1/2}}}|\mathcal{M}_{D_{1/2}}|^2 dE_1 dE_2. \qquad (3.151)$$

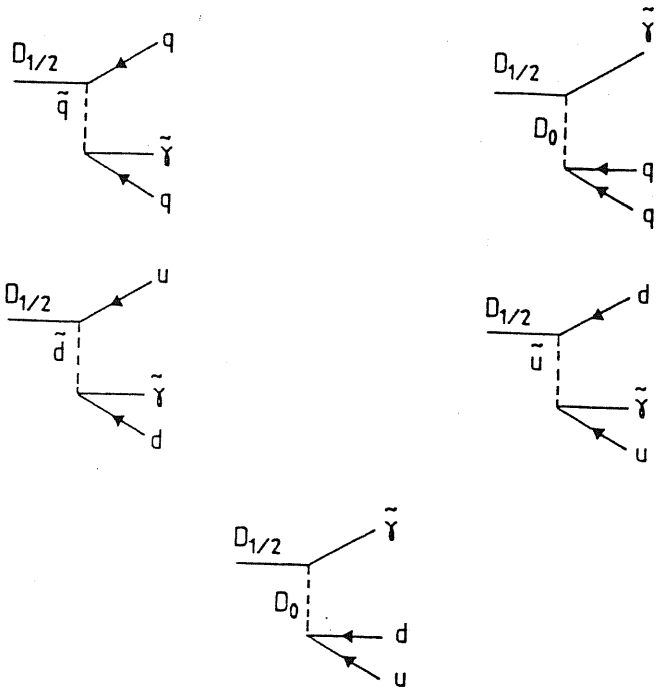

Figure 3.15: Tree diagrams contributing to the decay $D_{1/2} \to \overline{q}\overline{q}\tilde{\gamma}$.

The decay rate given by (3.149),(3.150) and (3.151) is a complicated function of $m_{D_{1/2}}/m_{\tilde{u},\tilde{d}}$. In the simplifying limit where $m_{D_{1/2}} << m_{\tilde{u},\tilde{d}}$ and neglecting quark masses and $m_{\tilde{\gamma}}$, we find

$$\begin{aligned}\Gamma &= \frac{1}{(2\pi)^3} m_{D_{1/2}}^5 \frac{1}{192} \\ &\times \{\lambda_C^2(\sqrt{2}e)^2 4[\frac{(1/3)^2}{m_{\tilde{d}_R}^4} + \frac{(-2/3)^2}{m_{\tilde{u}_R}^4} + \frac{(1/3)(-2/3)2}{m_{\tilde{d}_R}^2 m_{\tilde{u}_R}^2}] \\ &- \lambda_Q^2(\sqrt{2}e)^2 4[\frac{(-1/3)^2}{m_{\tilde{d}_L}^4} + \frac{(2/3)^2}{m_{\tilde{u}_L}^4} + \frac{(-1/3)(2/3)2}{m_{\tilde{u}_L}^2 m_{\tilde{d}_L}^2}]\}. \end{aligned} \quad (3.152)$$

Rather than use (3.149) in calculating the missing energy signature for $D_{1/2}$ production discussed in the previous subsection, we use simple phase space. We do not expect our results to be sensitive to this simplification.

Couplings to quark-lepton pairs

We now turn to the case (3.144). Single production of the scalar D is possible

in ep collisions via $e^-u \to D_0/\overline{D_0^c}$ ($e^+\overline{u} \to D_0^c/\overline{D_0}$), while $D_0/\overline{D_0^c} \to q+l$ ($D_0^c/\overline{D_0} \to \overline{q}\overline{l}$) decays dominate. The squared amplitudes for these decays are

$$|\mathcal{M}_{D_0}|^2 = 6\lambda_E^2 m_{D_0}^2, \quad |\mathcal{M}_{D_0^c}|^2 = 12\lambda_L^2 m_{D_0^c}^2. \tag{3.153}$$

Neglecting mixing, all of the D_0 decays are to jets + charged leptons, while the D_0^c has 50% branching ratios into (jets + charged leptons) and (jets + neutrinos). Again, we have no idea what the ratio of the couplings λ_E and λ_L might be. The cross section for the process $ep \to D_0/\overline{D_0^c} \to lq$ is given by

$$\begin{aligned} d\sigma &= \frac{d\hat{s}}{16\pi}\frac{\hat{s}}{s}\{u(\hat{s}/s) + \ldots\} \\ &\times \{\frac{2\lambda_L^4}{(\hat{s}-m_{D_0^c}^2)^2 + \Gamma_{D_0^c}^2 m_{D_0^c}^2} + \frac{\lambda_E^4}{(\hat{s}-m_{D_0}^2)^2 + \Gamma_{D_0}^2 m_{D_0}^2}\}, \end{aligned} \tag{3.154}$$

where $\sqrt{s} = \sqrt{4E_eE_p}$ is the centre-of-mass energy and $\hat{s}$ is the invariant mass squared of the colliding lepto-quark combination. In figure 3.16 we show the integrated cross section as a function of m_{D_0}, assuming $m_{D_0} = m_{D_0^c}$ and $\lambda_E^2 = \lambda_L^2 = \lambda'^2 = 4\pi\alpha_{em}F$ as in eq. (3.148). Results are presented for HERA: $\sqrt{s} = 314GeV$, and for two LHC/LEP options: $\sqrt{s} = 1.4TeV, 1.8TeV$.

These processes will appear experimentally as (lepton + jet) final states. the cases where the lepton is an electron must be compared with the background from the conventional process $e + p \to e + X$, whereas the cases where the lepton is a neutrino must be compared with the charged current cross sections for $e + p \to \nu + X$. There would be relatively little background if the D_0 decays into a μ or a τ, but flavour changing neutral current constraints severely restrict the possible couplings of these leptons.

We show in table 3.3 numerical calculations of the cross sections for $e^-p \to (D_0/\overline{D_0^c} \to e^-q) + X$, compared with the continuum background coming from the conventional electromagnetic and neutral current scattering $e^- + p \to e^- + X$. To estimate the background we have integrated over bins in x corresponding to the $e + jet$ mass resolution expected for the HERA detector ZEUS. We see that the

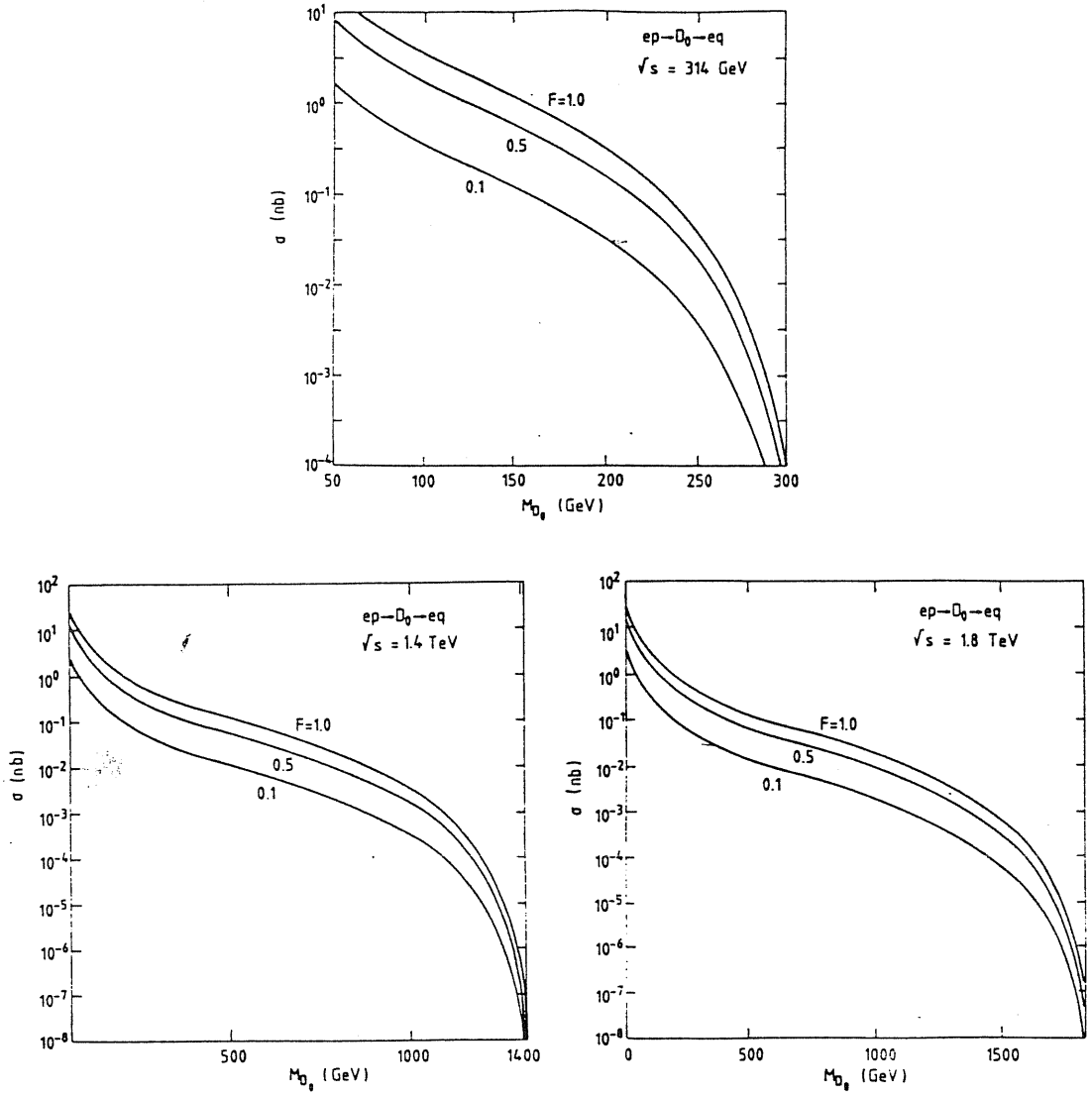

Figure 3.16: Total cross section for $ep \rightarrow (D_0/\overline{D_0^c} \rightarrow lq) + X$ at different ep colliders.

m_{D_0}	100	200	300
$x = m_D^2/s$	0.1	0.40	0.91
Background cross-sections $d\sigma/dx$ e_L^-(nb)	42.3	1.4	$2.0.10^{-4}$
e_R^-(nb)	24.6	0.7	$9.3.10^{-5}$
δm(GeV) ZEUS[22]	2.05	2.9	3.5
$\delta\sigma = 4m\delta m\sigma/s$(nb) (ZEUS)[22]	(L) 0.35 (R) 0.20	0.032 0.016	$8.4.10^{-6}$ $3.9.10^{-6}$
σ_{D_0} (F = 1) (nb)	3.6	0.32	$0.83.10^{-4}$

Table 3.3: Signal and background for scalar-D searches in *ep* collisions at HERA.

signal-to-background ratio are very favourable if $F = 1$, which may be an upper bound on the $D\bar{q}\bar{l}$ coupling. It should also be possible to detect the $D_0/\overline{D_0^c}$ even if F is considerably smaller than one. The process $e + q \rightarrow D_0/\overline{D_0^c} \rightarrow \nu q$ can be detected almost equally easily. The background from the standard model charged current reaction is slightly smaller than the that shown in table 3.3. The resolution for the mass bump in the $(\nu + q)$ channel is in the ZEUS detector only a factor ~ 1.6 worse than in the $(e+q)$ channel. The other HERA detector H1 is expected to have an $(e + q)$ mass resolution somewhat better (by a factor ~ 1.1) and a $(\nu + q)$ mass resolution somewhat worse (by a factor $\sim 1/1.7$) than the ZEUS detector. Similar calculations can be made for higher energy *ep* collider projects, with similar conclusions.

The squared amplitude for $D_{1/2} \rightarrow ql\tilde{\gamma}$ decay in the $D_{1/2}$ rest frame is given by

$$|\mathcal{M}_{D_{1/2}}|^2 = \lambda_L^2(\sqrt{2}e)^2 12 \times \{\frac{m_{D_{1/2}}E_q(\frac{1}{2}m_{D_{1/2}}^2 - \frac{1}{2}m_{\tilde{\gamma}}^2 - m_{D_{1/2}}E_q)}{(P^2 - m_{\tilde{e}_L}^2)^2}$$

$$
\begin{aligned}
&+ \left(\frac{1}{2}m_{D_{1/2}}^2 - \frac{1}{2}m_{\tilde{\gamma}}^2 - m_{D_{1/2}}E_l\right)m_{D_{1/2}}E_l\left[\frac{(2/3)^2}{(P^2-m_{\tilde{u}_L}^2)^2} + \frac{(1/3)^2}{(P^2-m_{\tilde{d}_L}^2)^2}\right] \\
&+ \frac{2(1/3)^2 m_{D_{1/2}}(m_{D_{1/2}} - E_q - E_l)(m_{D_{1/2}}(E_l+E_q) - \frac{1}{2}m_{D_{1/2}}^2 + \frac{1}{2}m_{\tilde{\gamma}}^2)}{(K^2 - m_{D_0^c}^2)^2} \\
&+ \frac{(2/3)(2m_{D_{1/2}}^2 E_l E_q - m_{D_{1/2}}^2(m_{D_{1/2}}(E_l+E_q) - \frac{1}{2}m_{D_{1/2}}^2 + \frac{1}{2}m_{\tilde{\gamma}}^2))}{(P^2-m_{\tilde{u}_L}^2)(P^2-m_{\tilde{e}_L}^2)} \\
&+ \frac{(1/3)m_{D_{1/2}}(m_{D_{1/2}}(E_l+E_q) - \frac{1}{2}m_{D_{1/2}}^2 + \frac{1}{2}m_{\tilde{\gamma}}^2)}{(K^2 - m_{D_0^c}^2)} \\
&\times \left[\frac{m_{D_{1/2}} - 2E_q}{(P^2-m_{\tilde{e}_L}^2)} + \frac{(m_{D_{1/2}} - 2E_l)(1/3)}{(P^2-m_{\tilde{d}_L}^2)} + \frac{(m_{D_{1/2}} - 2E_l)(-2/3)}{(P^2-m_{\tilde{u}_L}^2)}\right]\} \\
&+ \lambda_E^2(\sqrt{2}e)^2 12 \\
&\times \{\frac{(-2/3)^2 m_{D_{1/2}}E_l(\frac{1}{2}m_{D_{1/2}}^2 - \frac{1}{2}m_{\tilde{\gamma}}^2 - m_{D_{1/2}}E_l)}{(P^2-m_{\tilde{u}_R}^2)^2} \\
&+ \frac{m_{D_{1/2}}E_q(\frac{1}{2}m_{D_{1/2}}^2 - \frac{1}{2}m_{\tilde{\gamma}}^2 - m_{D_{1/2}}E_q)}{(P^2-m_{\tilde{e}_R}^2)^2} \\
&- \frac{(-2/3)(2m_{D_{1/2}}^2 E_l E_q - m_{D_{1/2}}^2(E_l+E_q) - \frac{1}{2}m_{D_{1/2}}^2 + \frac{1}{2}m_{\tilde{\gamma}}^2))}{(P^2-m_{\tilde{e}_R}^2)(P^2-m_{\tilde{u}_R}^2)} \\
&+ \frac{(1/3)^2 m_{D_{1/2}}(m_{D_{1/2}} - E_q - E_l)(m_{D_{1/2}}(E_l+E_q) - \frac{1}{2}m_{D_{1/2}}^2 + \frac{1}{2}m_{\tilde{\gamma}}^2)}{(K^2 - m_{D_0}^2)^2}\},
\end{aligned}
\tag{3.155}
$$

where:

$$
P^2 = m_{D_{1/2}}(m_{D_{1/2}} - 2E_{l,q}), \quad K^2 = 2E_l E_q(1-\cos\omega), \tag{3.156}
$$

ω is the angle between the final-state quark and lepton, E_q and E_l are their energies and $d\Gamma$ is given again by eq. (3.151). In the simplifying limit where $m_{D_{1/2}} << m_{\tilde{l}}, m_{\tilde{q}}$, we find

$$
\begin{aligned}
\Gamma &= \frac{1}{(2\pi)^3}\frac{m_{D_{1/2}}^5}{192} \\
&\times \{\lambda_L^2(\sqrt{2}e)^2 12[\frac{1}{m_{\tilde{e}_L}^4} - \frac{(2/3)^2}{m_{\tilde{u}_L}^4} - \frac{(-1/3)^2}{m_{\tilde{d}_L}^4} - \frac{2(2/3)^2}{m_{\tilde{u}_L}^2 m_{\tilde{e}_L}^2}] \\
&+ \lambda_E^2(\sqrt{2}e)^2 12[\frac{(-2/3)^2}{m_{\tilde{u}_R}^4} + \frac{1}{m_{\tilde{e}_R}^4} + \frac{2(-2/3)}{m_{\tilde{e}_R}^2 m_{\tilde{u}_R}^2}]\},
\end{aligned}
\tag{3.157}
$$

which is used in calculating signatures for $D_{1/2}$ production in the next subsection.

Couplings to quark-conjugate neutrino pairs

Finally, we turn to the case (3.145). Since in our model there is no D/d mixing, there is no single production of scalar D in either hadron-hadron or electron-hadron collisions. The dominant decays of the D_0 are to $d_R + \overline{\nu^c}$, which would have the same experimental missing-energy signature as conventional squark $\tilde{q} \rightarrow q + \tilde{\gamma}$ decay. The dominant decays of the $D_{1/2}$ in this case are to $d_R + \overline{\nu^c} + \tilde{\gamma}$ via the squared amplitude

$$|\mathcal{M}_{D_{1/2}}|^2 = \lambda_\nu^2(\sqrt{2}e)^2 12 \frac{(1/3)^2 m_{D_{1/2}} E_\nu (\frac{1}{2}m_{D_{1/2}}^2 - \frac{1}{2}m_{\tilde{\gamma}}^2 - m_{D_{1/2}}E_\nu)}{(P^2 - m_{\tilde{u}_R}^2)^2}, \tag{3.158}$$

$$P^2 = m_{D_{1/2}}(m_{D_{1/2}} - 2E_\nu), \tag{3.159}$$

where we have already taken the simplifying limit $m_{D_{1/2}} << m_{\tilde{l}}, m_{\tilde{q}}$ which is used in the phenomenological analysis of its missing energy signature in the following subsection.

3.5.3 Pair production in hadron-hadron collisions

In this subsection we discuss the possible cross sections and signatures for $p^{(}\overline{p}) \rightarrow D_0\overline{D_0}/D_0^c\overline{D_0^c} + X$ and $D_{1/2}\overline{D_{1/2}} + X$.

Cross sections

The forms of the parton-parton cross sections for $gg, \overline{q}q \rightarrow D_0\overline{D_0}/D_0^c\overline{D_0^c}$ are identical to those of $gg, \overline{q}q \rightarrow \tilde{q}\overline{\tilde{q}}$ if one compares the limits $m_{D_{1/2}} >> m_{D_0, D_0^c}$ and $m_{\tilde{g}} >> m_{\tilde{q}}$, due to the fact that $D_0/\overline{D_0^c}$ couplings to gluons are identical to those of $\tilde{q}$. The only difference between the total cross sections in these limits is therefore an overall combinatorial factor counting the total number of $D_0, \overline{D_0^c}$ or $\tilde{q}$ species. Previous works [65] generally assumed 5 approximately degenerate flavours of squarks($\tilde{u}$, $\tilde{d}$, $\tilde{s}$, $\tilde{c}$ and $\tilde{b}$) and added together both left- and right-handed quarks. Here we add together the $D_0/\overline{D_0^c}$ scalars expected from three generations. In this case, $\sigma(D_0\overline{D_0}/D_0^c\overline{D_0^c})/\sigma(\tilde{q}\overline{\tilde{q}}) = 3/5$.

The forms of the parton-parton cross sections for $gg, \bar{q}q \rightarrow D_{1/2}\overline{D_{1/2}}$ are identical to those of $gg, \bar{q}q \rightarrow \bar{t}t$ if one considers the limit $m_{D_0, D_0^c} >> m_{D_{1/2}}$. Equivalently, these parton-parton cross sections can be obtained from those for $gg, \bar{q}q \rightarrow \tilde{g}\tilde{g}$ in the limit $m_{\tilde{q}} >> m_{\tilde{g}}$ simply by adjusting the colour factors.

Possible signatures

As discussed in the previcus subsection, possible decays of the $D_0, \overline{D_0^c}$ are to $q\nu$, ql^- and $\overline{qq}$, while the $D_{1/2}$ may decay to $q\nu\tilde{\chi}$, $ql^-\tilde{\chi}$ or $\overline{qq}\tilde{\chi}$, where the $\tilde{\chi}$ is a weakly interacting neutral Majorana fermion similar to the photino, which can carry off missing energy. We therefore have the following possible event signatures:
Missing energy:

$$D_0\overline{D_0}/D_0^c\overline{D_0^c} \rightarrow (q\nu)(\overline{q\nu}) \tag{3.160}$$

$$D_{1/2}\overline{D_{1/2}} \rightarrow (\overline{qq}\tilde{\chi})(qq\tilde{\chi}) \;\; or \;\; (q\nu\tilde{\chi})(\overline{q\nu}\tilde{\chi}) \tag{3.161}$$

Charged lepton pairs:

$$D_0\overline{D_0}/D_0^c\overline{D_0^c} \rightarrow (ql^-)(\bar{q}l^+) \tag{3.162}$$

Leptons and missing energy:

$$D_{1/2}\overline{D_{1/2}} \rightarrow (ql^-\tilde{\chi})(\bar{q}l^+\tilde{\chi}) \tag{3.163}$$

Dijet mass bumps:

$$D_0\overline{D_0}/D_0^c\overline{D_0^c} \rightarrow (\overline{qq})(qq) \tag{3.164}$$

While the semileptonic decay of one D is not compatible with the simultaneous hadronic decay of another D, it is in principle possible to mix the semileptonic decay into a charged lepton of one D with the neutrino decay of another D. However, we will not discuss such dijet + lepton + missing energy final states. Nor we will discuss final states with two charged leptons of different flavours: $e^{\pm}\mu^{\mp}$, $e^{\pm}\tau^{\mp}$, $\mu^{\pm}\tau^{\mp}$. We concentrate on the missing energy signatures and on the charged lepton pair signatures. We present here results for $p\bar{p}$ collisions at $\sqrt{s} = 630GeV$

corresponding to the CERN collider, and $1600GeV$ corresponding to the Fermilab collider: results for pp collisions at $\sqrt{s} = 17TeV$ corresponding to the LHC will be presented elsewhere.

Missing energy signatures

To discuss these quantitatively we have used the same approach as in previous work on UA1 data. We divide missing energy events into the following categories. Monojets: only one cluster of hadronic energy within $\Delta R = \sqrt{(\Delta\Phi)^2 + (\Delta\eta)^2} = 1$ above a threshold of $E_T = 12GeV$, and missing transverse momentum p_T in excess of 4σ, where the measurement error $\sigma = 0.7\sqrt{E_T(GeV)}$; dijets: two such jet clusters and $p_T > 4\sigma$; trijets: three such jets, etc.. Our calculations include a somewhat more subtle characterization of the UA1 detector which is described in previous publications. However, a full description of the assignments of missing energy events to different categories is impossible in the absence of a full detector simulation. Therefore in this work we restrict ourselves to quoting cross sections for monojet events and multijet events, and emphasize that a realistic detector may shuffle events between these two categories.

$D_0/\overline{D_0^c} \rightarrow q\nu$. The signature for this decay is identical to that previously discussed for $\tilde{q} \rightarrow q\tilde{\gamma}$ with $m_{\tilde{\gamma}} = 0$. Figure 3.17a contains our predictions for monojets and multijets[4] from $D_0\overline{D_0}/D_0^c\overline{D_0^c}$ production at $\sqrt{s} = 630GeV$ including the factor of 3/5 in the cross section which was mentioned previously. The horizontal lines correspond to $\sigma = 7pb$ (solid line: five events in the present event sample of about $700nb^{-1}$), $\sigma = 1.4pb$ (dashed line: corresponding to one event in the present sample) and $\sigma = 0.28pb$ (dotted line: corresponding to perhaps five events at the $p\bar{p}$ collider with ACOL). We believe that a lower limit on the D_0/D_0^c mass could only be established by the UA1 collaboration itself. If it would establish an upper limit of five multijet events in the present data, that would correspond

[4]Note that in this and the next case the vast majority of multijet events only contain two jets.

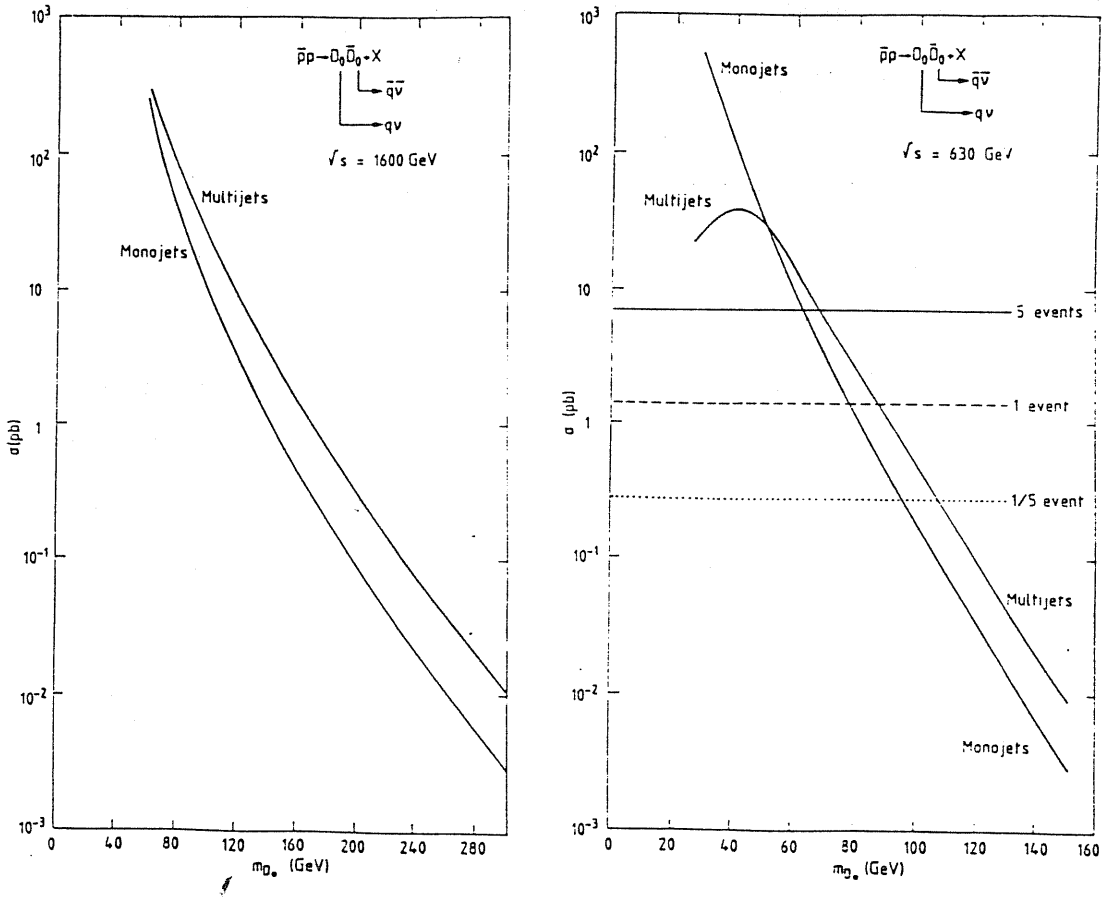

Figure 3.17: Total cross section for monojets and multijets from pairs of D-scalars having the quantum numbers of quark-neutrino pairs at the CERN (a) and Fermilab (b) colliders.

to $m_{D_0} \geq 60$ to $70GeV$. Figure 3.17b contains analogous cross section curves for $\sqrt{s} = 1600GeV$. At this energy, a sensitivity comparable to present CERN collider data would increase the possible limit to $m_{D_0} \geq 120$ to $130GeV$.

$\underline{D_{1/2} \to q\nu\tilde{\chi}}$. Here there is some additional ambiguity provided by the unknown mass of the $\tilde{\chi}$. The model analysis of the particle spectrum suggests that $m_{\tilde{\chi}} \geq 15GeV$, and it would be easily a large fraction of $m_{D_{1/2}}$. Therefore we plot in figure 3.18a our results for $\sqrt{s} = 630GeV$ as contours in the $(m_{D_{1/2}}, m_{\tilde{\chi}})$ plane corresponding to $\sigma = 7pb$ (solid lines), $1.4pb$ (dashed lines) and $0.28pb$ (dotted lines) as in fig. 3.17a. Naive interpolation between these contours will give cross sections accurate to better than a factor of 2, which is in any case the expected

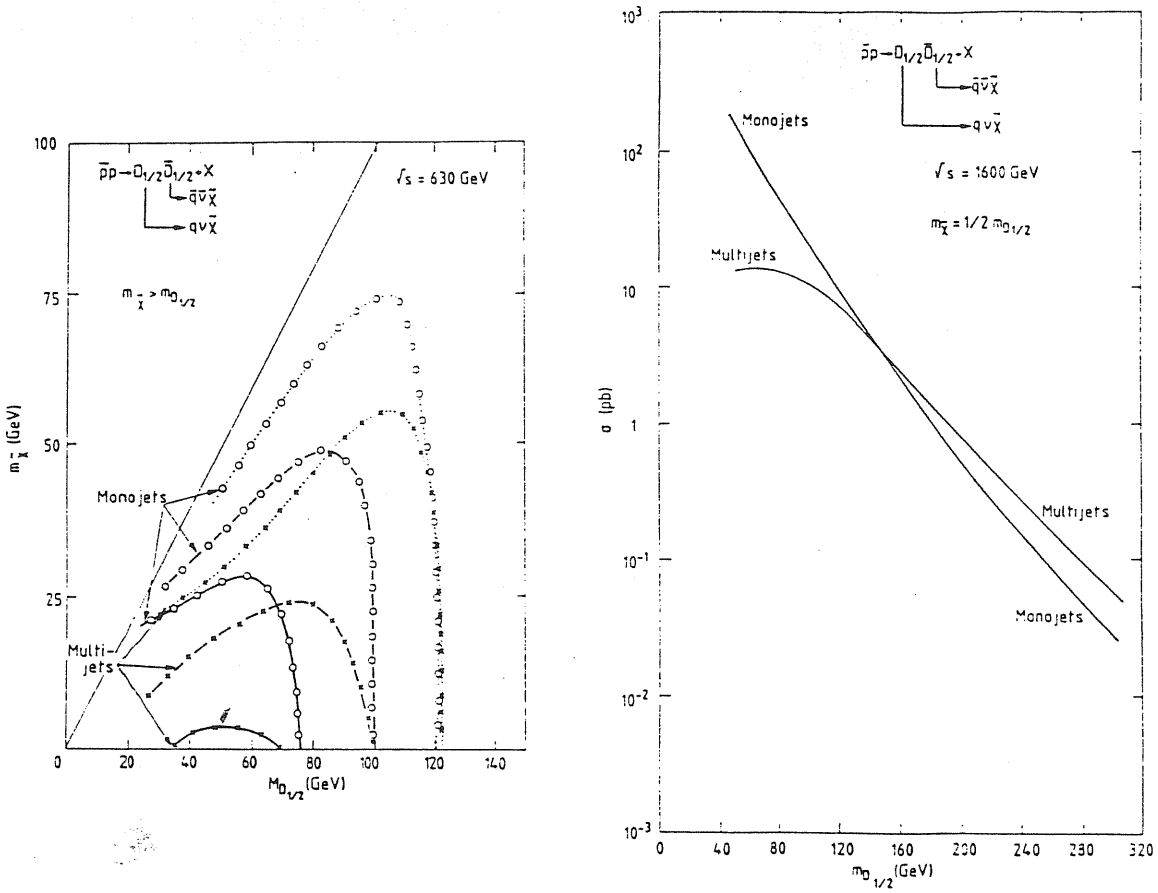

Figure 3.18: (*a*) Contours of cross sections for monojet (circles) and multijet (crosses) events from pair production of D-fermions with the quantum numbers of quark-neutrino pairs at the CERN collider; (*b*) total cross section for the same process at the Fermilab collider.

accuracy of our calculations. We see that monojets events are are always more copious than multijet events. We also see from fig. 3.18 that the UA1 sensitivity to $m_{D_{1/2}}$ is essentially unchanged for $0 \leq m_{\tilde{\chi}} \leq 15GeV$, but decreases significantly for larger $m_{\tilde{\chi}}$, and disappears in the limit $m_{\tilde{\chi}} \rightarrow m_{D_{1/2}}$. Less than five monojet events in the present UA1 data would correspond to $m_{D_{1/2}} \geq 70GeV$ if the $\tilde{\chi}$ is light, or $m_{\tilde{\chi}} \geq 50$ to $60GeV$ if $m_{\tilde{\chi}} = \frac{1}{2}m_{D_{1/2}}$. We plot in fig. 3.18b cross section curves for $\sqrt{s} = 1600GeV$ assuming for definiteness that $m_{\tilde{\chi}} = \frac{1}{2}m_{D_{1/2}}$. We see that a sensitivity comparable to present UA1 data would increase the possible limit to $m_{D_{1/2}} \geq 120GeV$.

$\underline{D_{1/2} \rightarrow \overline{q}q\tilde{\chi}}$. This is an alternative decay mode of the $D_{1/2}$ which has a signature similar to the conventional $\tilde{g} \rightarrow q\bar{q}\tilde{\gamma}$ decay, although the cross section is somewhat different and the mass of the $\tilde{\chi}$ may not be negligible. In fig. 3.19a we have plotted for $\sqrt{s} = 630GeV$ contours in the $(m_{D_{1/2}}, m_{\tilde{\chi}})$ plane corresponding to $\sigma = 7pb$ (solid lines), $1.4pb$ (dashed lines) and $0.28pb$ (dotted lines) as in fig. 3.18a. We see that the multijet cross sections are larger for low $m_{\tilde{\chi}}$ and large $m_{D_{1/2}}$, while the monojet cross sections are larger for bigger $m_{\tilde{\chi}}$. Thus monojet and multijet searches to some extent complement each other. An upper limit of five multijet events in the present data would correspond to $m_{D_{1/2}} \geq 80GeV$ for $m_{\tilde{\chi}} \leq 20GeV$, while an upper limit of five monojet events in the present data would correspond to $m_{D_{1/2}} \geq 60GeV$ if $m_{\tilde{\chi}} = \frac{1}{2}m_{D_{1/2}}$. Cross section curves for $\sqrt{s} = 1600GeV$ and $m_{\tilde{\chi}} = \frac{1}{2}m_{D_{1/2}}$ are plotted in figure 3.19b. Here we see that a multijet sensitivity comparable to that presently achieved by UA1 would reach $m_{D_{1/2}} \sim 150GeV$.

Charged lepton signatures

Taking our cue again from UA1, we have taken the following cuts on charged leptons: $|\eta_1| < 1.3$, $|\eta_2| < 2.0$, $m_{l^+l^-} > 6GeV$ and $p_T^{l_1}, p_T^{l_2} > 3GeV$ for muons, $p_T^{l_1}, p_T^{l_2} > 8GeV$ for electrons. We have also tried the effects of the isolation cuts:

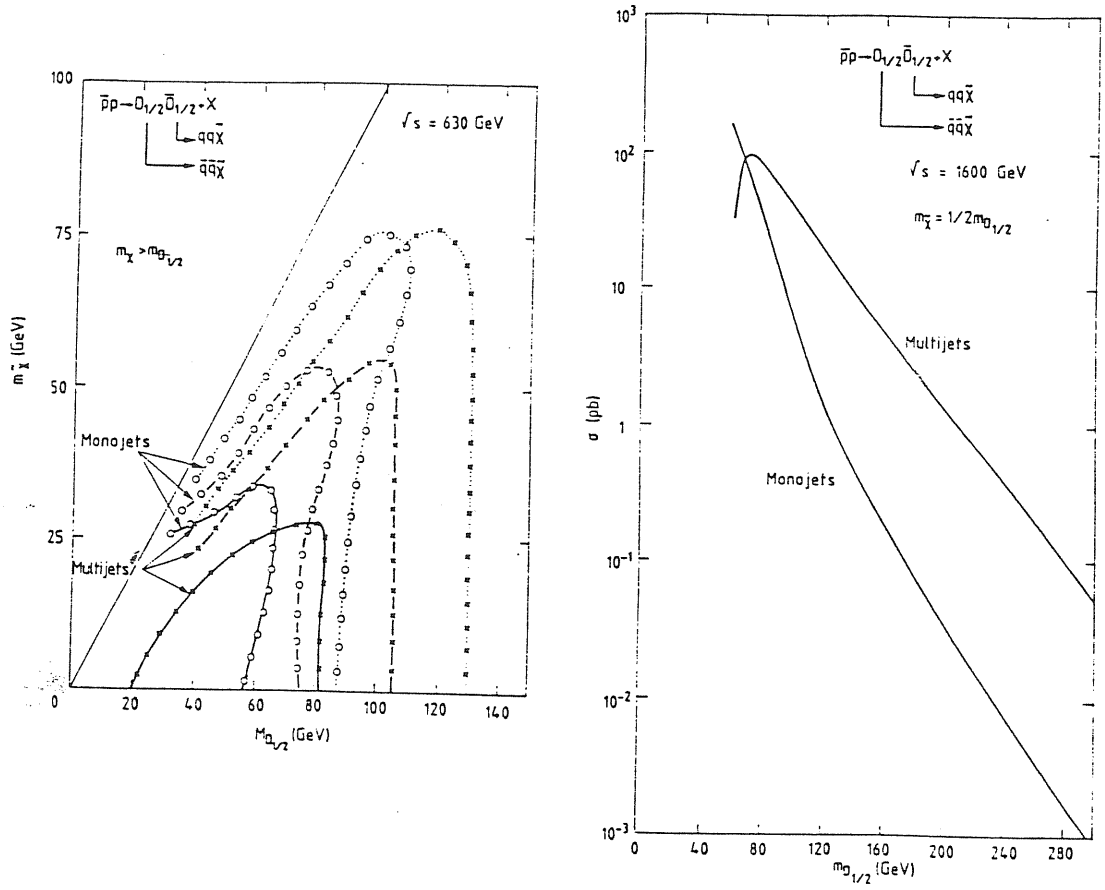

Figure 3.19: As in the previous figure for D-fermions having the quantum numbers of diquarks.

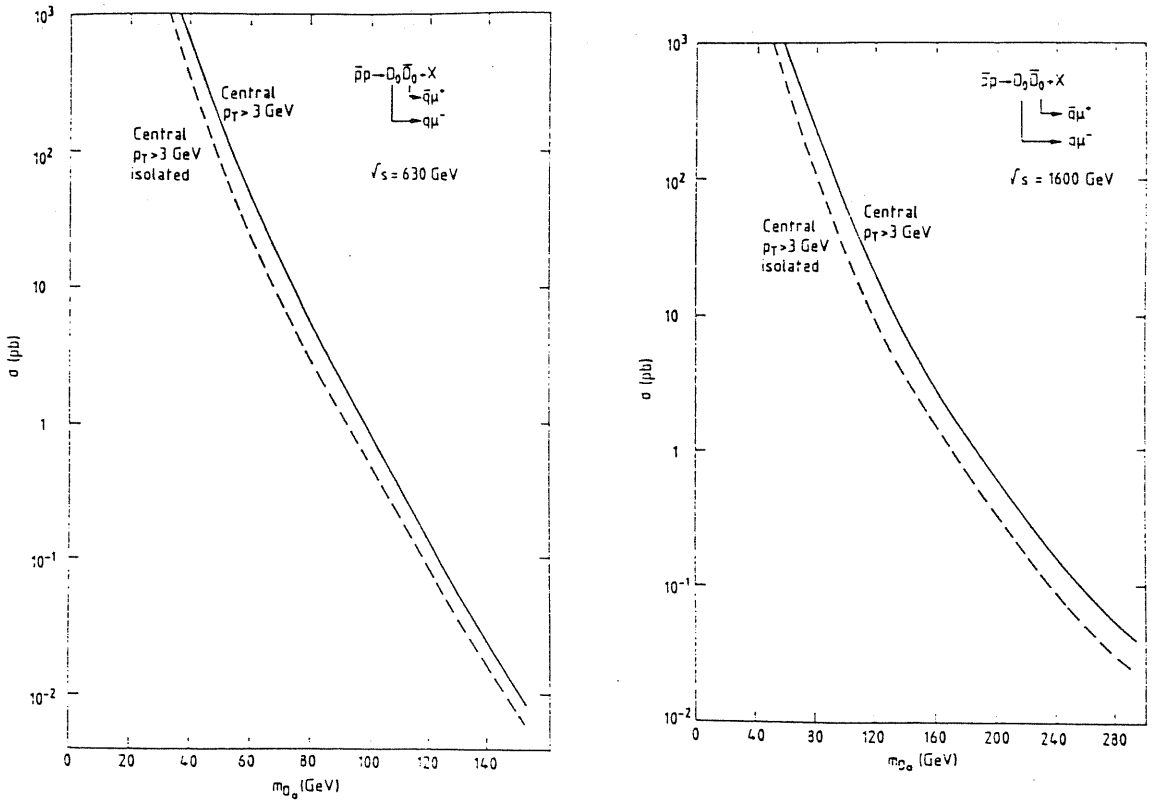

Figure 3.20: Total cross section for production of pairs of D-scalars with the quantum numbers of charged lepton-quark pairs at the CERN (a) and Fermilab (b) colliders. The centrality and isolation cuts are specified in the text.

$(\Sigma_{1,2}E_T^2) < 9GeV^2$ in the combination of cores with $\Delta R \equiv \sqrt{(\Delta\Phi)^2 + (\Delta\eta)^2} < 0.7$ around the two charged leptons. Thus we quote cross sections for $(\mu^+\mu^-)$ both total and isolated, and similarly for (e^+e^-) pairs.

$\underline{D_0/\overline{D_0^c} \to ql}$. Our results at $\sqrt{s} = 630GeV$ are shown in fig. 3.20a. The total (solid line) and isolated (dashed line) curves are for $\mu^+\mu^-$ pairs. The e^+e^- cross sections are indistinguishable for $m_{D_0} \geq 60GeV$ and differ by less than 10% even for $m_{D_0} = 40GeV$. Note that here we have assumed a 100% branching ratio into $q\mu^-$ for each of the three generations of $D_0/\overline{D_0^c}$ particles. This is probably unreasonable, a better guess being that at most one of the three generations of $D_0/\overline{D_0^c}$ particles would have a large branching ratio into $q\mu^-$. In this case, the cross sections in fig. 3.20 should be reduced by a factor of 3. Taking this point of view, an upper limit of five events in the present UA1 event sample would correspond to

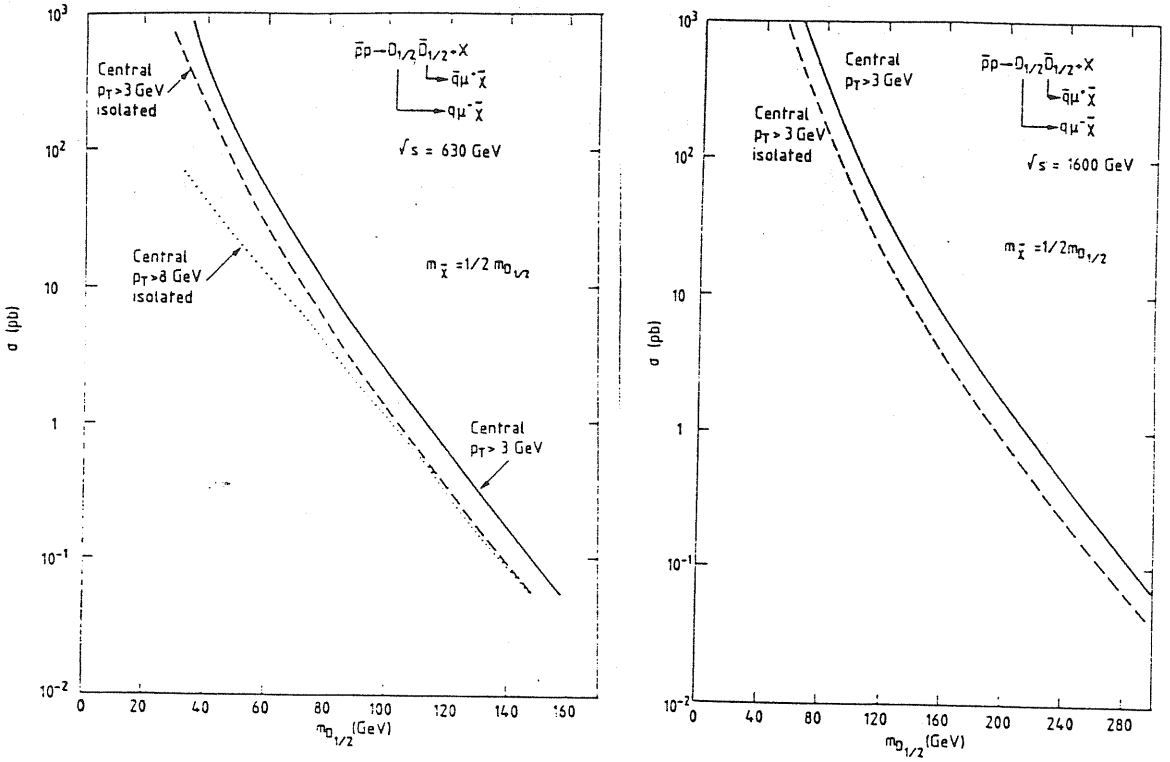

Figure 3.21: Same as in the previous figure for pairs of D-fermions.

$m_{D_0} \geq 60$ to $70GeV$. Corresponding cross sections for $\sqrt{s} = 1600GeV$ are shown in fig. 3.20b. A sensitivity comparable to UA1's present achievement would then yield $m_{D_0} \geq 140GeV$.

$\underline{D_{1/2} \to ql\tilde{\chi}}$. Here we meet again the ambiguity in the mass of the $\tilde{\chi}$. If these events are treated simply as possible missing energy events, and no attempt is made to identify the charged leptons, then the result of fig. 3.19 are directly applicable. Alternatively, they could be analyzed as (l^+l^-) events with no attempt made to measure missing energy. In this case, their signature would be similar to that of $D_0/\overline{D_0^c} \to ql$. Fig. 3.21a and 3.21b show cross section curves at $\sqrt{s} = 630GeV$ and $1600GeV$ respectively, assuming $m_{\tilde{\chi}} = \frac{1}{2}m_{D_{1/2}}$. We see from fig. 3.21a that an upper bound of five events in the present UA1 sample would yield $m_{D_{1/2}} \geq 80GeV$, while comparable sensitivity at the Fermilab collider would yield $m_{D_{1/2}} \geq 160GeV$.

Chapter 4

New Z Bosons from E_6

In this chapter we shall consider the possibility of an extra neutral gauge boson, Z' (in addition to the photon and the Z of the standard model), with mass in the range 100 GeV–few TeV, associated to a flavour-conserving neutral current of E_6. Superstrings are the most recent theoretical motivation for such a study, but not the only one: even conventional grand unification in a simple group of rank higher than four, like $SO(10)$ or E_6, can give rise to a scenario of this type. We shall therefore try to perform our analysis, as far as possible, in a model-independent way.

In section 4.1 a convenient parametrization will be introduced [66], assuming only unification in E_6 or a subgroup of it [thus including, for example, the case of $SO(10)$]. Section 4.2 will examine the structure of the neutral gauge boson mass matrix [67], exploring possible constraints on masses and mixing angles. Section 4.3 will collect the present experimental data on neutral currents in a suitable set of phenomenological parameters [68]. In section 4.4 we will extract from them the corresponding limits on the mass and the mixing of the new Z in the case of three representative superstring-inspired models [68]. The possibilities for detecting signals of a Z' at present and future colliders will be reviewed in section 4.5, where a detailed analysis [66,67] of the expectations for hadronic colliders will be presented.

	γ	Z^0
v^u	$\frac{2}{3}e$	$\frac{e}{s_W c_W}\left(\frac{1}{4}-\frac{2}{3}s_W^2\right)$
a^u	0	$-\frac{e}{s_W c_W}\frac{1}{4}$
v^d	$-\frac{1}{3}e$	$\frac{e}{s_W c_W}\left(-\frac{1}{4}+\frac{1}{3}s_W^2\right)$
a^d	0	$\frac{e}{s_W c_W}\frac{1}{4}$
v^e	$-e$	$\frac{e}{s_W c_W}\left(-\frac{1}{4}+s_W^2\right)$
a^e	0	$\frac{e}{s_W c_W}\frac{1}{4}$
v^ν	0	$\frac{e}{s_W c_W}\frac{1}{4}$
a^ν	0	$-\frac{e}{s_W c_W}\frac{1}{4}$

Table 4.1: Standard model couplings of the known fermions ($u \equiv u, c, t$; $d \equiv d, s, b$; $e \equiv e, \mu, \tau$; $\nu \equiv \nu_e, \nu_\mu, \nu_\tau$) to the electroweak gauge bosons γ and Z^0.

4.1 General parametrization

Since E_6 has rank $r = 6$, there can be at most four gauge bosons, neutral under $SU(3)_C \times U(1)_Q$, associated to flavour-conserving currents. The most general form of the corresponding lagrangian is:

$$\mathcal{L}_{NC} = \overline{\psi}^k \gamma_\mu (v_\alpha^k + a_\alpha^k \gamma_5) \psi^k Z_\alpha^\mu, \tag{4.1}$$

where summation over repeated indices is understood and $Z_\alpha (\alpha = 1, \ldots, N; 2 \leq N \leq 4)$ stand for the physical vector bosons of definite mass M_α and width Γ_α: $\alpha = 1$ corresponds to the photon ($M_1 = 0, \Gamma_1 = 0$), $\alpha = 2$ to the observed Z ($M_2 = 92.6 \pm 1.7 GeV, \Gamma_2 < 4.6 GeV$), $\alpha = 3, 4$ to possible extra gauge bosons. The index k runs over the different fermions. For the standard model $N = 2$, and the corresponding vector and axial couplings $v_\alpha^k, a_\alpha^k (\alpha = 1, 2)$ for the observed quarks and leptons are given in table 4.1. Here and in the following we adopt the conventions $\gamma \equiv s_W A_3 + c_W B$ and $Z^0 \equiv c_W A_3 - s_W B$, where $s_W \equiv \sin\theta_W$, $c_W \equiv \cos\theta_W$ and A_3 and B are the gauge bosons associated to T_{3L} and Y, respectively. Finally, e denotes the (running) positron charge.

A convenient way of parametrizing the neutral current lagrangian (4.1) is to

	T_{3L}	$\sqrt{\frac{5}{3}}Y$	$\sqrt{\frac{5}{3}}Y'$	Y''
$\begin{pmatrix} u_L \\ d_{1L} \end{pmatrix}$	$\begin{pmatrix} 1/2 \\ -1/2 \end{pmatrix}$	1/6	1/3	0
d_{2L}	0	−1/3	−2/3	0
u^c_L	0	−2/3	1/3	0
d^c_{1L}	0	1/3	−1/6	1/2
d^c_{2L}	0	1/3	−1/6	−1/2
$\begin{pmatrix} \nu_{1L} \\ e_{1L} \end{pmatrix}$	$\begin{pmatrix} 1/2 \\ -1/2 \end{pmatrix}$	−1/2	−1/6	1/2
$\begin{pmatrix} \nu_{2L} \\ e_{2L} \end{pmatrix}$	$\begin{pmatrix} 1/2 \\ -1/2 \end{pmatrix}$	−1/2	−1/6	−1/2
$\begin{pmatrix} e^c_{2L} \\ \nu_{3L} \end{pmatrix}$	$\begin{pmatrix} 1/2 \\ -1/2 \end{pmatrix}$	1/2	−2/3	0
e^c_{1L}	0	1	1/3	0
ν_{4L}	0	0	5/6	−1/2
ν_{5L}	0	0	5/6	1/2

Table 4.2: Action of the orthogonal basis (T_{3L}, Y, Y', Y'') for E_6 neutral currents on the fundamental representation, 27.

rewrite it in the following form:

$$\mathcal{L}_{NC} = J_{\mu\beta} C_{\beta\alpha} Z^{\mu}_{\alpha}, \tag{4.2}$$

where: $J_{\mu\beta} = \overline{\psi_L}^k \gamma_\mu T^{kk}_\beta \psi^k_L$ [all fields are taken to be left-handed, $L \equiv (1-\gamma_5)/2$] are four fixed (diagonal) neutral currents with properly normalized orthogonal generators, obtained by expanding the $SU(3)_C \times U(1)_Q$-neutral E_6 Cartan subalgebra. We choose for convenience T_β to be T_{3L}, Y, Y', Y'' (their action on the E_6 fundamental representation is given in table 4.2) . Then, all the model-dependence (apart from the fermion assignments in the currents $J_{\mu\beta}$, which will be discussed later) is carried by the $4 \times N$ entries of the matrix $C_{\beta\alpha}$.

Let us consider, for the sake of simplicity, the case in which only one extra gauge boson (Z_3) survives at low energy: the extension to the case of two extra gauge bosons can be found in ref. [66] . Then the index α in (4.2) runs from 1 to 3 and we can call it j, and $C_{\beta j}$ are 12 model-dependent parameters. An equivalent

set of parameters is obtained by writing

$$C_{\beta j} = O_{\beta i}\tilde{g}_i O'_{ij} \quad (\beta = 1,2,3,4;\ \ i,j = 1,2,3), \tag{4.3}$$

where $O_{\beta i}$ are the first three columns of a 4×4 orthogonal matrix, $\tilde{g}_i$ is a 3×3 diagonal matrix and O'_{ij} is a 3×3 orthogonal matrix, providing altogether an equivalent set of $6+3+3 = 12$ parameters. In the absence of intermediate breaking scales, the matrices O, $\tilde{g}$ and O' have a definite physical meaning. $O_{\beta i}$ defines the rotation from the E_6 current basis conventionally chosen to the one which is multiplicatively renormalized and $\tilde{g}_i$ defines the corresponding renormalized gauge coupling constants. O'_{ij} is the rotation diagonalizing the gauge boson mass matrix. In E_6 superstring-inspired models, the set of 12 free parameters reduces to three when the different physical constraints are taken into account. Actually,

$$O_{\beta i} \equiv \begin{matrix} T_{3L} \\ Y \\ Y' \\ Y'' \end{matrix} \begin{pmatrix} 1 & 0 & 0 \\ 0 & c_1 & s_1 \\ 0 & -s_1 c_2 & c_1 c_2 \\ 0 & s_1 s_2 & -c_1 s_2 \end{pmatrix} \quad \left(-\frac{\pi}{2} \leq \theta_{1,2} < \frac{\pi}{2}\right), \tag{4.4}$$

depends on two angles $\theta_{1,2}$ ($c_{1,2} \equiv \cos\theta_{1,2}$, $s_{1,2} \equiv \sin\theta_{1,2}$) instead of six, because $SU(2)_L$ is a good symmetry at low energy and T_{3L} does not mix with other generators. Besides the remaining two currents must include the hypercharge Y, and a combination $\hat{Y}$ of the other two E_6 currents fixed by θ_2, $\hat{Y} \equiv c_2 Y' - s_2 Y''$. The orthogonal generator $s_2 Y' + c_2 Y''$ is assumed to be broken at high energy and the associated current decouples from the low-energy theory. The mixing of Y with $\hat{Y}$ is given by θ_1: a non-zero θ_1 can be generated by renormalization of gauge couplings in presence of incomplete matter representations, or if there is rescaling of gauge couplings at the compactification scale. Moreover, as we argue below, θ_2 can only take two different values, depending on the mechanism lowering the rank of E_6: $c_2 = 1$, $s_2 = 0$ for non-abelian flux breaking and $c_2 = \sqrt{3/8}$, $s_2 = \sqrt{5/8}$ for a large VEV of one of the standard model singlets in the $(27 + \overline{27})$. Out of the three coupling constants $\tilde{g}_i$, only one is not fixed, but it is in principle calculable

and its order of magnitude known. If charged currents are described by $SU(2)_L$,

$$\tilde{g}_1^2 \equiv g_{SU(2)_L}^2 = \frac{G_F}{\sqrt{2}} 8 M_W^2 \tag{4.5}$$

is fixed by the measured M_W mass and by the Fermi constant G_F. The running positron electric charge e can be used to fix one combination of the other two couplings,

$$\frac{c_1^2}{\tilde{g}_2^2} + \frac{s_1^2}{\tilde{g}_3^2} = \frac{3}{5}\left(\frac{1}{e^2} - \frac{1}{\tilde{g}_1^2}\right). \tag{4.6}$$

We choose the remaining free parameter to be

$$\lambda \equiv \frac{\tilde{g}_2}{\tilde{g}_3}, \tag{4.7}$$

which is a number of order one in any realistic model. In the simple case $\theta_1 = 0$, $\tilde{g}_2$ and $\tilde{g}_3$ have a clear physical meaning: $\tilde{g}_2 = g_Y$, $\tilde{g}_3 = g_{\hat{Y}}$. The fact that the photon must couple to the electric charge $Q = T_{3L} + Y$ always allows us to decompose O' as

$$O'_{ij} \equiv \begin{pmatrix} s'_1 & c'_1 & 0 \\ c'_2 c'_1 & -c'_2 s'_1 & s'_2 \\ s'_2 c'_1 & -s'_2 s'_1 & -c'_2 \end{pmatrix} \begin{pmatrix} 1 & 0 & 0 \\ 0 & c_3 & s_3 \\ 0 & -s_3 & c_3 \end{pmatrix}, \tag{4.8}$$

with

$$s'_1 = s_W = \frac{e}{\tilde{g}_1}, \quad c'_1 = c_W, \tag{4.9}$$

$$s'_2 = \sqrt{\frac{5}{3}} \frac{e s_1}{c_W \tilde{g}_3}, \quad c'_2 = \sqrt{\frac{5}{3}} \frac{e c_1}{c_W \tilde{g}_2} \tag{4.10}$$

and

$$c_3 \equiv \cos\theta_3, \quad s_3 \equiv \sin\theta_3, \quad -\frac{\pi}{2} \leq \theta_3 < \frac{\pi}{2}. \tag{4.11}$$

[We have chosen to parametrize O' in such a way that for $\theta_3 = 0$ the second column of $C_{\beta j}$ corresponds to the standard Z^0 current. This greatly simplifies physical applications]. If the Higgs sector lies in fundamental E_6 representations, as happens in the models we consider, then θ_3 is known up to a sign in terms of the standard model prediction $M_{Z^0}^2 = M_W^2/c_W^2$ and of the neutral gauge bosons masses $M_{2,3}$, as will be explained in the following section. Finally, we comment

C_{11}	=	e
C_{12}	=	$\frac{ec_W}{s_W}c_3$
C_{13}	=	$\frac{ec_W}{s_W}s_3$
C_{21}	=	$\sqrt{\frac{5}{3}}e$
C_{22}	=	$-\sqrt{\frac{5}{3}}\frac{e}{c_W}[c_3 s_W + s_3 s_1 c_1(\lambda - 1/\lambda)]$
C_{23}	=	$-\sqrt{\frac{5}{3}}\frac{e}{c_W}[s_3 s_W - c_3 s_1 c_1(\lambda - 1/\lambda)]$
C_{31}	=	0
C_{32}	=	$\sqrt{\frac{5}{3}}\frac{e}{c_W}s_3(c_1^2/\lambda + \lambda s_1^2)c_2$
C_{33}	=	$-\sqrt{\frac{5}{3}}\frac{e}{c_W}c_3(c_1^2/\lambda + \lambda s_1^2)c_2$
C_{41}	=	0
C_{42}	=	$-\sqrt{\frac{5}{3}}\frac{e}{c_W}s_3(c_1^2/\lambda + \lambda s_1^2)s_2$
C_{43}	=	$\sqrt{\frac{5}{3}}\frac{e}{c_W}c_3(c_1^2/\lambda + \lambda s_1^2)s_2$

Table 4.3: Neutral current couplings for the photon, $C_{\alpha 1}$, the observed Z, $C_{\alpha 2}$, and a new (E_6) gauge boson Z_3, $C_{\alpha 3}$, in the current basis of table 4.2.

on the range of variation of $\theta_{1,2,3}$ and λ. It is not restrictive to assume that $-\pi/2 \leq \theta_{1,2,3} < \pi/2$, noting that the global sign of c_1, s_1 does not enter $C_{\beta j}$ and that the sign of $J_\beta O_{\beta i}\tilde{g}_i O'_{ij}$ cannot be measured. On the other hand, we can assume $\lambda \geq 1$, because interchanging $\tilde{g}_2$ and $\tilde{g}_3$ amounts to redefining θ_1 ($\theta_1 \to \theta_1 \pm \pi/2$).

In summary, the 12 model-dependent numbers $C_{\beta j}$ can be parametrized in terms of two angles $\theta_{1,2}$ (although θ_2 can only take two different values) and a ratio of coupling constants λ: their explicit expressions are given in table 4.3. To determine completely the lagrangian (4.2), the masses of the gauge bosons $Z_{2,3}$ have to be specified [M_2 has already been measured], as well as the fermion assignments in the currents J_β.

We now discuss the fermion assignments in the J_β currents entering the lagrangian of eq. (4.2). A more detailed discussion can be found in ref. [51]. Out of the many angles which can be introduced to describe the mixing of all fermions with the same $SU(3)_C \times U(1)_Q$ quantum numbers in E_6 superstring-inspired models, we will consider only one. Its precise determination, as that of other poorly

known angles, requires the study of the interactions of the new fermions expected in these models. This is not our concern here.

Matter fields lie in fundamental representations, 27, of E_6, whose field content has been given in table 4.2. We assume, as suggested by the smallness of flavour-changing neutral currents, that the fermion assignments within the 27 are the same for all generations. Moreover, it is believed that a good approximation to the pattern of fermion masses can be obtained as a result of large $\Delta T_L = 0$ [$SU(2)_L$ invariant] masses and small $\Delta T_L = \frac{1}{2}$ [$SU(2)_L$ breaking] masses. In that case, three angles are required to describe the mixing within the 27, which rotate $d^c_{1,2L}$, $(\nu_{1,2L}\ \ e_{1,2L})$ and $\nu_{4,5L}$ respectively. We will only consider the common angle defined by the rotation of the current eigenstates $f^c_{1(2)} = [d^c_{1(2)L}, (\nu_{1(2)L}, e_{1(2)L}), \nu_{5(4)L}]$ in table 4.2 to the mass eigenstates $f_{1(2)}$,

$$\begin{pmatrix} f_1 \\ f_2 \end{pmatrix} = \begin{pmatrix} \cos\beta & \sin\beta \\ -\sin\beta & \cos\beta \end{pmatrix} \begin{pmatrix} f^c_1 \\ f^c_2 \end{pmatrix}, \tag{4.12}$$

fixing to zero the other two angles. In the above equation $f_{1(2)}$ stands for known (new) fermions, and $\beta = 0$ corresponds to the standard assignments of known fermions in the $[16]_{SO(10)} \in [27]_{E_6}$.

Taking β into account, the E_6 superstring-inspired models with one extra gauge boson introduced before can be described by only two values of θ_2. They correspond to the two known ways of going from E_6 to a low-energy group $SU(3)_C \times SU(2)_L \times U(1) \times U(1)$. One is non-abelian flux breaking, which lowers the rank by one unit and implies $\theta_2 = 0$. The second one is abelian flux breaking, which conserves the rank, followed by Higgs breaking at a large scale. For Higgs breaking, we have only two $SU(2)_L \times U(1)_Y$ singlets at our disposal in the fundamental 27 representation of E_6, $\tilde{\nu_4}$ and $\tilde{\nu_5}$ [1]. These two singlets form an $SU(2)_N$ doublet, where $SU(2)_N$ is an E_6 subgroup which commutes with the standard model subgroup, already introduced in chapter 2. For the rank-6 group H surviving after compactification

[1] θ_2 is arbitrary in E_6 models with arbitrary Higgs sectors.

there are two alternatives: H contains or does not contain $SU(2)_N$. In the first case, one can assume without loss of generality that $<\tilde{\nu}_4>=0$ and $<\tilde{\nu}_5>\neq 0$. This configuration can be reached from any combination with $<\tilde{\nu}_4>\neq 0$, $<\tilde{\nu}_5>\neq 0$ by means of a suitable $SU(2)_N$ transformation. Therefore, using the quantum number assignments in table 4.1, one finds $c_2=\sqrt{3/8}$, $s_2=\sqrt{5/8}$. In the second case, if one starts from $<\tilde{\nu}_4>\neq 0$, $<\tilde{\nu}_5>\neq 0$, the rotation considered before is no longer allowed, because $SU(2)_N$ is broken and $\tilde{\nu}_4$ and $\tilde{\nu}_5$ have different quantum numbers under the residual group H. Therefore, since we are interested in lowering the rank only by one unit, we have to assume that either $\tilde{\nu}_4$ or $\tilde{\nu}_5$ acquires a non-vanishing VEV, but not both. The two cases are equivalent, as we prove now. Using eq. (4.12), one can see that any model with $<\tilde{\nu}_4>=0$, $<\tilde{\nu}_5>\neq 0$ and given β is equivalent to a model with $<\tilde{\nu}_4>\neq 0$, $<\tilde{\nu}_5>=0$ and $\beta\rightarrow\beta+\pi/2$. Therefore, it is not restrictive to assume $<\tilde{\nu}_4>=0$, $<\tilde{\nu}_5>\neq 0$, and then $c_2=\sqrt{3/8}$, $s_2=\sqrt{5/8}$. Note that, if one is only concerned with the standard quarks and leptons $[d_L^c,(\nu_L,e_L)]\in f_1$ in eq. (4.12)], a variation in θ_2 can mimic a variation in β by properly redefining the other parameters. However, these two angles are physically different. The difference becomes apparent only when the exotic quarks and leptons $[D_L^c,(\overline{H}^0,\overline{H}^-)\in f_2$ in eq. (4.12)] are considered. For example, $\beta\neq 0,\pi/2$ implies a non-zero $\overline{D_L^c}d_L^cZ_3$ coupling, which can never be reproduced varying θ_2 if $\beta=0,\pi/2$.

Summarizing, in the models under consideration we allow only for one non-zero angle β in the fermion assignments within the 27 of E_6. This removes the possible double degeneracy for θ_2 in the case of a large Higgs VEV.

Comparing (4.2) with (4.1) and using table 4.2 and (4.12), v_α^k and a_α^k can be expressed as functions of $C_{\beta\alpha}$. The result is given in table 4.4. As there are four independent currents, all v_α^k, a_α^k can be written as functions of four of them, e.g. v_α^u, a_α^u, $v_\alpha^{d_1}$ and $a_\alpha^{d_1}$. Using now table 4.3, we obtain, for the case of one extra gauge boson, the vector and axial couplings that are needed for phenomenological

$$
\begin{array}{lcl}
v_\alpha^u & = & \frac{1}{4}C_{1\alpha} + \frac{5}{12}\sqrt{\frac{3}{5}}C_{2\alpha} \\
a_\alpha^u & = & -\frac{1}{4}C_{1\alpha} + \frac{1}{4}\sqrt{\frac{3}{5}}C_{2\alpha} - \frac{1}{3}\sqrt{\frac{3}{5}}C_{3\alpha} \\
v_\alpha^{d_1} & = & -\frac{1}{4}C_{1\alpha} - \frac{1}{12}\sqrt{\frac{3}{5}}C_{2\alpha} + \frac{1}{4}\sqrt{\frac{3}{5}}C_{3\alpha} - \frac{1}{4}\cos 2\beta C_{4\alpha} \\
a_\alpha^{d_1} & = & \frac{1}{4}C_{1\alpha} - \frac{1}{4}\sqrt{\frac{3}{5}}C_{2\alpha} - \frac{1}{12}\sqrt{\frac{3}{5}}C_{3\alpha} - \frac{1}{4}\cos 2\beta C_{4\alpha} \\
\hline
v_\alpha^{e_1} & = & -2v_\alpha^u - v_\alpha^{d_1} \\
a_\alpha^{e_1} & = & a_\alpha^{d_1} \\
v_\alpha^{d_2} & = & -v_\alpha^u - v_\alpha^{d_1} \\
a_\alpha^{d_2} & = & -a_\alpha^u - a_\alpha^{d_1} \\
v_\alpha^{e_2} & = & v_\alpha^{d_1} - v_\alpha^u \\
a_\alpha^{e_2} & = & -a_\alpha^u - a_\alpha^{d_1} \\
v_\alpha^{\nu_1} & = & -v_\alpha^{d_1} - \frac{1}{2}v_\alpha^u - \frac{1}{2}a_\alpha^u \\
v_\alpha^{\nu_2} & = & a_\alpha^{d_1} \\
v_\alpha^{\nu_3} & = & a_\alpha^u \\
v_\alpha^{\nu_4} & = & v_\alpha^{d_1} + \frac{1}{2}v_\alpha^u - \frac{1}{2}a_\alpha^u \\
v_\alpha^{\nu_5} & = & -a_\alpha^u - a_\alpha^{d_1} \\
a_\alpha^{\nu_i} & = & -v_\alpha^{\nu_i} \quad (i = 1, 2, \ldots, 5) \\
\hline
v_\alpha^{d_1 d_2} & = & -\tan 2\beta \frac{1}{4}(v_\alpha^u + a_\alpha^u + 2v_\alpha^{d_1} + 2a_\alpha^{d_1}) \\
v_\alpha^{e_1 e_2} & = & v_\alpha^{\nu_1 \nu_2} = v_\alpha^{\nu_4 \nu_5} = -v_\alpha^{d_1 d_2} \\
a_\alpha^{d_1 d_2} & = & a_\alpha^{e_1 e_2} = a_\alpha^{\nu_1 \nu_2} = a_\alpha^{\nu_4 \nu_5} = v_\alpha^{d_1 d_2}
\end{array}
$$

Table 4.4: Vector(v) and axial (a) couplings of the matter fields in the fundamental E_6 representation, 27, as functions of the current couplings, $C_{\beta\alpha}$.

applications. They are given in table 4.5.

To make the discussion more concrete, we shall work in the following, when giving numerical predictions, with three representative superstring-inspired models, specified in table 4.6. All these models are obtained by fixing $\lambda = 1$, in which case physical quantities do not depend on θ_1. Model (a) is characterized by $(c_2, s_2) = (1, 0)$, and is nothing else than the minimal model [26] discussed in great detail in chapter 3: for this model physical quantities do not depend on β. Models (b) [17] and (c) [27] correspond to two different realizations of the intermediate mass scale scenario, discussed in chapter 2, with $(c_2, s_2) = (\sqrt{3/8}, \sqrt{5/8})$: they are characterized by $\beta = 0$ and $\beta = \pi/2$, respectively, corresponding to two different assignments of the conventional quarks and leptons inside the 27 of E_6, which we believe are the most natural ones.

$$
\begin{array}{lcl}
v_1^u & = & \frac{2}{3}e \\
v_2^u & = & \frac{e}{s_W c_W}\left[c_3\left(\frac{1}{4}-\frac{2}{3}s_W^2\right)-s_3\frac{5}{12}s_W s_1 c_1\left(\lambda-\frac{1}{\lambda}\right)\right] \\
v_3^u & = & \frac{e}{s_W c_W}\left[s_3\left(\frac{1}{4}-\frac{2}{3}s_W^2\right)+c_3\frac{5}{12}s_W s_1 c_1\left(\lambda-\frac{1}{\lambda}\right)\right] \\
\hline
a_1^u & = & 0 \\
a_2^u & = & \frac{e}{s_W c_W}\left\{-c_3\frac{1}{4}-s_3 s_W\frac{1}{\lambda}\left[\frac{1}{4}s_1 c_1(\lambda^2-1)+\frac{1}{3}(c_1^2+\lambda^2 s_1^2)c_2\right]\right\} \\
a_3^u & = & \frac{e}{s_W c_W}\left\{-s_3\frac{1}{4}+c_3 s_W\frac{1}{\lambda}\left[\frac{1}{4}s_1 c_1(\lambda^2-1)+\frac{1}{3}(c_1^2+\lambda^2 s_1^2)c_2\right]\right\} \\
\hline
v_1^{d_1} & = & -\frac{1}{3}e \\
v_2^{d_1} & = & \frac{e}{s_W c_W}\left\{c_3\left(-\frac{1}{4}+\frac{1}{3}s_W^2\right)+s_3\frac{1}{4}s_W\frac{1}{\lambda}\left[\frac{1}{3}s_1 c_1(\lambda^2-1)\right.\right. \\
 & + & \left.\left.(c_1^2+\lambda^2 s_1^2)(c_2+\sqrt{\frac{5}{3}}s_2\cos 2\beta)\right]\right\} \\
v_3^{d_1} & = & \frac{e}{s_W c_W}\left\{s_3\left(-\frac{1}{4}+\frac{1}{3}s_W^2\right)-c_3\frac{1}{4}s_W\frac{1}{\lambda}\left[\frac{1}{3}s_1 c_1(\lambda^2-1)\right.\right. \\
 & + & \left.\left.(c_1^2+\lambda^2 s_1^2)\left(c_2+\sqrt{\frac{5}{3}}s_2\cos 2\beta\right)\right]\right\} \\
\hline
a_1^{d_1} & = & 0 \\
a_2^{d_1} & = & \frac{e}{s_W c_W}\left\{c_3\frac{1}{4}+s_3\frac{1}{4}s_W\frac{1}{\lambda}\left[s_1 c_1(\lambda^2-1)+(c_1^2+\lambda^2 s_1^2)\left(-\frac{1}{3}c_2+\sqrt{\frac{5}{3}}s_2\cos 2\beta\right)\right]\right\} \\
a_3^{d_1} & = & \frac{e}{s_W c_W}\left\{s_3\frac{1}{4}-c_3\frac{1}{4}s_W\frac{1}{\lambda}\left[s_1 c_1(\lambda^2-1)+(c_1^2+\lambda^2 s_1^2)\left(-\frac{1}{3}c_2+\sqrt{\frac{5}{3}}s_2\cos 2\beta\right)\right]\right\}
\end{array}
$$

Table 4.5: Vector (v) and axial (a) couplings for the up (u,c,t) and down (d,s,b) quarks in E_6 superstring-inspired models with one extra gauge boson. The remaining couplings can be trivially computed using the relations of table 4.4.

	(c_2, s_2)	$\sin\beta$	model
(a)	$(1, 0)$	-	minimal
(b)	$(\sqrt{3/8}, \sqrt{5/8})$	0	IMS (ref. [17])
(c)	$(\sqrt{3/8}, \sqrt{5/8})$	1	IMS (ref. [27])

Table 4.6: Values of the parameters θ_2 and β corresponding to the three models considered in the text. It is assumed that $\lambda = 1$, which implies no dependence on θ_1.

4.2 Structure of the mass matrix

Any extension of the standard model with one extra neutral gauge boson gives rise, after removing the photon, to a mass matrix $\mathcal{M}^2$ of the form

$$\mathcal{M}^2 = \begin{pmatrix} A & C \\ C & B \end{pmatrix}, \tag{4.13}$$

where the first entry corresponds to the standard current eigenstate Z^0 and the second one to the new Z. Such a matrix is diagonalized by means of an orthogonal transformation,

$$\begin{pmatrix} M_2^2 & 0 \\ 0 & M_3^2 \end{pmatrix} = \begin{pmatrix} c_3 & -s_3 \\ s_3 & c_3 \end{pmatrix} \begin{pmatrix} A & C \\ C & B \end{pmatrix} \begin{pmatrix} c_3 & s_3 \\ -s_3 & c_3 \end{pmatrix}, \tag{4.14}$$

where we assume, for definiteness, that the eigenvalues satisfy $M_3^2 > M_2^2$. The mixing angle $\theta_3 \in [-\pi/2, \pi/2)$ is given by

$$s_3 = sign(C)\sqrt{\frac{A - M_2^2}{M_3^2 - M_2^2}}, \quad c_3 = \sqrt{\frac{M_3^2 - A}{M_3^2 - M_2^2}}. \tag{4.15}$$

At first sight A, B and C or, equivalently, M_2^2, M_3^2 and θ_3 seem to be three independent parameters, the only constraint on them coming from the fact that the matrix $\mathcal{M}^2$ must be positive-definite. However, this is not the case in general, and in particular in models where the Higgs sector contains only standard $SU(2)_L \times U(1)_Y$ doublets and singlets, transforming non-trivially under the new gauge interactions (as it happens in E_6 superstring-inspired models). This will allow us to extract information on M_3 from measurements of M_2. The main point is that A and M_2^2 can be measured (B can be traded for M_2^2 if $M_2^2 \neq A$), whereas C, which is a model-dependent quantity, is bounded from above. This bound is translated into an upper bound on M_3, for

$$M_3^2 = A + \frac{C^2}{A - M_2^2}. \tag{4.16}$$

Eq. (4.16) follows from eq. (4.14), noting that

$$M_2^2 + M_3^2 = A + B, \tag{4.17}$$

$$M_2^2 M_3^2 = AB - C^2. \tag{4.18}$$

Let us then discuss the determination of the right-hand side of eq. (4.16): a study of this constraint in the minimal model has already been presented in chapter 3.

In the basis we choose for $\mathcal{M}^2$ in (4.13):

$$A = M_{Z_0}^2 = \frac{M_W^2}{c_W^2} = \frac{\pi\alpha}{\sqrt{2}G_F s_W^2}\frac{1}{c_W^2}, \tag{4.19}$$

where G_F is the Fermi constant and α the electromagnetic fine structure constant. That is the standard model prediction[2] for M_2^2. We assume that at the scale under consideration charged currents are described by $SU(2)_L$. Therefore, A can be measured by measuring m_W; another determination of $M_{Z^0}^2$ can come from a (model-dependent) fit of s_W^2 to low-energy neutral current data, as we will see later. On the other hand, M_2^2 is expected to be measured with high precision at SLC and LEP. Thus, knowledge of C in eq. (4.16) will fix M_3^2. C only depends on the $SU(2)_L \times U(1)_Y$ doublet vacuum expectation values through a definite combination. We find

$$C = \frac{s_W}{\lambda} M_{Z^0}^2 \left\{ (1-\lambda^2) s_1 c_1 + (c_1^2 + \lambda^2 s_1^2) \left[\frac{c_2}{3}(-4+5\xi) + \sqrt{\frac{5}{3}} s_2 \xi (-1+2\eta) \right] \right\}, \tag{4.20}$$

where

$$\xi \equiv \frac{|<\tilde{\nu}_1>|^2 + |<\tilde{\nu}_2>|^2}{|<\tilde{\nu}_1>|^2 + |<\tilde{\nu}_2>|^2 + |<\tilde{\nu}_3>|^2}, \quad (\xi \in [0,1]), \tag{4.21}$$

$$\eta \equiv \frac{|<\tilde{\nu}_1>|^2}{|<\tilde{\nu}_1>|^2 + |<\tilde{\nu}_2>|^2}, \quad (\eta \in [0,1]). \tag{4.22}$$

For conventional assignments of quarks and leptons inside the $[16]_{SO(10)} \subset [27]_{E_6}$, $\tilde{\nu}_L \equiv \tilde{\nu}_1$, $\overline{H}^0 \equiv \tilde{\nu}_2$, $H^0 \equiv \tilde{\nu}_3$, where $\overline{H}(H)$ denotes, as in chapter 3, the Higgs of hypercharge $Y = -\frac{1}{2}(\frac{1}{2})$ which couples to down (up) quarks. In general, standard

[2]Of course, the precise standard model prediction M_{Z^0} depends, via radiative corrections, on unknown parameters like the top and the Higgs masses. We assume here three fermion generations and $m_{top} \sim 40GeV$, taking into account only the leading standard model corrections to α : $\alpha = \alpha(M_{Z^0}) = [127.7]^{-1}$. Other smaller radiative corrections to A, due to different values of m_{top}, the Higgs sector, exotic fermions, supersymmetric partners and extra gauge bosons, will be neglected in the present analysis, where we focus on tree-level mixing effects.

left-handed sneutrinos are a combination of the $\tilde{\nu}_{1,2}$ directions

$$\begin{pmatrix} \tilde{\nu}_L \\ \overline{H}^0 \end{pmatrix} = \begin{pmatrix} \cos\beta & \sin\beta \\ -\sin\beta & \cos\beta \end{pmatrix} \begin{pmatrix} \tilde{\nu}_1 \\ \tilde{\nu}_2 \end{pmatrix}, \tag{4.23}$$

where the angle β is the one defined in eq. (4.12). Then lepton number conservation, $< \tilde{\nu}_L >= 0$, implies $\eta = \sin^2\beta$. The conventional assignment corresponds to $\beta = 0$ ($\eta = 0$), but $\beta(\eta)$ can be different from zero in general.

Using eqs. (4.16), (4.19) and (4.20), constraints on the parameter space (M_2, M_3, M_{Z^0}) can be extracted for every E_6 superstring-inspired model, and in particular for the representative examples we have decided to consider. Note that ξ, in principle, can vary between 0 and 1. However, for $\xi = 0(1)$ the down (up) quarks would be massless. Moreover, detailed model calculations of radiative electroweak breaking restrict $\xi \in [0.04, 0.27]$ in the minimal model (a); similarly, one obtains $\xi \in [0.04, 0.41]$ in model (c). In case (b) C is independent of ξ.

Since direct measurements of M_2 and M_W already exist at the CERN collider, we will assume in what follows that both masses lie within the one standard deviation ellipse of fig. 4.1, obtained averaging the UA1 and UA2 determinations [69]

$$M_2 = 92.6 \pm 1.7 GeV \tag{4.24}$$

$$M_W = 81.8 \pm 1.5 GeV. \tag{4.25}$$

Fig. 4.1 also displays the line corresponding to the standard model predictions (4.19) for (M_{Z^0}, M_W), varying the angle θ_W. The values of (M_2, M_W) compatible with (4.24), (4.25) and with the existence of a Z_3 are represented by the shaded area. We have checked that this values can be obtained in any model for a suitable pattern of VEVs. In fig. 4.2 we plot eq. (4.16) for the three representative models of table 4.6. We fix M_{Z^0} by choosing M_W equal to its central value at the CERN collider [eq. (4.25)] $M_W = 81.8 GeV$, whereas the range in M_2 corresponds to the 1σ limit given in fig. 4.1. M_2^2 has to be smaller than $M_{Z^0}^2$ as required by eqs. (4.17) and (4.18). In the limiting case in which M_2^2 coincides with the standard

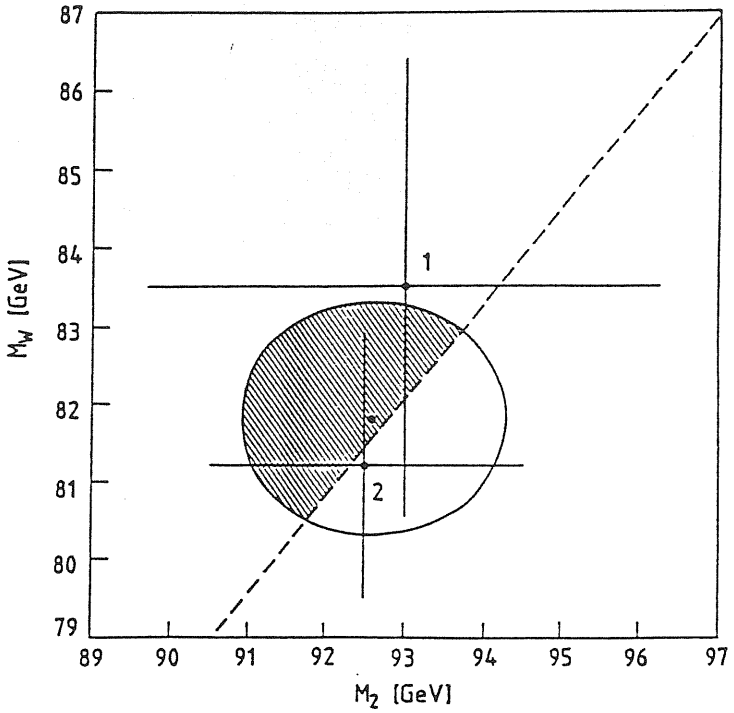

Figure 4.1: Allowed region of the (M_2, M_W) plane according to the present collider data.

value $M^2_{Z^0}$, no constraint on M_3^2 can be drawn. This happens in model (a) for $\xi = 0.8$ and in model (c) for $\xi = 0.4$: it is not possible in model (b), where C is independent of ξ and non-zero. Then $C = 0$ and Z_3 and Z^0 do not mix. This is possible only in model (c) within the favoured range of ξ. But if M_2 happens to be smaller than M_{Z^0}, an upper bound on M_3 is obtained. For instance, for $M_W = 81.8GeV$ and our favoured range of ξ, if M_2 were $92GeV$, then our bound would be $M_3 < 435GeV$ (a), $M_3 < 290GeV$ (b) and $M_3 < 264GeV$ (c).

4.3 Phenomenological analysis of neutral current data

In this section we present new, model-independent fits of the observables in low-energy neutral current experiments in the νq, νl, lq and ll sectors (ν = neutrino or antineutrino, l = charged lepton or antilepton, q = quark or antiquark). A detailed description of the different pieces of experimental information and of our

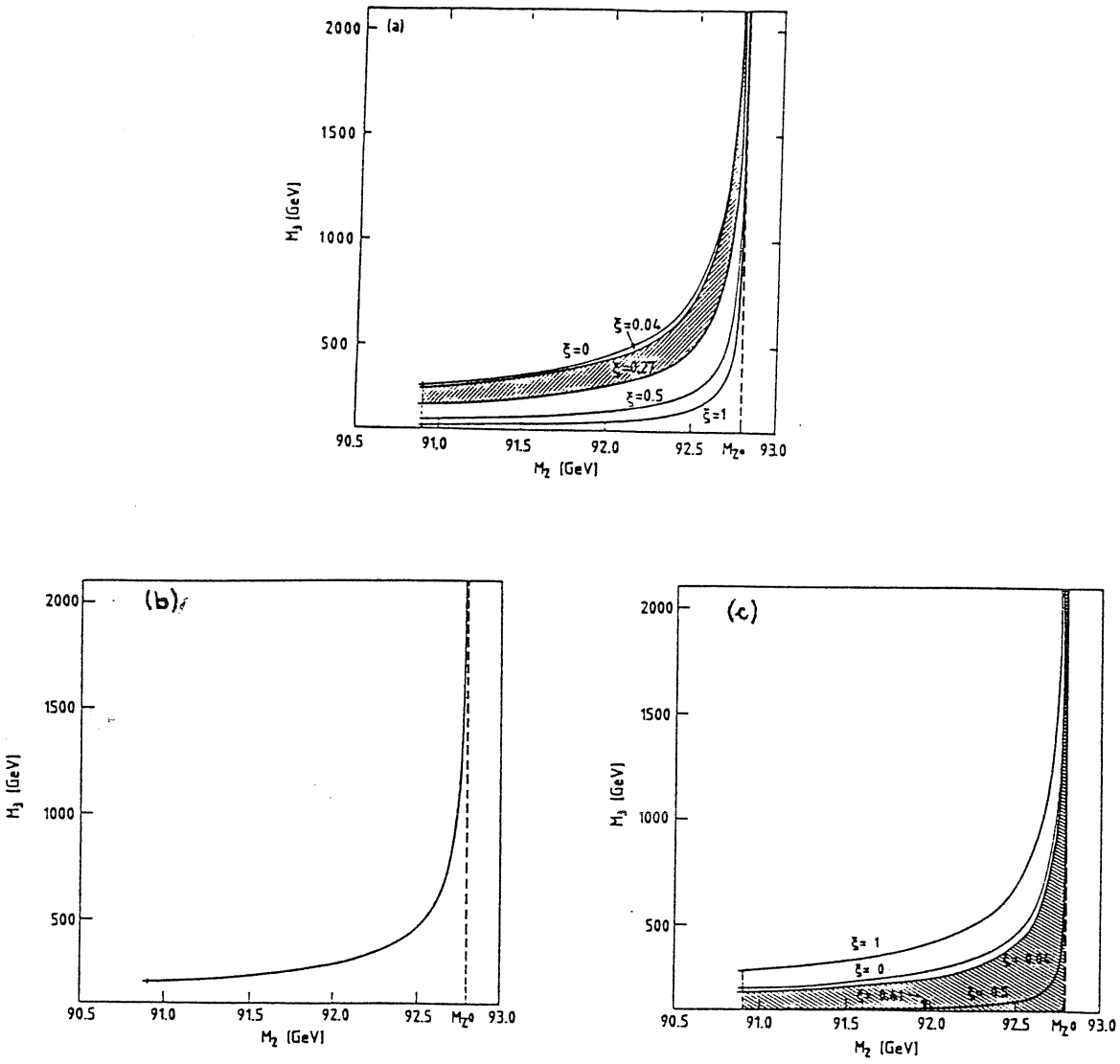

Figure 4.2: Allowed region in the (M_2, M_3) plane for the models (a), (b) and (c) of table 4.6.

analysis procedures can be found in ref. [68]. Here we limit ourselves to a summary, focusing mainly on the results which consist, for each sector, in best fit values of convenient model independent parameters. In the next section these results will be combined with the collider data on the $W^{\pm}$, Z_2 masses to derive limits on the mass and the mixing angle of the extra Z' in the three representative models introduced before.

Before going into details, a general remark is in order. Even if we are working in extended electroweak models, radiative corrections, which *must* be applied to the model-independent parameters, will be evaluated in the framework of the standard model. This approximation is justified because we know that the standard model is consistent with all present experimental data, and therefore we can anticipate that in any acceptable model the effects of the extra Z' on measurable quantities are small perturbations of the standard model predictions. Thus the effects of radiative corrections involving Z' itself are expected to be a second order perturbation, and will be neglected altogether.

4.3.1 Neutrino-quark sector

The phenomenological lagrangian parametrizing the effective neutral-current interactions in the neutrino-quark sector is

$$\mathcal{L}_{eff}^{(\nu q)} = -\frac{G_F}{\sqrt{2}} \; [\overline{\nu}\gamma_\mu(1-\gamma_5)\nu] \; [u_L\overline{u}\gamma^\mu(1-\gamma_5)u + d_L\overline{d}\gamma^\mu(1-\gamma_5)d + u_R\overline{u}\gamma^\mu(1+\gamma_5)u + d_R\overline{d}\gamma^\mu(1+\gamma_5)d]. \quad (4.26)$$

Among the different processes described by eq. (4.26) (deep-inelastic scattering, pion production, elastic scattering, etc.), deep inelastic neutrino-hadron scattering is by far the most important. Making use of 38 independent experimental measurements on isoscalar and on n and p targets, and applying the QCD-improved quark-parton model and the standard model radiative corrections, one can determine the four squared chiral couplings u_L^2, d_L^2, u_R^2 and d_R^2 with the corresponding

errors. From the squared chiral couplings one can then derive the linear ones, removing the sign ambiguities by a comparison with other processes sensitive to these choices. Adding together in quadrature the experimental errors (statistical + systematic) and the theoretical uncertainties, one finds:

$$\begin{aligned} u_L &= 0.356 \pm 0.020, \\ d_L &= -0.417 \pm 0.018, \\ u_R &= -0.164 \pm 0.027, \\ d_R &= 0.058 \pm 0.080, \end{aligned} \tag{4.27}$$

with a correlation matrix

$$\rho = \begin{pmatrix} 1 & 0.963 & 0.388 & 0.378 \\ & 1 & 0.361 & 0.412 \\ & & 1 & 0.896 \\ & & & 1 \end{pmatrix}. \tag{4.28}$$

4.3.2 Neutrino-electron sector

The effective neutral current lagrangian for the neutrino-electron sector is given by

$$\mathcal{L}_{eff}^{(\nu e)} = -\frac{G_F}{\sqrt{2}}[\overline{\nu}\gamma_\mu(1-\gamma_5)\nu][g_L\bar{e}\gamma^\mu(1-\gamma_5)e + g_R\bar{e}\gamma^\mu(1+\gamma_5)e]. \tag{4.29}$$

Neutrino-electron scattering (which by the way is associated to the historical discovery of neutral currents) is free from all the theoretical uncertainties of strong interactions that plague neutrino-hadron scattering. However, due to the smallness of the cross-section, statistical errors are presently much larger. A combined analysis of all the existing data on $(\overline{\nu})_\mu$ and $(\overline{\nu})_e e$, including radiative corrections (even if they are still small compared to the experimental errors), gives

$$\begin{aligned} g_L &= -0.273 \pm 0.018, \\ g_R &= 0.228 \pm 0.022, \end{aligned} \tag{4.30}$$

with a correlation

$$\rho = 0.042. \tag{4.31}$$

4.3.3 Charged lepton - quark sector

The neutral current interactions of this sector which are relevant to our analysis are described by the effective lagrangian

$$\begin{aligned}\mathcal{L}_{eff}^{(lq)} = \frac{G_F}{\sqrt{2}} \quad & [(\bar{e}\gamma_\mu\gamma_5 e)(C_{1u}\bar{u}\gamma^\mu u + C_{1d}\bar{d}\gamma^\mu d) \\ & +(\bar{e}\gamma_\mu e)(C_{2u}\bar{u}\gamma^\mu\gamma_5 u + C_{2d}\bar{d}\gamma^\mu\gamma_5 d) \\ & +(\bar{e}\gamma_\mu e)(h^u_{AA}\bar{u}\gamma^\mu\gamma_5 u + h^d_{AA}\bar{d}\gamma^\mu\gamma_5 d)] \end{aligned} \tag{4.32}$$

and are probed by three different classes of experiments: parity violation effects in atoms, asymmetries in deep inelastic eD and μC scattering, asymmetries in $e^+e^- \to q\bar{q}$.

Parity violation in atoms

Experiments measuring parity violation in heavy atoms give informations on the coefficients C_{1u} and C_{1d} in (4.32): they are characterized by different experimental methods, atomic elements and transitions observed. After including some theoretical input and radiative corrections, one is able to extract from each experiment the quantity $C_{1u}+\zeta C_{1d}$, where $\zeta \equiv (Z+2N)/(2Z+N)$ depends on the element under consideration. We use here data from 11 different experiments: the corresponding values of $C_{1u} + \zeta C_{1d}$ can be found in ref. [68].

Asymmetries in $e-q$ and $\mu-q$ interactions

A parity violating asymmetry $A_D \equiv (\sigma_R - \sigma_L)/(\sigma_R + \sigma_L)$ was measured at SLAC in the inelastic scattering of longitudinally polarized electrons by deuterium:

$$e^-_{L,R}(E_0) + D \to e^-(E') + X. \tag{4.33}$$

The measured asymmetries at different values of the kinematical parameters can be fitted to the formula

$$\frac{A_D}{Q^2} = K\left[\left(C_{1u} - \frac{1}{2}C_{1d}\right) + F(y)\left(C_{2u} - \frac{1}{2}C_{2d}\right)\right], \tag{4.34}$$

where $K = (3G_F)/(5\sqrt{2}\pi\alpha) = 2.158 \times 10^{-4} GeV^{-2}$, $y \equiv (E_0 - E')/E_0$ and $F(y) \equiv [1-(1-y)^2]/[1+(1+y)^2]$. In order to determine the two combinations $(C_{1u}-\frac{1}{2}C_{1d})$,

$(C_{2u} - \frac{1}{2}C_{2d})$ and their correlation ρ, we have performed a fit to the published data, obtaining

$$C_{1u} - \frac{1}{2}C_{1d} = -0.45 \pm 0.12, \tag{4.35}$$

$$C_{2u} - \frac{1}{2}C_{2d} = 0.21 \pm 0.38, \tag{4.36}$$

$$\rho = -0.954. \tag{4.37}$$

For the consistency of our approach, the above results should be corrected for the complete one-loop standard model corrections. These additional corrections depend on y and Q^2, and range from 0.4% to 4%: therefore, they can be safely neglected when compared with the experimental errors which range from 15% to 50%.

A different kind of asymmetry has been measured in the deep inelastic scattering of longitudinally polarized muons by an isoscalar carbon target:

$$B = \frac{\sigma^+(-|\lambda|) - \sigma^-(+|\lambda|)}{\sigma^+(-|\lambda|) + \sigma^-(+|\lambda|)}, \tag{4.38}$$

where $\sigma^{\pm}(\lambda)$ is the cross section for $\mu^{\pm}$ with polarization λ for the reaction $\mu^{\pm}C \rightarrow \mu^{\pm}X$. Correcting the data for one loop standard model corrections, and fitting them to the theoretical expression

$$B = -\frac{3G_F F(y)Q^2}{5\sqrt{2}\pi\alpha}[(h^u_{AA} - \frac{1}{2}h^d_{AA}) + \lambda(C_{2u} - \frac{1}{2}C_{2d})], \tag{4.39}$$

one finds:

$$(h^u_{AA} - \frac{1}{2}h^d_{AA}) + |\lambda|(C_{2u} - \frac{1}{2}C_{2d}) = \begin{cases} 0.81 \pm 0.35 & for \quad |\lambda| = 0.66 \\ 0.68 \pm 0.17 & for \quad |\lambda| = 0.81 \end{cases} \tag{4.40}$$

Forward-backward asymmetry in $e^+e^- \rightarrow q\bar{q}$

The forward-backward asymmetry has been measured in $e^+e^- \rightarrow q\bar{q}$ reactions at PETRA and PEP. The main experimental problems are flavour identification and the distinction between quark and antiquark, and no reliable method has been found for the light quarks u,d s. In the case of the c quark, two methods have been

used: a) direct observation of $D^{0,\pm}$, $D^{*\pm}$; b) observation of direct leptons in decays $c \to l\nu X$ $(l = e, \mu)$. In the case of the b quark, only the observation of direct leptons in decays $b \to l\nu X$ is available. In both cases all the experiments have the common feature of low yields and high backgrounds, and the errors are rather large. For this reason one can neglect radiative corrections and fit the measured asymmetries $A_{FB}^{(c)}$ and $A_{FB}^{(b)}$ to the linear expressions in s:

$$A_{FB}^{(c)}(s) = a^{(c)}s, \quad A_{FB}^{(b)}(s) = a^{(b)}s. \tag{4.41}$$

To improve the approximation, one can also apply s dependent but model independent theoretical corrections which compensate for neglecting the terms $O(s^2)$. After these corrections, considering 8 different experiments in each case we obtain the best fit

$$\begin{aligned} a^{(c)} &= (-1.28 \pm 0.32) \times 10^{-4} GeV^{-2}, \\ a^{(b)} &= (-1.98 \pm 0.40) \times 10^{-4} GeV^{-2}. \end{aligned} \tag{4.42}$$

One can now collect the different pieces of information on the $l - q$ sector and perform a fit to the parameters appearing in eq. (4.32). The result is:

$$\begin{aligned} C_{1u} &= -0.1809 \pm 0.0551, \\ C_{1d} &= 0.3274 \pm 0.0490, \\ C_{2u} - \frac{1}{2}C_{2d} &= -0.1213 \pm 0.2344, \\ h_{AA}^{u} &= 0.6048 \pm 0.1515, \\ h_{AA}^{d} &= -0.5112 \pm 0.1052, \end{aligned} \tag{4.43}$$

with a correlation matrix given by:

$$\rho = \begin{pmatrix} 1 & -0.979 & -0.892 & 0.564 & -0.172 \\ & 1 & 0.885 & -0.559 & 0.171 \\ & & 1 & -0.640 & 0.163 \\ & & & 1 & 0.059 \\ & & & & 1 \end{pmatrix}. \tag{4.44}$$

4.3.4 Charged lepton - charged lepton sector

This sector is probed in the reactions $e^+e^- \to \mu^+\mu^-$, $\tau^+\tau^-$, whose forward-backward asymmetries have been measured at PEP and PETRA. To keep the analysis at a model-independent level, we fit the measured asymmetries A_{FB}^{ex} to the following approximate theoretical expression:

$$A_{FB}^{th} = As + Bs^2, \tag{4.45}$$

so that all the information can be condensed into the parameters A and B (which in turn can be used as inputs in any fit to a specific model with an extra Z'). The asymmetries A_{FB}^{ex} presented by the experimental groups already include corrections for detection efficiency, bremsstrahlung events of the type $e^+e^- \to l^+l^-\gamma$ and other QED radiative corrections: all these corrections are experiment-dependent. Before comparing A_{FB}^{ex} with A_{FB}^{th}, two further corrections are in order. The first one takes care of the left-over standard model radiative corrections. The second one takes care of the difference between the full tree-level theoretical expression for the asymmetry and the approximate formula (4.45): this correction depends strongly on the value of s, but it is practically model-independent within a reasonable range of variation for the model parameters. Fitting the existing 28 independent experimental data we obtain :

$$\begin{aligned} A &= (-0.56 \pm 0.13) \times 10^{-4} GeV^{-2}, \\ B &= (-1.38 \pm 0.96) \times 10^{-8} GeV^{-4}, \end{aligned} \tag{4.46}$$

with a correlation $\rho = -0.947$ and $\chi^2/d.o.f. = 23.5/26$.

4.4 Limits on the mass and the mixing of a Z'

We use now the information collected in the previous section, together with the direct determinations of M_W and M_2, to establish [68] a lower limit on the mass M_3 of the extra Z_3 boson and an upper limit on the magnitude of the angle θ_3

describing its mixing with the observed Z_2, in the three superstring inspired models of table 4.6[3]. In order to do this, we must be able to express the phenomenological parameters of eqs. (4.27), (4.30),(4.43) and (4.46) in terms of the vector and axial couplings of table 4.5 and of the gauge boson masses M_2 and M_3. Some trivial algebraic computations give ($d \equiv d_1$, $e \equiv e_1$, $\nu \equiv \nu_1$ in the notation of section 4.1):

$$u, d_{L,R} = \sum_{i=2}^{3} \left(\frac{A_C}{M_i}\right)^2 [v_i^{\nu} - a_i^{\nu}][v_i^{u,d} \mp a_i^{u,d}], \tag{4.47}$$

$$g_{L,R} = \sum_{i=2}^{3} \left(\frac{A_C}{M_i}\right)^2 [v_i^{\nu} - a_i^{\nu}][v_i^{e} \mp a_i^{e}], \tag{4.48}$$

$$C_{1u,d} = -8 \sum_{i=2}^{3} \left(\frac{A_C}{M_i}\right)^2 a_i^e v_i^{u,d}, \tag{4.49}$$

$$C_{2u,d} = -8 \sum_{i=2}^{3} \left(\frac{A_C}{M_i}\right)^2 v_i^e a_i^{u,d}, \tag{4.50}$$

$$h_{AA}^{(u,d)} = -8 \sum_{i=2}^{3} \left(\frac{A_C}{M_i}\right)^2 a_i^e a_i^{u,d}, \tag{4.51}$$

$$A = -\frac{3}{2}\left[\left(\frac{a_2^e}{M_2}\right)^2 + \left(\frac{a_3^e}{M_3}\right)^2\right], \tag{4.52}$$

$$B = -\frac{3}{2}\left\{\left(\frac{a_2^e}{M_2^2}\right)^2 + \left(\frac{a_3^e}{M_3^2}\right)^2 - \frac{(v_2^e a_3^e + v_3^e a_2^e)^2 - 2[(a_2^e v_3^e)^2 + (a_3^e v_2^e)^2]}{M_2^2 M_3^2}\right\}, \tag{4.53}$$

where $A_C^2 \equiv \frac{\pi\alpha}{\sqrt{2}G_F}\frac{1}{1-\Delta r}$ and $\Delta r = 0.0711 \pm 0.0013$.

The models of table 4.6 are characterized by specific values of the parameters θ_2 and β, and since we have assumed $\lambda = 1$ physical quantities do not depend on θ_1. Moreover, as explained in section 4.2, their mass matrices can be characterized by only two parameters, for example θ_3 and M_3. For each separate model, therefore, the parameters to be fitted are just three: the weak angle θ_W, the mass M_3 and the mixing angle θ_3. Using eqs. (4.27), (4.30), (4.43) and (4.46), plus the additional information that can be extracted from the UA1 and UA2 determinations of the $W^{\pm}$ and Z_2 masses [69], we have performed a least squares fit using the

[3]For related work, see ref. [70].

computer program MINUIT. The results for the three models under consideration are summarized below.

Model (a)

$$\left.\begin{array}{l} M_3 > 157GeV \\ \theta_3| < 0.11 \end{array}\right\} \quad (at\ 1\sigma), \tag{4.54}$$

$$s_W^2 = 0.231 \pm 0.006. \tag{4.55}$$

Model (b)

$$\left.\begin{array}{l} M_3 > 377GeV \\ |\theta_3| < 0.04 \end{array}\right\} \quad (at\ 1\sigma), \tag{4.56}$$

$$s_W^2 = 0.230 \pm 0.006. \tag{4.57}$$

Model (c)

$$\left.\begin{array}{l} M_3 > 207GeV \\ |\theta_3| < 0.04 \end{array}\right\} \quad (at\ 1\sigma), \tag{4.58}$$

$$s_W^2 = 0.228 \pm 0.006. \tag{4.59}$$

4.5 Prospects for present and future colliders

In the previous section we have seen that the present limits on new Z_3 bosons, coming from low-energy neutral current data and from the measurements of the $W^{\pm}$ and Z_2 masses, are not very stringent. It is therefore interesting to study the possible signals of these new bosons at the existing and planned high-energy machines.

One way of detecting a new Z_3 boson could be the observation of its indirect effects at future e^+e^- and ep colliders. At SLC and LEP one will be able to perform precise measurements of the Z_2 mass and of cross sections and asymmetries around the Z_2 peak. At HERA (and perhaps at the LHC in an ep configuration) one could look at parity and charge asymmetries. On these topics there exists already a wide literature [71].

The most attractive possibility, however, is the direct production of Z_3 bosons at present and future hadronic colliders [72]: $Sp\bar{p}S$ (+ ACOL), Tevatron, LHC

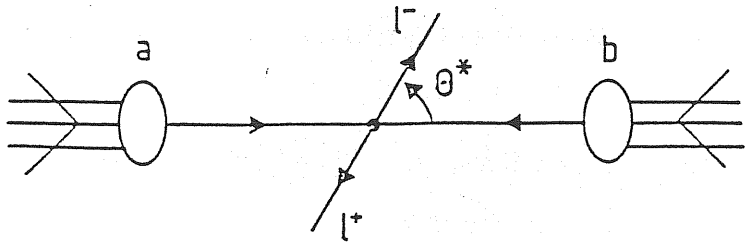

$\sqrt{s}$ = ab center of mass energy
$M^2 = (p_{l^+} + p_{l^-})^2$
$\frac{M}{2}(e^y - e^{-y}) = (p_{l^+} + p_{l^-})_{\|}$
θ^* = al^- scattering angle in the l^+l^- center of mass

Figure 4.3: Production of l^+l^- pairs in hadron collisions. 'a' always denotes a proton and 'b' a proton or an antiproton, depending on the collider. $l^\pm$ corresponds to $e^\pm$, $\mu^\pm$ or $\tau^\pm$.

and SSC. The most promising decay channel for the discovery of a new Z_3 is, obviously, the one into charged lepton-antilepton pairs, which led in the past to the discovery of the Z_2. Another interesting channel, which could give some useful complementary information, but is generally less favourable than the previous one, is the one into W^+W^- pairs (through the mixing between Z_2 and Z_3). These two decay channels will be studied in detail in the rest of this section. Decays into ordinary quark-antiquark pairs appear to be undetectable, due to the huge QCD background. Other fancier possibilities require the presence of exotic fermions or supersymmetric particles in the final state, and will not be considered here.

4.5.1 Decays into lepton-antilepton pairs

The unpolarized differential cross section for the process $p(\overline{p}) \to l^+l^-X$ depends on the lepton invariant mass M, on the rapidity y and on the angle θ^* in the centre of mass of the colliding partons (see fig. 4.3). The general form of this cross section is, for tree level amplitudes,

$$\frac{d\sigma}{dM\,dy\,d\cos\theta^*} = \Sigma_q[g_q^S(y,M)S_q(M)(1+\cos^2\theta^*) + g_q^A(y,M)A_q(M)2\cos\theta^*], \quad (4.60)$$

where the index q runs over the different quark flavours, S_q,A_q (which are the only model-dependent quantities) involve the vector and axial couplings of quarks and leptons to the different neutral gauge bosons, while g_q^S, g_q^A involve the parton distribution functions of the colliding hadrons: the precise definitions will be given below. One usually integrates the θ^* dependence, which only reflects the spin structure of the interaction. One can also integrate the y-dependence, which gives the parton distribution within the hadrons and is an input, or the M dependence, given that almost all the events concentrate on the resonant peak. However, one loses in principle a lot of information in both cases. If the rapidity dependence is integrated out, given that the structure functions weigh differently the (anti)quark distributions for different y values, one gets only one average of S_q and A_q, while keeping explicitly the y-dependence one might probe different combinations of S_q and A_q. On the other hand, if the M-dependence is integrated out, one loses in a similar way relevant interference effects, as S_q and A_q are sums of products of coupling constants and propagators. If a signal is detected, the best way of analyzing the data would be to perform a fit to (4.60), given that the θ^* and y dependences for the production of a new Z are calculable. For this the general parametrization of the E_6 models we introduced in section 4.1 is convenient, because the preferred model can be singled out at once. However, the only sensible thing to do at present (in the absence of any experimental indication of a new Z) is to give numerical examples of differential cross sections and asymmetries, integrating out θ^* and y or θ^* and M, respectively.

Experimentally, the situation can be more complicated. To discriminate among different models, the lepton charges have to be identified and the momenta measured with a sufficient resolution: this could be non trivial at LHC and SSC. Moreover, to take cuts and detection efficiency into account, one should multiply the lepton cross section by an experiment dependent function of M, y and θ^*.

Finally, the results depend on the parton distribution functions: in our calcu-

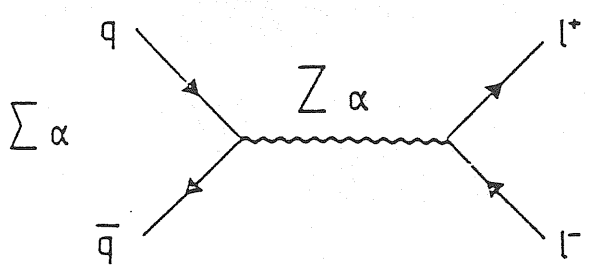

Figure 4.4: Lowest order graphs contributing to the process $q\bar{q} \to l^+l^-$.

lations we use those by Duke and Owens [73], set 1; other choices would not affect significantly the results of our analysis. QCD corrections can also be non-negligible, and in particular partons can carry a non-vanishing transverse momentum. Here we neglect all these effects.

At hadron colliders, the production of lepton-antilepton pairs is described, at the quark level, by the graphs of fig. 4.4. Searching for isolated lepton-antilepton pairs with large transverse energy one can observe the Z and possibly new neutral gauge bosons. The corresponding differential cross section is given by eq. (4.60), with

$$g_q^{S,A}(y,M) = \frac{M}{48\pi} x_a x_b [f_q^{(a)}(x_a,M^2) f_{\bar{q}}^{(b)}(x_b,M^2) \pm f_{\bar{q}}^{(a)}(x_a,M^2) f_q^{(b)}(x_b,M^2)], \tag{4.61}$$

where the sign $+(-)$ corresponds to $S(A)$, and

$$S_q = \Sigma_{\alpha,\beta} \frac{(v_\alpha^q v_\beta^q + a_\alpha^q a_\beta^q)(v_\alpha^e v_\beta^e + a_\alpha^e a_\beta^e)}{(M^2 - M_\alpha^2 + iM_\alpha\Gamma_\alpha)(M^2 - M_\beta^2 - iM_\beta\Gamma_\beta)}, \tag{4.62}$$

$$A_q = \Sigma_{\alpha,\beta} \frac{(v_\alpha^q a_\beta^q + a_\alpha^q v_\beta^q)(v_\alpha^e a_\beta^e + a_\alpha^e v_\beta^e)}{(M^2 - M_\alpha^2 + iM_\alpha\Gamma_\alpha)(M^2 - M_\beta^2 - iM_\beta\Gamma_\beta)}. \tag{4.63}$$

We follow standard conventions and the notation of ref. [74] if not otherwise stated. Quark and lepton masses are neglected. a and b are the two colliding hadrons at centre of mass energy $\sqrt{s}$, x_a and x_b being the momentum fractions of the colliding partons in a and b respectively (see fig. 4.3). M is the lepton-antilepton invariant

mass, y the rapidity ($x_{a,b} = M/\sqrt{s}e^{\pm y}$) and θ^* the scattering angle (al^-) in the centre of mass of the parton system $q\bar{q}$. Finally, $f_{q(\bar{q})}^{(a(b))}(x_{a(b)}, M^2)$ are the relevant parton distribution functions.

All the model dependence in eq. (4.60) is in S_q and A_q. Then it is sensible to integrate over θ^*. We will present plots of the differential cross section

$$\left(\frac{d\sigma}{dM}\right)^S = \int_{\log(M/\sqrt{s})}^{\log(\sqrt{s}/M)} dy \int_{-1}^{1} d\cos\theta^* \frac{d\sigma}{dM dy d\cos\theta^*}, \tag{4.64}$$

testing the dependence of S_q on the model parameters, and the asymmetry for $p\bar{p}$

$$A^{p\bar{p}}(M) = \frac{(d\sigma/dM)^{A^{p\bar{p}}}}{(d\sigma/dM)^S} = \frac{\int_{\log(M/\sqrt{s})}^{\log(\sqrt{s}/M)} dy \left(\int_0^1 - \int_{-1}^0\right) d\cos\theta^* \frac{d\sigma}{dM dy d\cos\theta^*}}{(d\sigma/dM)^S}, \tag{4.65}$$

and for pp

$$A^{pp}(M) = \frac{(d\sigma/dM)^{A^{pp}}}{(d\sigma/dM)^S} \leq \frac{\left(\int_0^{\log(\sqrt{s}/M)} - \int_{\log(M/\sqrt{s})}^0\right) dy \left(\int_0^1 - \int_{-1}^0\right) d\cos\theta^* \frac{d\sigma}{dM dy d\cos\theta^*}}{(d\sigma/dM)^S}, \tag{4.66}$$

testing the A_q dependence (for a sizeable differential cross section). We also give the differential cross section $(d\sigma/dMdy)^S_{M=M_3}$ at the resonant peak $M = M_3$ and the corresponding asymmetry

$$A(y) = \frac{(d\sigma/dMdy)^A_{M=M_3}}{(d\sigma/dMdy)^S_{M=M_3}} = \frac{\left(\int_0^1 - \int_{-1}^0\right) d\cos\theta^* \frac{d\sigma}{dM dy d\cos\theta^*}\Big|_{M=M_3}}{\int_{-1}^1 d\cos\theta^* \frac{d\sigma}{dM dy d\cos\theta^*}\Big|_{M=M_3}}. \tag{4.67}$$

Equations (4.64)-(4.67) are our main concern in the rest of this subsection. To calculate v_α^k and a_α^k and the cross sections, one should also fix the value of θ_3. We put it equal to zero in all cases. In fact, θ_3 is known to be small ($|\theta_3| < 0.11$ from the analysis of the previous section, but this limit rapidly improves as M_3 increases from its lower bound) and for the Z_3 decays into l^+l^- we are concerned with, it can be safely neglected. This small mixing can be important to obtain bounds on

M_3^2, as seen in section 4.2, and for the decay of Z_3 into W^+W^-, as we will see in the next subsection. However, its contribution to the Z_3 width and the Z_3-fermion couplings, which are the relevant quantities here, is at most a few per cent. Note that the absence of Z^0Z_3 mixing does not mean that there are not interference effects: they result from the addition of the different amplitudes in fig. 4.4 and could give important information when measured.

We plot here the lepton differential cross section, $(d\sigma/dM)^S$ in eq. (4.64), and the asymmetry, $A^{p\bar{p}}(M)$ or $A^{pp}(M)$ depending on the collider in eqs. (4.65),(4.66), for the three representative E_6 superstring-inspired models of table 4.6. Fig. 4.5 and 4.6 correspond to the CERN collider $(a,b,\sqrt{s}) = (p,\bar{p},630GeV)$; fig. 4.7 and 4.8 to LHC, $(a,b,\sqrt{s}) = (p,p,17TeV)$; analogous figures for the Tevatron and the SSC can be found in ref. [66]. In all cases we use the Duke and Owens parton distribution functions, set 1 and we assume $M_W = 81.8GeV$, $M_2 = M_{Z^0}^{th} = 92.8GeV$ and $\Gamma_2 = \Gamma_{Z^0}^{th} = 2.8GeV$ ($\theta_3 = 0$, see above), and $\alpha(M_{Z^0}) = e^2/4\pi = (127.7)^{-1}$, v_α^k and a_α^k are those of tables 4.4 and 4.5. M_3 is fixed for illustration purposes equal to $150GeV$ for the CERN collider and $1TeV$ for LHC. The Z_3 width, Γ_3, is calculated in the two extreme cases: (i) Z_3 can decay only into the observed fermions (including the top quark); (ii) Z_3 can decay into three families of 27 fermions and the corresponding sfermions. This illustrates the possible range of variation of Γ_3, which we calculate using the decay rates

$$\Gamma(Z_3 \to f\bar{f}) = \frac{M_3}{12\pi}(1-4\eta_f)^{1/2}C_f\{(v_3^f)^2 + (a_3^f)^2 + 2[(v_3^f)^2 - 2(a_3^f)^2]\eta_f\}, \quad (4.68)$$

for fermions, and

$$\Gamma(Z_3 \to \tilde{f}_{L,R}\bar{\tilde{f}}_{L,R}) = \frac{M_3}{12\pi}(1-4\eta_{\tilde{f}})^{3/2}\frac{1}{4}C_f(v_3^f \mp a_3^f)^2, \quad (4.69)$$

for sfermions, where $\eta_a \equiv (m_a/M_3)^2$ with m_a $(a = f, \tilde{f})$ the fermion and sfermion masses and the colour factor C_f equal to 1(3) for $SU(3)_C$ singlets (triplets). In doing numerical estimates, we neglect finite mass effects in the final state: they

can be trivially included using eqs. (4.68) and (4.69), but in case (i) they are negligible; in case (ii) they can be sizeable, but neglecting them we obtain an upper bound for the total width Γ_3. In table 4.7 we give numerical values for the relevant quantities Γ_3/M_3 and $B(l^+l^-) \equiv \Gamma(Z_3 \to e^+e^-)/\Gamma_3 \equiv \Gamma(Z_3 \to \mu^+\mu^-)/\Gamma_3$. We consider cases (i) and (ii) above for the three models previously introduced. Γ_3/M_3 does not depend on M_3 (in the massless limit for the decay products) and is given in units of 10^3, so that the numbers in table 4.7 correspond to the width (in GeV) of a $1TeV$ Z_3.

In figs. 4.9-4.11 we plot $(d\sigma/dMdy)^S_{M=M_3}$ and $A(y)$ in eq. (4.67), for the same models and colliders and with the same assumptions as before. Finally, in figs. 4.12, 4.13 we give the total cross section for the production of Z_3 decaying into e^+e^- (or $\mu^+\mu^-$). The number of events corresponds to integrated luminosities, $\int \mathcal{L}dt$, of $0.37pb^{-1}$ ($Sp\bar{p}S$) and $10pb^{-1}$ ($Sp\bar{p}S + ACOL$), fig. 4.12 and of 10^4pb^{-1} (LHC), fig. 4.13. The horizontal line in fig. 4.12 corresponds to $\sigma = 3pb$, the present upper bound (at 90%$c.l.$) from the UA1 and UA2 data: it can be easily translated into a lower bound on M_3 for the different models.

Looking at the different figures, two final comments are in order. First, the hadron colliders, through the identification of charged lepton pairs, could detect quite heavy neutral gauge bosons or impose strong limits on their existence (fig. 4.13). Second, the width of these new gauge bosons is quite small (table 4.7 and fig. 4.5 and 4.7, and distinguishing among different models might require good resolution detectors. This point is raised and quantitatively discussed in ref. [75].

4.5.2 Decays into W^+W^- pairs

We have seen in the previous subsection that, if a new gauge boson Z_3 exists, it can decay into pairs of fermions, $f\bar{f}$ (and possibly of sfermions $\tilde{f}\bar{\tilde{f}}$ if a supersymmetric model is considered) independently of a possible sizeable mixing with the Z^0. In

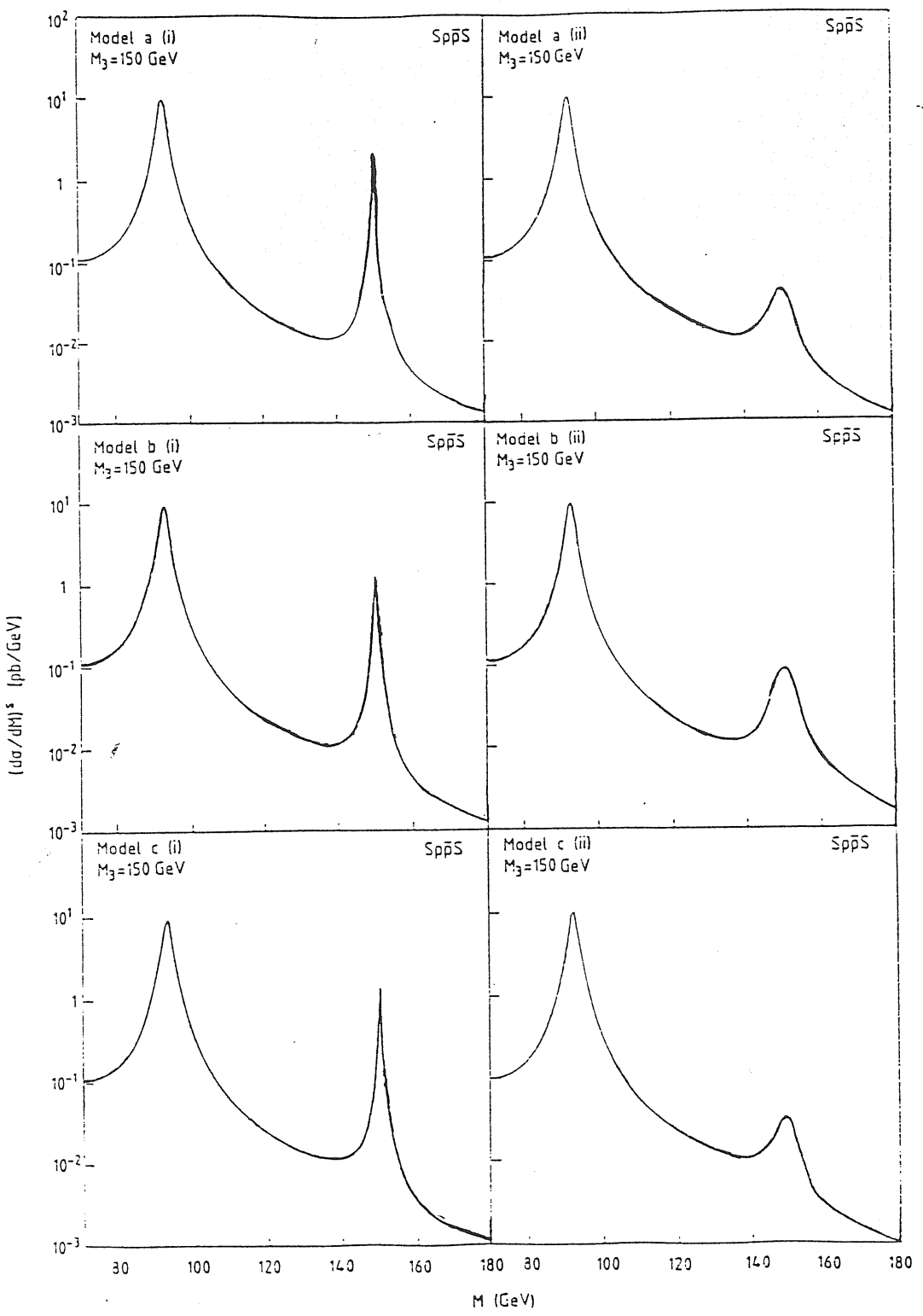

Figure 4.5: Lepton differential cross section $(d\sigma/dM)^S$ as a function of the lepton invariant mass M for the $Sp\bar{p}S$, models (a), (b) and (c) and cases (i) and (ii). $M_3 = 150GeV$ is assumed.

	(i)	(i)	(ii)	(ii)
	$10^3 \times \Gamma_3/M_3$	$B(e^+e^-)\%$	$10^3 \times \Gamma_3/M_3$	$B(e^+e^-)\%$
Model (a)	6.5	3.6	38	0.6
Model (b)	12	5.9	38	1.8
Model (c)	6.5	5.4	38	0.9

Table 4.7: Width and branching ratios into electron-positron pairs for the Z_3 of three representative models.

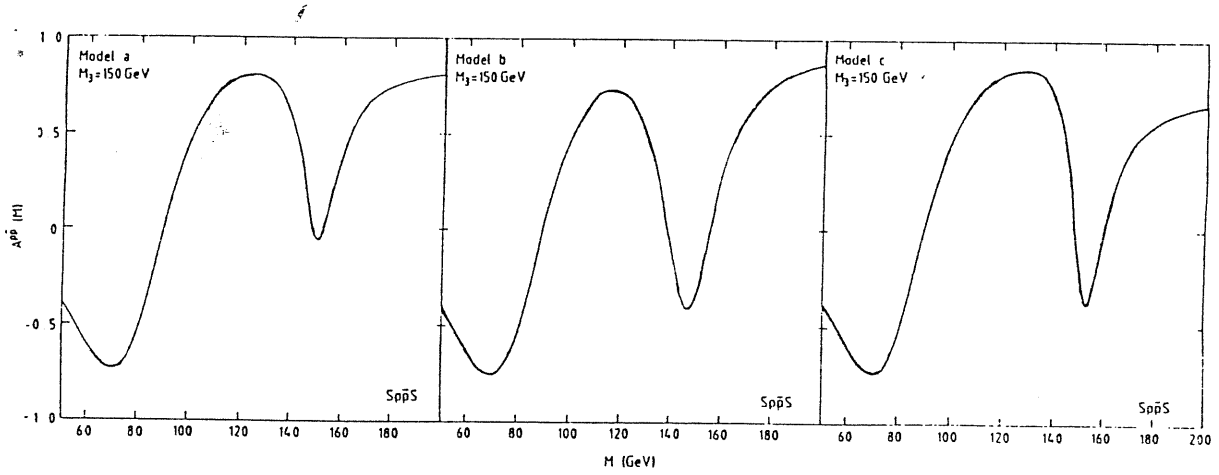

Figure 4.6: Lepton asymmetry $A^{p\bar{p}}(M)$ as a function of the lepton invariant mass M, for $Sp\bar{p}S$, $M_3 = 150GeV$, models (a), (b) and (c) and case (i) only; the figure is essentially unchanged for case (ii).

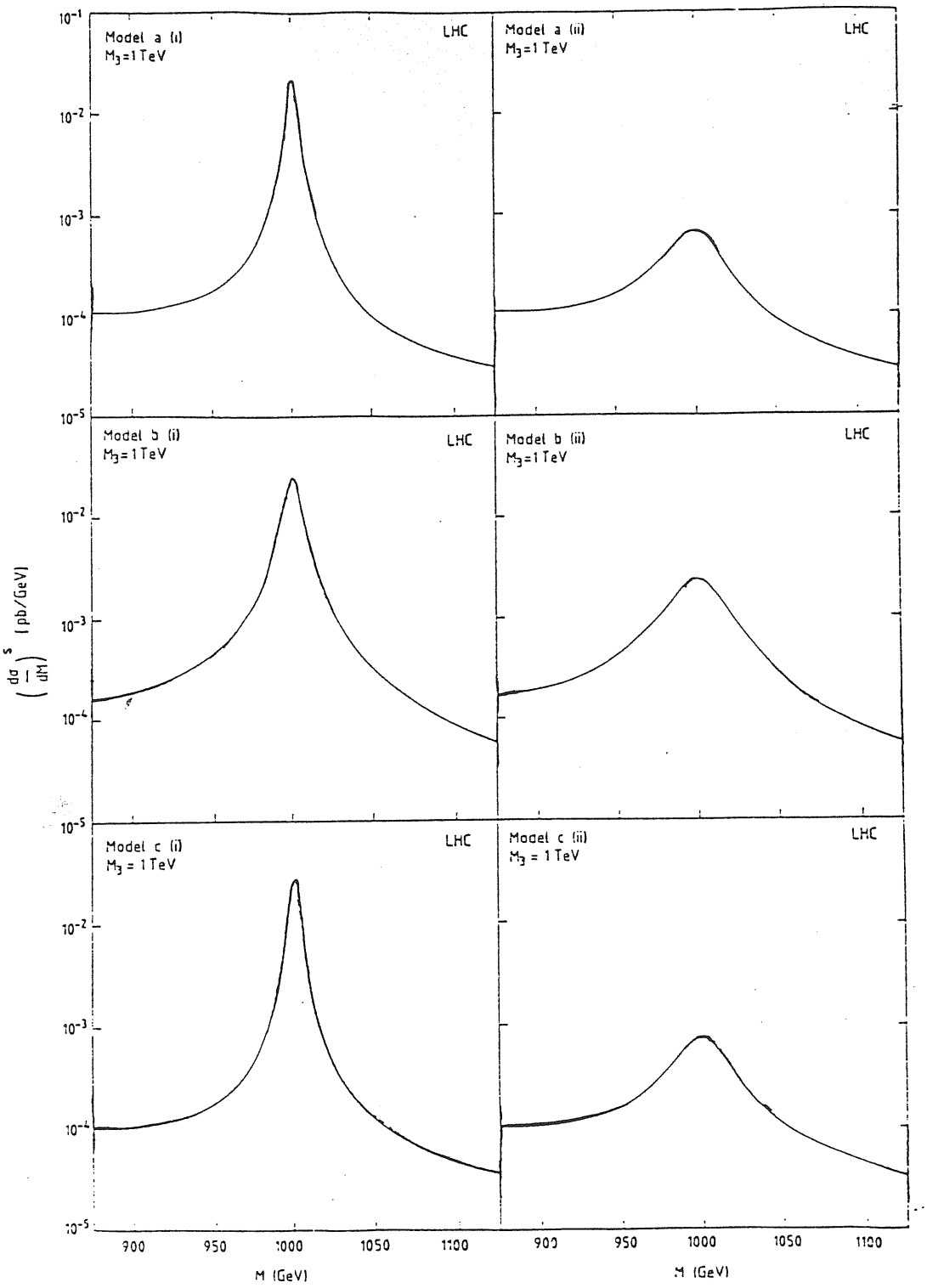

Figure 4.7: The same as in fig 4.5 but for the LHC and $M_3 = 1TeV$.

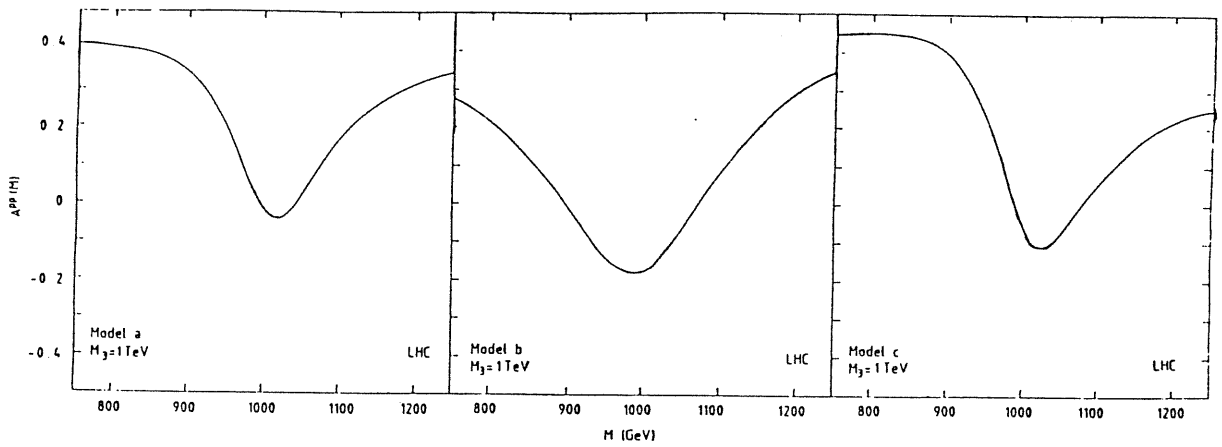

Figure 4.8: Lepton asymmetry $A^{pp}(M)$ as in fig. 4.6 but for the LHC, $M_3 = 1TeV$ and case (ii); the figure is essentially unchanged for case (i).

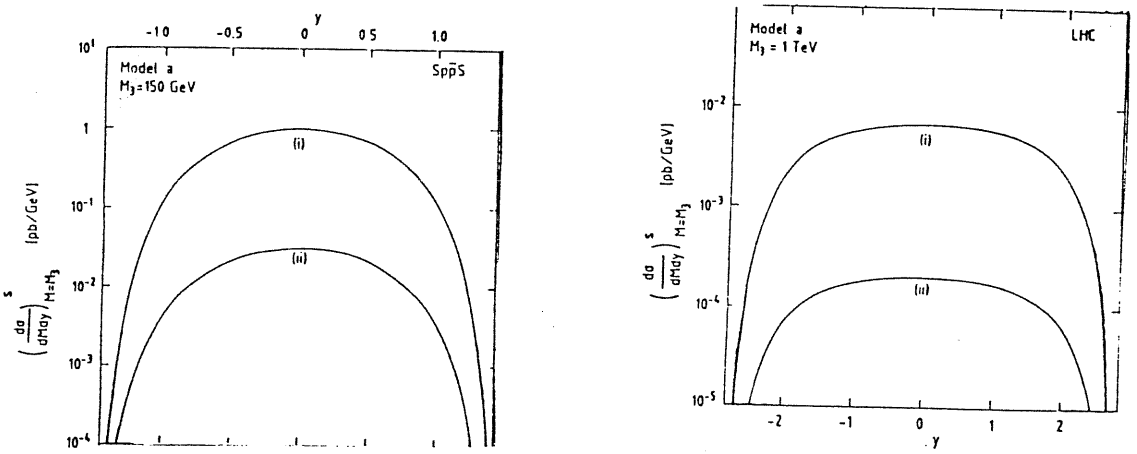

Figure 4.9: Lepton differential cross section at the Z_3 peak $(d\sigma/dMdy)_{M=M_3}$ as a function of the rapidity for model (a) and cases (i) and (ii). For the $Sp\bar{p}S$, $M_3 = 150GeV$; for the LHC, $M_3 = 1TeV$. The figures corresponding to models (b) and (c) are quite similar.

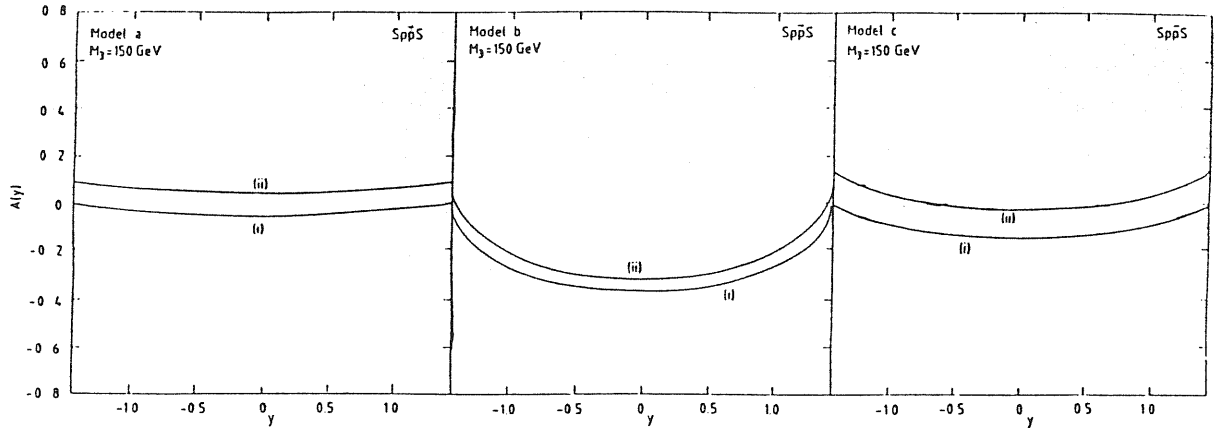

Figure 4.10: Lepton asymmetry at the Z_3 peak as a function of the rapidity A(y) for the $Sp\bar{p}S$, $M_3 = 150GeV$, models (a), (b) and (c) and cases (i) and (ii).

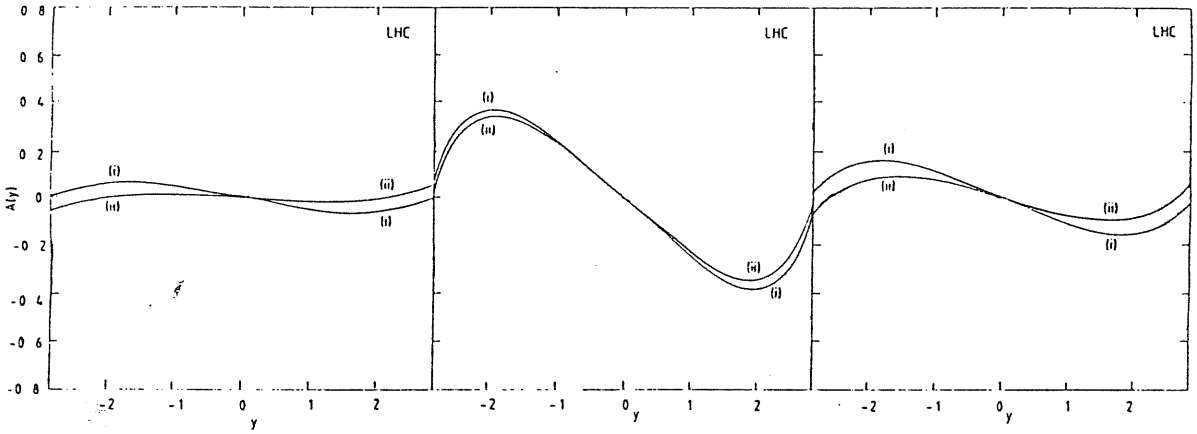

Figure 4.11: The same as in fig. 4.10 but for the LHC and $M_3 = 1TeV$.

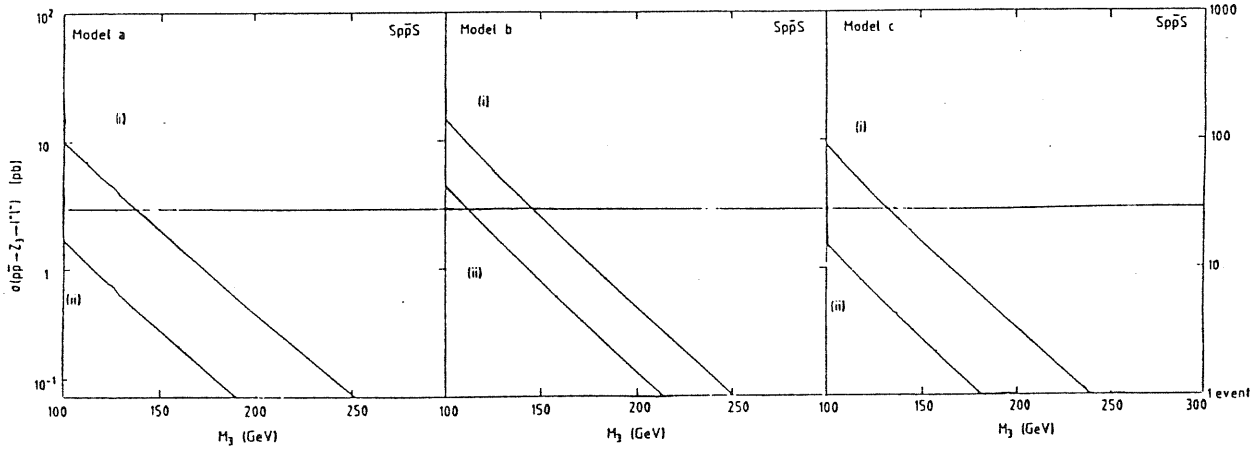

Figure 4.12: Total cross section for the production of Z_3 decaying into l^+l^- at the $Sp\bar{p}S$.

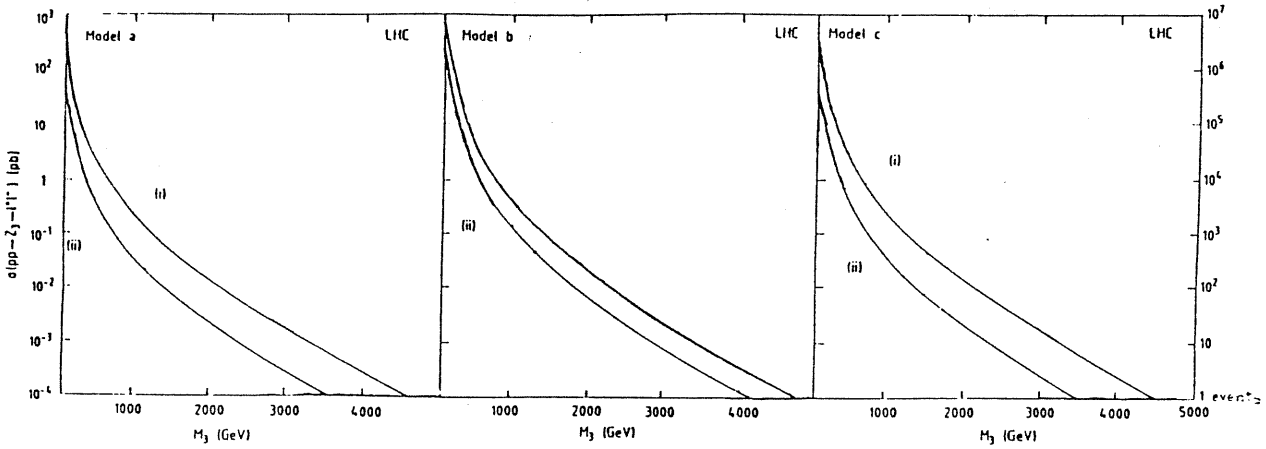

Figure 4.13: The same as in fig. 4.12 but for the LHC and an integrated luminosity of $10^4 pb^{-1}$.

addition, Z_3 can decay into W-pairs if $M_3 > 2M_W$ and it has a non-zero mixing with the Z^0 [4]. The coupling of the Z_3 to W pairs is illustrated in fig. 4.14 and the corresponding decay rate is found to be

$$\Gamma(Z_3 \to W^+W^-) = \frac{M_3}{12\pi}(1-4\eta_W)^{3/2}(1+20\eta_W+12\eta_W^2)\eta_W^{-2}\frac{\delta^2}{16}. \qquad (4.70)$$

In the above equation, δ is the coupling constant associated to the vertex $Z_3W^+W^-$, $\eta_W \equiv (M_W/M_3)^2$. As can be observed comparing (4.68), (4.69) and (4.70), the W^+W^- channel can be very important for a heavy enough Z_3 (small enough η_W), unless δ is negligibly small. Actually, in the physically relevant limit $M_3^2 >> M_W^2$,

$$\frac{\Gamma(Z_3 \to W^+W^-)}{\Gamma(Z_3 \to \Sigma_f f\bar{f}, \Sigma_f \tilde{f}\bar{\tilde{f}})} \simeq \frac{1}{24}\left(\frac{M_3}{M_W}\right)^4 \frac{\delta^2}{\Sigma_f C_f[(v_3^f)^2+(a_3^f)^2]}, \qquad (4.71)$$

where sfermion masses $m_{\tilde{f}}$ have been neglected with respect to M_3. (If sfermions are not considered, there is an enhancement factor of 3/2).

Formulae (4.70),(4.71) are model independent. If $\delta = O(1)$, $\Gamma_{W+W-} \sim O(M_3^4/M_W^4)\Gamma_{f\bar{f}}$, implying a very wide (heavy) Z_3 decaying only into W pairs. But this is never the case in extended electroweak models, where δ always scales as M_3^{-2} (see below).

[4]Decays into gaugino pairs can be safely neglected for they are suppressed by a factor $(M_W/M_3)^4$ with respect to decays into W pairs.

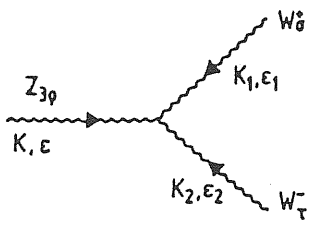

$$i\delta\,[K^\tau g^{\rho\sigma} - K^\sigma g^{\rho\tau} + K_1^\rho g^{\tau\sigma} - K_1^\tau g^{\rho\sigma} + K_2^\sigma g^{\rho\tau} - K_2^\rho g^{\tau\sigma}]$$

Figure 4.14: Feynman rule for the coupling of the Z_3 to W pairs.

Still, however, the W^+W^- sample from Z_3 decays will appear to be experimentally sizeable in hadron colliders.

In general,

$$\delta = \tilde{g}_1 c_W s_3. \tag{4.72}$$

This follows from the observation that W^+W^- only couple to W_3, with strength $\tilde{g}_1$. Then, it is only through its mixing with W_3 that a new Z can couple to (and decay into) W^+W^-. However, any heavy gauge boson can mix with W_3 at most proportionally to c_W, for W_3 mixes with the photon proportionally to s_W. In the standard model, there is only one massive gauge boson, Z_0, and it saturates c_W, then coupling to W^+W^- with strength $\tilde{g}_1 c_W$. Defining Z_0 in the same way in models with one extra gauge boson, the new Z_3 will couple to W^+W^- through its mixing with Z_0, s_3, and proportionally to the Z_0 coupling, $\tilde{g}_1 c_W$, proving eq. (4.72). Using now eqs. (4.15) and (4.16), we can write

$$s_3 = \frac{C}{\sqrt{(M_3^2 - A)(M_3^2 - M_2^2)}}. \tag{4.73}$$

This proves that, if C is bounded, as it happens in any $SU(3)_C \times SU(2)_L \times U(1)_Y \times U(1)_{\tilde{Y}}$ model, then s_3 scales as M_3^{-2}. In fact, M_2^2 has been measured and A and C are essentially bounded, up to Clebsch-Gordan coefficients and ratios of coupling constants, by M_W. This follows from the observation that any VEV contributing to A and C has $Q = 0$ and T_{3L} and $Y \neq 0$, then contributing also to M_W^2. In this

case eq. (4.71) reduces to

$$\frac{\Gamma(Z_3 \to W^+W^-)}{\Gamma(Z_3 \to \sum_f f\bar{f}, \sum_f \tilde{f}\bar{\tilde{f}})} \simeq \frac{C^2}{M_W^4} \frac{e^2 c_W^2}{24 s_W^2 \sum_f C_f[(v_3^f)^2 + (a_3^f)^2]}, \qquad (4.74)$$

which does not scale with M_3: C is bounded and so is eq. (4.74).

To get some insight in the size of the W^+W^- signal for E_6 superstring-inspired models, let us compare $\Gamma(Z_3 \to W^+W^-)$ with $\Gamma(Z_3 \to e^+e^-)$, which are easily computed using the results of sections 4.1 and 4.2. Figure 4.15 gives the ratio $R \equiv \Gamma(Z_3 \to W^+W^-)/\Gamma(Z_3 \to e^+e^-)$ for the models (a), (b) and (c) of table 4.6 as a function of M_3 for different values of ξ. For values of ξ for which there is no Z_3Z_0 mixing, $\delta = 0$ and so is $\Gamma(Z_3 \to W^+W^-)$. In all cases M_2 is required to lie in the shaded area of fig. 4.1. For this range of M_2 and for given (model dependent) ξ values, M_3 cannot be arbitrarily small. Then, in some cases the corresponding line in fig. 4.15 starts at values of M_3 larger than the threshold $M_3 = 2M_W$. We can observe in fig. 4.15 that the ratio R depends mainly om ξ, changing little for different M_2 and M_3 values as can be guessed from eq. (4.74).

From fig. 4.15, it is clear that the W^+W^- signal is of experimental interest, as it is comparable to the e^+e^- one. However, in general it is not the main signal, due to the penalizing factor for W pair identification with respect to lepton pairs. The detection of W^+W^- appears to rely on the chain $Z_3 \to W^+W^- \to (l\nu)(jj)$ where $l = e, \mu$. Taking into account the branching ratios for $W \to e\nu, jj$ and the detector efficiency, a (optimistic) 'discovery limit' of 20 $Z_3 \to W^+W^-$ has been estimated. In figs. 4.16 and 4.17 we plot the total cross section $\sigma(ab \to Z_3 \to W^+W^-)$ for the CERN collider, $(a, b, \sqrt{s}) = (p, \bar{p}, 630GeV)$ and the LHC, $(a, b, \sqrt{s}) = (p, p, 17TeV)$, respectively. We also give the corresponding number of events for an integrated luminosity, $\int \mathcal{L}dt$, of $0.73pb^{-1}$ ($Sp\bar{p}S$) and $10pb^{-1}$ ($Sp\bar{p}S$ + ACOL) in fig. 4.16, and of 10^4pb^{-1} (LHC) in fig. 4.17. In each figure, we present plots for the models (a), (b) and (c) of table 4.6. The calculation of the W^+W^- cross section is standard, but we use for the Z_3 production and for its decay

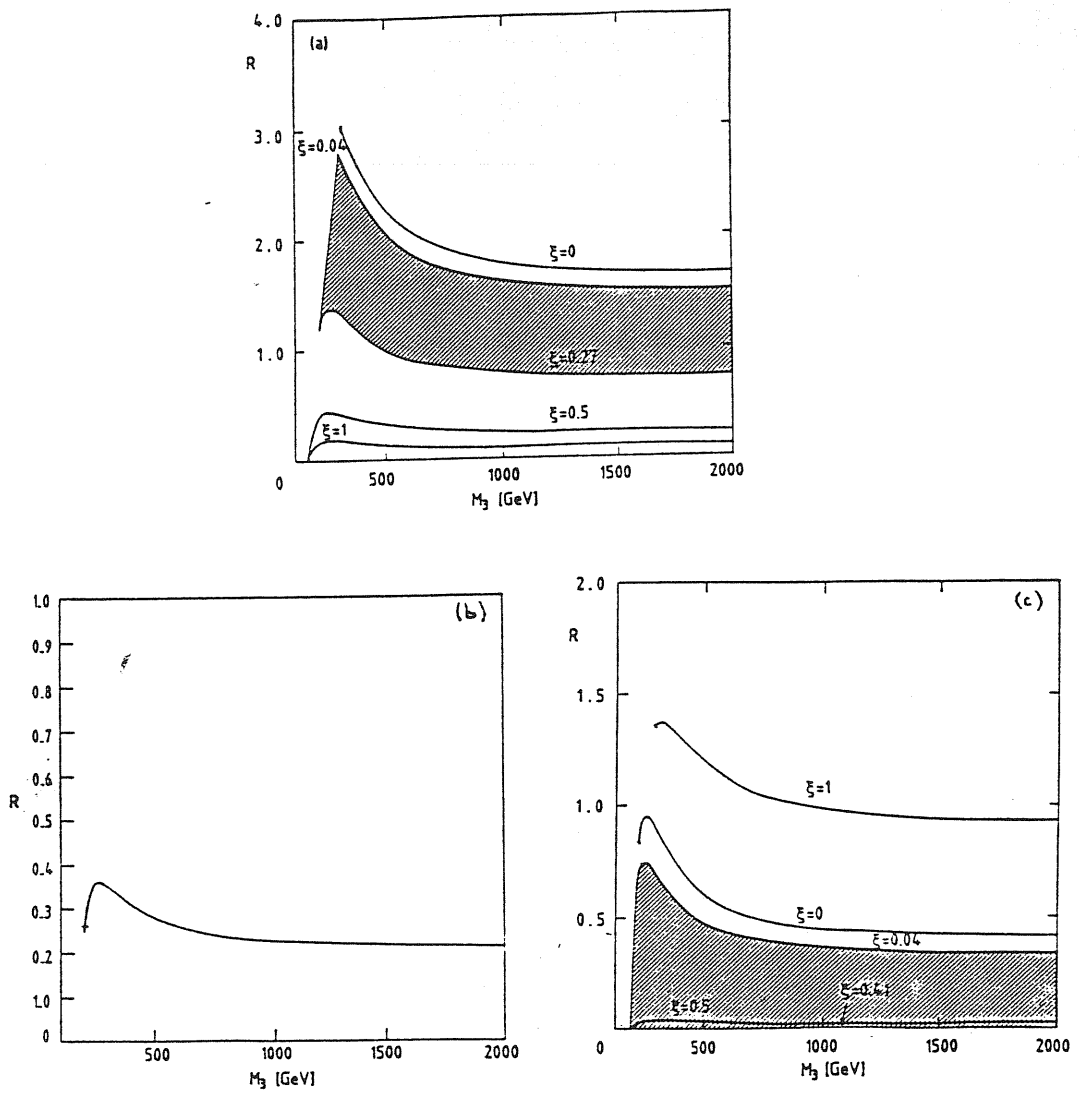

Figure 4.15: Allowed values of the relative branching ratio R defined in the text, as a function of M_3, for the models (a), (b) and (c) of table 4.6. The choice of parameters is the same as in fig. 4.2

into W^+W^- (usually not considered) the coupling in fig. 4.14, together with the results of sections 4.1 and 4.2. Our parton distribution functions are as before those of Duke and Owens, set 1. We assume that only three standard fermion generations are kinematically accessible. If Z_3 is allowed to decay into all fermions and sfermions in the 27 representations of E_6, the cross sections would be reduced by a factor $\sim \frac{1}{2}$. Besides a factor of 2 of uncertainty characterizes the parton distribution functions. As in fig. 4.15, lines corresponding to $\xi = 0, 0.5$ and 1 are shown, while the shaded areas correspond to the favoured values of ξ. As before, we fix $M_W = 81.8GeV$ and we allow M_2 to vary inside the shaded area of fig. 4.1. Comparing the W^+W^- cross section with the 20 events discovery limit, we observe that to detect (or exclude) a new Z_3 through its W^+W^- signal, we have to wait for LHC (fig. 4.17) or SSC, the CERN collider being out of question (fig. 4.16). This allows to comment on the two unusual events which are present in the W sample of UA1 [76]. It was speculated [77] from the kinematics of these events that they could result from the decay of a new boson of mass $\sim 250GeV$ into W^+W^-. It is clear from fig. 4.16 that no Z_3 arising from an E_6 superstring-inspired model can give the presently needed cross-section: they are off by more than one order of magnitude. Moreover, as explained before, it is a general fact that the $W^+W^-Z_3$ coupling is $\tilde{g}_1 c_W s_3$, where $\tilde{g}_1 c_W$ is the Z_0 coupling and s_3 the $Z_0 Z_3$ mixing. Present experimental limits require that in extended electroweak models (even more general than the E_6 superstring-inspired ones) $s_3 < 0.1$ for $M_3 \sim 250GeV$. Therefore, the cross section required by the $Z_3 \to W^+W^-$ interpretation of the present UA1 data is one order of magnitude larger than expected in any extended gauge theory.

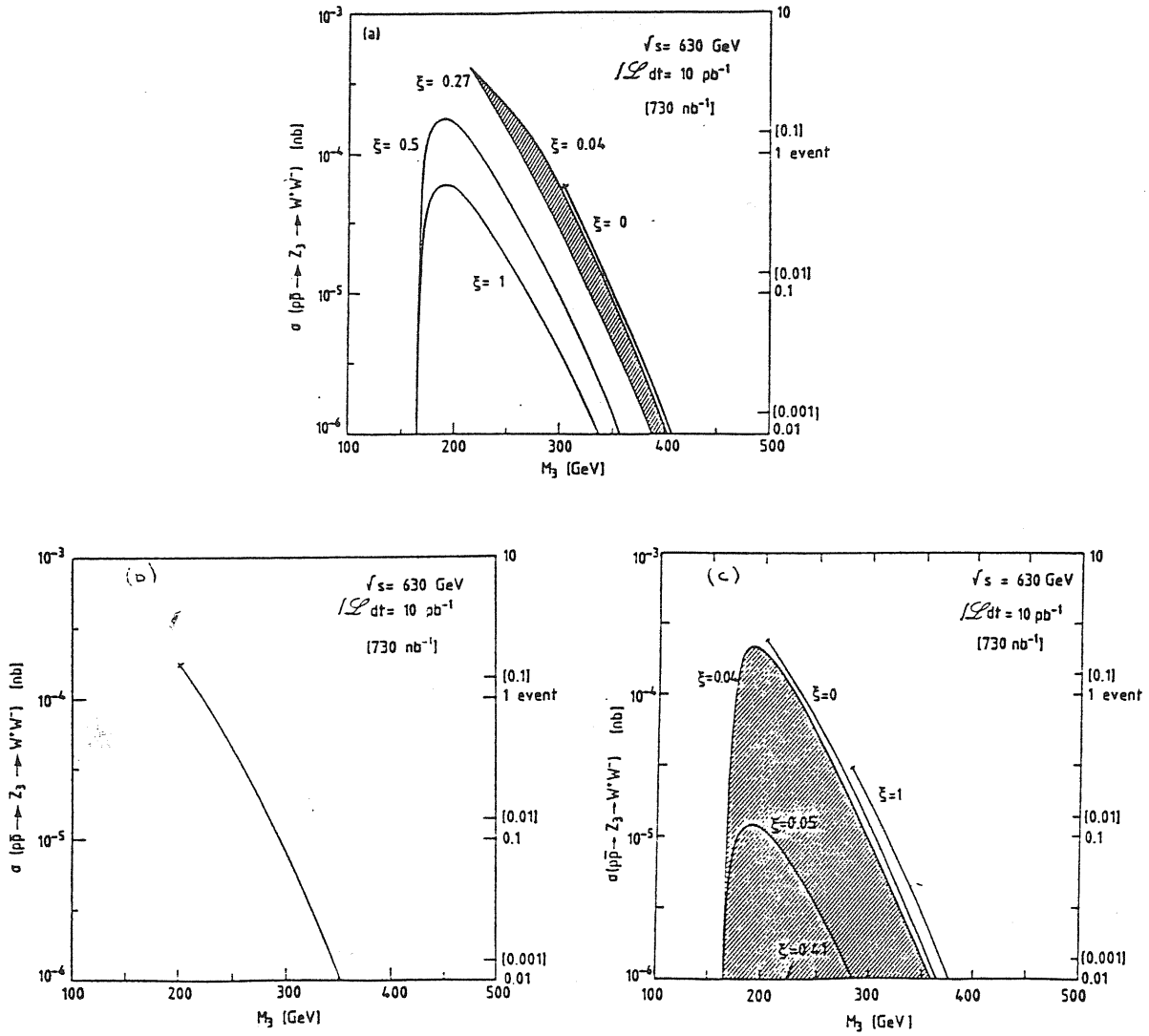

Figure 4.16: Total cross section and expected number of events for W^+W^- production at the Z_3 peak ($Sp\bar{p}S$).

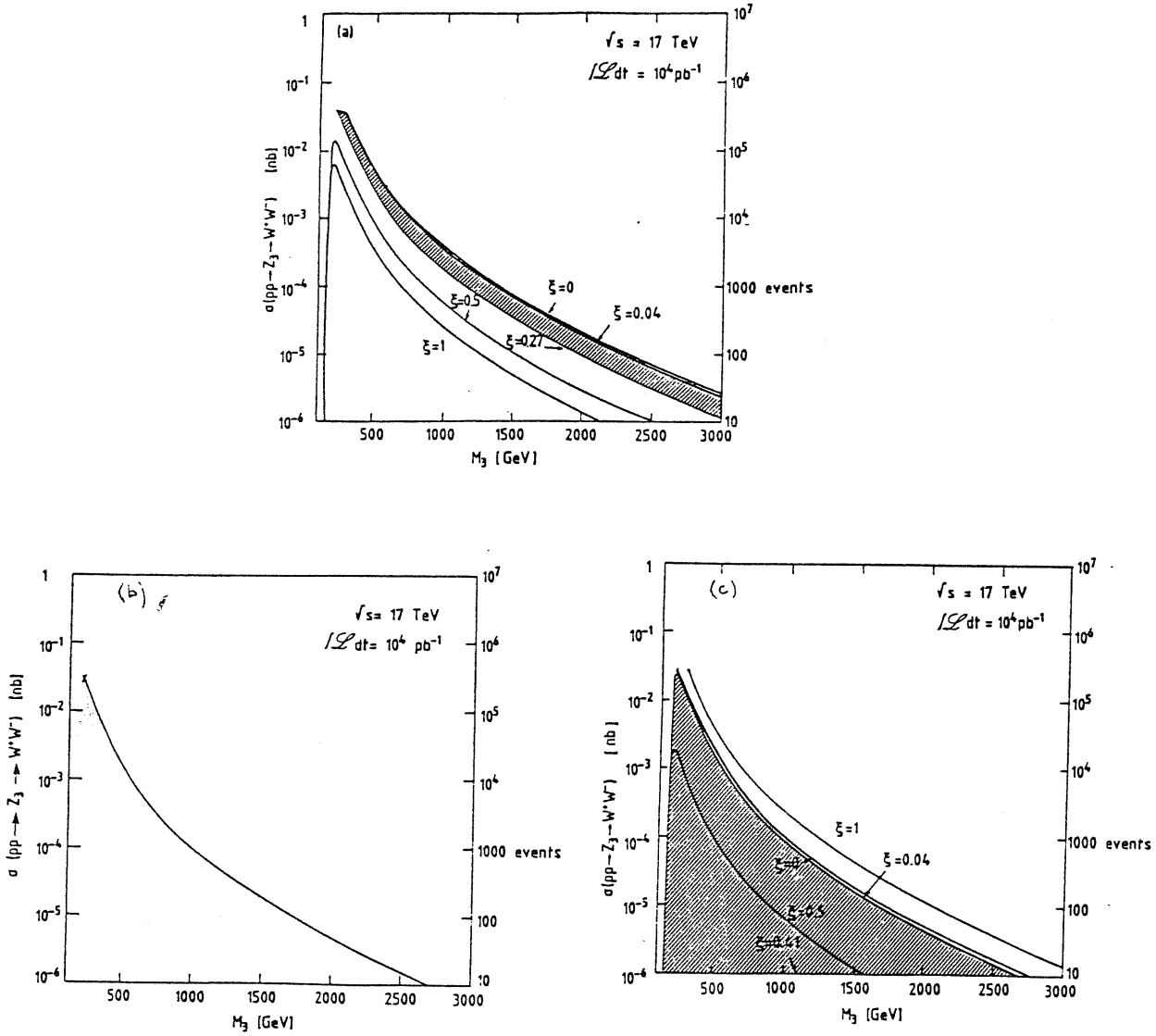

Figure 4.17: The same as in fig. 4.16 but for the LHC.

Chapter 5

Concluding remarks

In this work we have considered some phenomenological $N = 1$, $d = 4$ supergravity models that can be regarded as possible low-energy limits of the $E_8 \times E_8'$ heterotic superstring, compactified on some Calabi-Yau manifold. After explaining the philosophy of our approach in chapter 1, we have reviewed some general features of these superstring motivated models in chapter 2. In chapter 3 we have discussed in detail a prototype model, characterized by the gauge group $SU(3)_C \times SU(2)_L \times U(1)_Y \times U(1)_E$ and by three families of 27 chiral superfields with the quantum numbers of the fundamental representation of E_6, mainly focusing on those features that make it different from conventional supergravity models. In chapter 4 we have examined, in a general framework, the possible existence of extra Z' bosons (in addition to the Z observed at the CERN collider), associated to flavour conserving neutral currents of E_6. We have established limits on their masses and mixing angles from the analysis of the present experimental data, and we have studied the prospects for their detection at existing and future accelerators.

It must be stressed once again that, at the time of this writing, there is no sound way of extracting incontrovertible phenomenological predictions from superstring theories. Much progress is needed before such a connection (if any) can be established. It seems however that, if the low-energy limit of superstrings is going to be just the standard model (with or without supersymmetry), it will be

extremely difficult to find even some circumstantial evidence in favour or against them. This is what motivated our investigation of possible *new* phenomena that might be related to this theoretical framework.

This situation is expected to improve in the near future. On the theoretical side, it could be interesting to compare the class of low-energy models we have considered with the ones corresponding to some other recent proposals, like orbifolds or four-dimensional superstrings, to understand differences and similarities. On the experimental side, the forthcoming colliders will give us an unprecedented chance of exploring the TeV region. If none of the new phenomena considered in this analysis will be detected, this will restrict significantly the possible phenomenologically acceptable options. On the other hand, the discovery of just one of them could give us the clue for what is beyond the standard model.

References

1. See, for example, the Proceedings of the XXIII International Conference on High Energy Physics, Berkeley, July 16-23, 1986.

2. For reviews and references see, for example: P. Langacker, Phys. Rep. 72 (1981) 185; J. Ellis, in Gauge Theories in High Energy Physics, Les Houches, Session XXXVI, 1981, edited by M. K. Gaillard and R. Stora (North-Holland, Amsterdam, 1983).

3. For reviews and references see, for example: H. P. Nilles, Phys. Rep. 110 (1984) 1; A. B. Lahanas and D. V. Nanopoulos, Phys. Rep. 145 (1987) 1.

4. For a review and references see, for example: Superstring Theory, by M. B. Green, J. H. Schwarz and E. Witten, Cambridge University Press, 1986.

5. Recent reviews on superstring phenomenology are: J. Ellis, CERN preprint TH. 4439/86 (1986); H.-P. Nilles, CERN preprint TH. 4444/86 (1986); L. E. Ibáñez, CERN preprint TH.4459/86 (1986).

6. D. J. Gross, J. A. Harvey, E. Martinec and R. Rohm, Phys. Rev. Lett. 54 (1985) 502; Nucl. Phys. B256 (1985) 253; Nucl. Phys. B267 (1986) 75.

7. E. Calabi, in Algebraic Geometry and Topology: a Symposium in Honor of S. Lefschetz, p.78 (Princeton University Press, 1955); S. T. Yau, Proc. Natl. Acad. Sci. 74 (1977) 1798.

8. P. Candelas, G. T. Horowitz, A. Strominger and E. Witten, Nucl. Phys. B258 (1985) 46.

9. E. Witten, Nucl. Phys B268 (1986) 79.

10. L. Dixon, J. A. Harvey, C. Vafa and E. Witten, Nucl. Phys. B261 (1985) 678; B274 (1986) 285.

11. K. S. Narain, Phys. Lett. 169B (1986) 41; I. Antoniadis, C. P. Bachas, C. Kounnas and P. Windey, Phys. Lett. 171B (1986) 51; H. Kawai, D. C. Lewellen and S.-H. H. Tye, Phys. Rev. Lett. 57 (1986) 1832; Cornell University preprint CLNS 86/751 (1986); I. Antoniadis, C. P. Bachas and C. Kounnas, Ecole Polytechnique preprint A761.1286 or Lawrence Berkeley Laboratory preprint LBL-22709 (1986); W. Lerche, D. Lüst and A. N. Schellekens, CERN preprint TH.4590/86 (1986).

12. D. J. Gross and E.Witten, Nucl. Phys. B277 (1986) 1; M. T. Grisaru, A. E. M. van de Ven and D. Zanon, Phys. Lett. 173B (1986) 423, Nucl. Phys. B277 (1986) 388 and 409; M. T. Grisaru and D. Zanon, Phys. Lett. 177B (1986) 347; M. D. Freeman and C. N. Pope, Phys. Lett. 174B (1986) 48; C. N. Pope, M. F. Sohnius and K. S. Stelle, Nucl. Phys. B283 (1987) 192.

13. L. Witten and E. Witten, Nucl. Phys B281 (1987) 109; D. Nemeschansky and A. Sen, Phys. Lett. 178B (1986) 370; P. Candelas, M. D. Freeman, C. N. Pope, M. F. Sohnius and K. S. Stelle, Phys. Lett. 177B (1986) 341.

14. E. Witten, Nucl. Phys. B258 (1985) 75.

15. Y. Hosotani, Phys. Lett. 129B (1983) 193.

16. M. Dine, V. Kaplunovsky, M. Mangano, C. Nappi and N. Seiberg, Nucl. Phys. B259 (1985) 549; J. Breit, B. Ovrut and G Segre, Phys. Lett. 158B

(1985) 33; S. Cecotti, J.-P. Derendinger, S. Ferrara, L. Girardello and M. Roncadelli, Phys. Lett. 156B (1985) 318.

17. F. del Aguila, G. Blair, M. Daniel and G. G. Ross, Nucl. Phys. B272 (1986) 413.

18. E. Witten, Phys. Lett. 155B (1985) 151.

19. A. H. Chamseddine, Nucl. Phys. B185 (1981) 403; E. Bergshoeff, M. de Roo, B. de Wit and P. van Nieuwenhuizen, Nucl. Phys. B195 (1982) 97; G. F. Chapline and N. S. Manton, Phys. Lett. 120B (1983) 105.

20. E. Cremmer, S. Ferrara, L. Girardello and A. van Proeyen, Nucl. Phys. B212 (1983) 413.

21. E. Cremmer, S. Ferrara, C. Kounnas and D. V. Nanopoulos, Phys. Lett. 133B (1983) 61; J. Ellis, C. Kounnas and D. V. Nanopoulos, Nucl. Phys. B241 (1984) 406 and B247 (1985) 373.

22. C. P. Burgess, A. Font and F. Quevedo, Nucl. Phys. B272 (1986) 661.

23. S. Ferrara, C. Kounnas and M. Porrati, Phys. Lett. B181 (1986) 263.

24. S. Ferrara, L. Girardello, C. Kounnas and M. Porrati, preprint LBL-22905, UCLA/87/TEP/2, UCB/TPH/87/4 (1987); I. Antoniadis, J. Ellis, E. Floratos, D. V. Nanopoulos and T. Tomaras, preprint CERN-TH.4651/87 (1987).

25. P. Binetruy, S. Dawson, I. Hinchliffe and M. Sher, Nucl. Phys. B273 (1986) 501; J.-P. Derendinger, L. E. Ibáñez and H. P. Nilles, Nucl. Phys. B267 (1986) 365.

26. E. Cohen, J. Ellis,K. Enqvist and D. V. Nanopoulos, Phys. Lett. 165B (1985) 76; J. Ellis, K. Enqvist, D. V. Nanopoulos and F. Zwirner, Nucl. Phys. B276 (1986) 14 and Mod. Phys. Lett. A1 (1986) 57.

27. L. E. Ibáñez and J. Mas, CERN preprint TH.4426/86 (1986).

28. B. R. Greene, K. H. Kirklin, P. Miron and G. G. Ross, Phys. Lett. 180B (1986) 69; Nucl. Phis. B278 (1986) 667 and Oxford University preprint 11/87 (1987).

29. For a comprehensive review see: G. Costa and F. Zwirner, Riv. Nuo. Cim., Vol.9, n.3 (1986) 1.

30. S. Nandi and U. Sarkar, Phys. Rev. Lett. 56 (1986) 564.

31. R. N. Mohapatra, Phys. Rev. Lett. 56 (1986) 561

32. B. Campbell, J. Ellis, M. K. Gaillard, D. V. Nanopoulos and K. Olive, Phys. Lett. 180B (1986) 77; B. A. Campbell, J. Ellis, K. Enqvist, M. K. Gaillard and D. V. Nanopoulos, preprint CERN-TH.4473/86 (1986).

33. G. Costa, F. Feruglio, F. Gabbiani and F. Zwirner, University of Padova preprint DFPD 18/86 (1986).

34. K. Enqvist, D, V, Nanopoulos and M. Quirós, Phys. Lett. 169B (1986) 343; J. Ellis, K. Enqvist, D. V. Nanopoulos and K. Olive, preprint CERN-TH.4613/86 (1986).

35. M. Dine, N. Seiberg, X.-G. Wen and E. Witten, Nucl. Phys. B278 (1986) 769 and Princeton preprint (1987); J. Ellis, C. Gómez, D. V. Nanopoulos and M. Quirós, Phys. Lett. 173B (1986) 59 + (E) 174B (1986) 465.

36. J. Ellis, K. Enqvist, D. V. Nanopoulos, K. Olive, M. Quirós and F. Zwirner, Phys. Lett. 176B (1986) 403.

37. S. Ferrara, L. Girardello and H. P. Nilles, Phys. Lett. 125B (1983) 457.

38. J.-P. Derendinger, L. E. Ibáñez and H. P. Nilles, Phys. Lett. 155B (1985) 65; M. Dine, R. Rohm, N. Seiberg and E. Witten, Phys. Lett. 156B (1985) 55.

39. Y. J. Ahn and J. D. Breit, Nucl. Phys. B273 (1986) 75; M. Quirós, Phys. Lett.173B (1986) 265.

40. J. D. Breit, B. A. Ovrut and G. Segrè, Phys. Lett. 162B (1985) 303; P. Binetruy and M. K. Gaillard, Phys. Lett. 168B (1986) 347.

41. P. Binetruy, S. Dawson and I. Hinchliffe, Phys. Lett. 179B (1986) 262.

42. J. Ellis, D. V. Nanopoulos, M. Quirós and F. Zwirner, Phys. Lett. 180B (1986) 83; J. Ellis, A. B. Lahanas, D. V. Nanopoulos, M. Quirós and F. Zwirner, preprint CERN-TH.4626/86 (1986).

43. P. Majumdar, Mod. Phys. Lett. A2 (1987) 49.

44. P. Binetruy, S. Dawson, I. Hinchliffe and M. K. Gaillard, preprint LBL-22339 (1986); P. Binetruy, S. Dawson and I. Hinchliffe, preprint LBL-22322 (1986).

45. C. Kounnas and M. Porrati, preprint UCB-PTH-86/7 (1986).

46. M. Dine, N. Seiberg and E. Witten, Princeton preprint IASSNS-HEP-87/1 (1987).

47. S. Ferrara, C. Kounnas and F. Zwirner, in preparation.

48. J. Ellis, D. V. Nanopoulos, S. T. Petcov and F. Zwirner, Nucl. Phys. B283 (1987) 93.

49. V. D. Angelopoulos, J. Ellis, H. Kowalski, D. V. Nanopoulos, N. Tracas and F. Zwirner, preprint CERN-TH.4578/86 (1986).

50. B. A. Campbell, J. Ellis and D. V. Nanopoulos, Phys. Lett. 181B (1986) 283.

51. F. del Aguila, G. A. Blair, M. Daniel and G. G. Ross, Nucl. Phys. B283 (1987) 50.

52. A. Strominger and E. Witten, Comm. Math. Phys. 101 (1985) 341; A. Strominger, Phys. Rev. Lett. 55 (1985) 2547.

53. S. Komamiya, in Proc. Int. Symposium on Lepton and Photon Interactions at High Energies, Kyoto, 1985.

54. R. M. Barnett, H. E. Haber and G. L. Kane, Phys. Rev. Lett. 54 (1985) 1983.

55. J. Ellis, J. S. Hagelin, D. V. Nanopoulos, K. Olive and M. Srednicki, Nucl. Phys. B238 (1984) 453.

56. J. Yang, M. S. Turner, G. Steigman, D. N. Schramm and K. A. Olive, Ap. J. 281 (1984) 493.

57. G. Steigman, K. A. Olive, D. N. Schramm and M. S. Turner, Phys. Lett. 176B (1986) 33.

58. J. Ellis, K. Enqvist, D.V. Nanopoulos and S. Sarkar, Phys. Lett. 167B (1986) 457.

59. C. Rubbia, in Proc. Int. Symposium on Lepton and Photon Interactions at High Energies, Kyoto, 1985.

60. C. Hearty et al. (ASP Collaboration), preprint SLAC-PUB-4114 (1987).

61. H. E. Haber and M. Sher, preprint SCIPP-86/66 (1986); M. Drees, preprint MAD/PH/313 (1986).

62. H. Baer et al., in Physics at LEP, CERN Yellow Report 86-02, Vol. 1, p. 297 (1986).

63. W. Buchmüller et al., in Physics at LEP, CERN Yellow Report 86-02, Vol. 1, p. 203 (1986).

64. J. L. Rosner, Comm. Nucl. Part. Phys. 15 (1986) 195; R. Robinett, Phys. Rev. D33 (1986) 1908; V. Barger, N. Deshpande, R. J. N. Phillips and K. Whisnant, Phys. Rev. D33 (1986) 1912 + (E) D35 (1987) 1741; W. Buchmüller, R. Rückl and D. Wyler, preprint DESY 86/150 (1986); A. Dobado, M. J. Herrero and C. Muñoz, preprint FTUAM/87-4 (1987).

65. J. Ellis and H. Kowalski, Phys. Lett. 142B (1984) 441; Nucl. Phys. B246 (1984) 189 and B259 (1985) 109.

66. F. del Aguila, M. Quirós and F. Zwirner, CERN preprint TH.4536/86 (1986), to appear on Nucl. Phys. B (1987).

67. F. del Aguila, M. Quirós and F. Zwirner, Nucl. Phys. B284 (1987) 530.

68. G. Costa, J. Ellis, G. L. Fogli, D. V. Nanopoulos and F. Zwirner, CERN preprint TH.4675/87 (1987).

69. G. Arnison et al. (UA1 Collaboration), Phys. Lett. 166B (1986) 484; J. Appel et al. (UA2 Collaboration), Z. Phys. C30 (1986) 1; Review of Particle Properties, Phys. Lett. 170B (1986) 95.

70. L. S. Durkin and P. Langacker, Phys. Lett. 166B (1986) 436; V. Barger, N. G. Deshpande and K. Whisnant, Phys. Rev. Lett. 56 (1986) 30; D. London and J. L. Rosner, Phys. Rev. D34 (1986) 1530.

71. V. Angelopoulos, J. Ellis, D. V. Nanopoulos and N. Tracas, Phys. Lett. 176B (1986) 203; C. Vaz an D. Wurmser, Phys. Rev. D33 (1986) 2578; G.

Belanger and S. Godfrey, Phys. Rev. D34 (1986) 1309; P. J. Franzini and F. J. Gilman, Phys. Rev. D35 (1987) 855; M. Cvetic and B. W. Lynn, Phys. Rev. D35 (1987) 51; F. Cornet and R. Rückl, Phys. Lett. 184B (1987) 263.

72. P. Langacker, R. W. Robinett and J.L. Rosner, Phys. Rev. D30 (1984) 1470; V. Barger, N. G. Deshpande, J. L. Rosner and K. Whisnant, preprint MAD/PH/299 (1986); P. Chiappetta and J. P. Guillet, preprint CERN-TH.4628/86 (1986).

73. D. W. Duke and J. F. Owens, Phys. Rev. D30 (1984) 49.

74. J. D. Bjorken and S. D. Drell, Relativistic Quantum Fields, Mc-Graw Hill, New York, 1965.

75. B. Adeva, F. del Aguila, D. V. Nanopoulos, M. Quirós and F. Zwirner, CERN preprint TH.4535/86 (1986), to appear in the Proceedings of the Snowmass '86 Workshop on the SSC.

76. UA1 Collaboration, presented by D. Denegri at the 6th International Conference on $p\bar{p}$ Physics, Aachen, July 1986.

77. R. Kleiss and W. J. Stirling, Phys. Lett. 180B (1986) 171.